



DEVELOPMENT OF STORAGE COEFFICIENTS FOR CARBON DIOXIDE STORAGE IN DEEP SALINE FORMATIONS

Technical Study

Report No. 2009/13

Bcj Ya VYf 2009

*This document has been prepared for the Executive Committee of the IEA GHG Programme.
It is not a publication of the Operating Agent, International Energy Agency or its Secretariat.*

INTERNATIONAL ENERGY AGENCY

The International Energy Agency (IEA) was established in 1974 within the framework of the Organisation for Economic Co-operation and Development (OECD) to implement an international energy programme. The IEA fosters co-operation amongst its 26 member countries and the European Commission, and with the other countries, in order to increase energy security by improved efficiency of energy use, development of alternative energy sources and research, development and demonstration on matters of energy supply and use. This is achieved through a series of collaborative activities, organised under more than 40 Implementing Agreements. These agreements cover more than 200 individual items of research, development and demonstration. The IEA Greenhouse Gas R&D Programme is one of these Implementing Agreements.

ACKNOWLEDGEMENTS AND CITATIONS

This report was prepared as an account of the work sponsored by the IEA Greenhouse Gas R&D Programme. The views and opinions of the authors expressed herein do not necessarily reflect those of the IEA Greenhouse Gas R&D Programme, its members, the International Energy Agency, the organisations listed below, nor any employee or persons acting on behalf of any of them. In addition, none of these make any warranty, express or implied, assumes any liability or responsibility for the accuracy, completeness or usefulness of any information, apparatus, product of process disclosed or represents that its use would not infringe privately owned rights, including any parties intellectual property rights. Reference herein to any commercial product, process, service or trade name, trade mark or manufacturer does not necessarily constitute or imply any endorsement, recommendation or any favouring of such products.

COPYRIGHT

Copyright © IEA Environmental Projects Ltd. (Greenhouse Gas R&D Programme) 2009.

All rights reserved.

ACKNOWLEDGEMENTS AND CITATIONS

This report describes research sponsored by the IEA Greenhouse Gas R&D Programme. This report was prepared by:

EERC, University of North Dakota, USA

With co-funding and support from:

US Department of Energy (DOE) National Energy Technology Laboratory Cooperative Agreement No. DE-FC26-08NT43291.

The principal researchers were:

- C. Gorecki, EERC,
- J. Sorensen, EERC,
- J. Bremer, EERC,
- S. Ayash, EERC,
- D. Knudsen, EERC,
- Y. Holubnyak, EERC,
- S. Smith, EERC,
- E. Steadman, EERC,
- J. Harju, EERC.

To ensure the quality and technical integrity of the research undertaken by the IEA Greenhouse Gas R&D Programme (IEA GHG) each study is managed by an appointed IEA GHG manager. The report is also reviewed by a panel of independent technical experts before its release.

The IEA GHG managers for this report were: Neil Wildgust
& Toby Aiken

The expert reviewers for this report included:

- John Bradshaw, GGSS, Australia,
- John Wilkinson, Exxon Mobil, USA,
- Stefan Knopf & Klaus Reinhold, BGR, Germany,
- Karsten Michael, CO2CRC, Australia,
- Steve Cawley, BP Alternative Energy, United Kingdom,
- Malcolm Wilson, University of Regina, Canada,

The report should be cited in literature as follows:

IEA Greenhouse Gas R&D Programme (IEA GHG), "Development of Storage Coefficients for CO₂ Storage in Deep Saline Formations", 2009/13, October 2009.

Further information or copies of the report can be obtained by contacting the IEA Greenhouse Gas R&D Programme at:

IEA Greenhouse Gas R&D Programme, Orchard Business Centre,
Stoke Orchard, Cheltenham, Glos., GL52 7RZ, UK
Tel: +44 1242 680753 Fax: +44 1242 680758
E-mail: mail@ieaghg.org
www.ieagreen.org.uk

OVERVIEW: DEVELOPMENT OF STORAGE COEFFICIENTS FOR CARBON DIOXIDE STORAGE IN DEEP SALINE FORMATIONS

Background to the Study

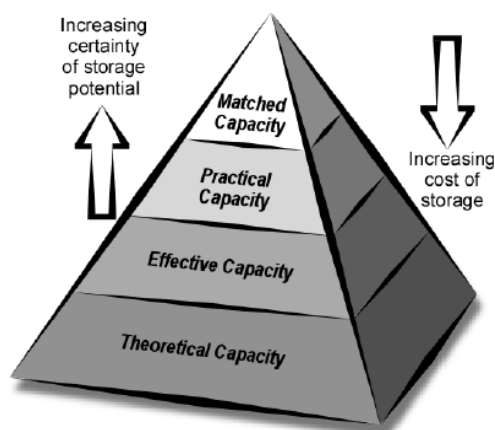
The IEA Greenhouse Gas R&D Programme (IEA GHG) commissioned the Energy and Environmental Research Centre (EERC), from the University of North Dakota, to undertake a study to develop storage coefficients for carbon dioxide (CO₂) storage in deep saline formations. The project was co-sponsored by the US Department of Energy (US DOE).

Various Carbon Sequestration Leadership Forum (CSLF) and IEA GHG publications have documented the complexity associated with estimating storage resources, and the ability to represent the information in a manner that truly reflects and expresses the uncertainty involved. A key criteria that remains unresolved, is how to take theoretical resources and convert them to realistic or viable capacities at a regional level. Existing published papers state that “storage coefficients” need to be applied to regional estimates to achieve this. Such coefficients would be dependent on storage type (i.e. deep saline formations, depleted gas or oilfield) and geological characteristics of storage formations.

The aim of this study was to define a series of such coefficients, which can be applied to regional calculations to provide more realistic estimates. Coefficients were considered and derived principally for deep saline formations, reflecting the large storage potential but associated inherent complexity and uncertainty.

The CSLF has published three papers through their Technical Group Taskforce on Storage Capacity Estimation Methodologies to document the issues involved. The CSLF Phase I report (2005) provided critical analysis of previous regional or wider scale capacity estimates and the methodologies employed in their derivation. The Phase I report emphasised the huge variations in capacity estimates obtained with varying methodologies and underlying assumptions by different authors. Estimates of total storage CO₂ capacity in Europe, for example, were shown to vary widely, under and over 1,000 Gt. The report also detailed the concept of the techno-economic pyramid for resource classification, as illustrated in the diagram below.

Figure 1: *CSLF Techno-Economic Resource Pyramid*





The Phase II CSLF report (2007) summarised key aspects of the Phase I report and suggested methodologies for estimating capacity according to storage scenario. A series of equations were presented for calculation of capacity in oil and gas reservoirs and saline aquifers.

The Phase III report (2008) supplemented the Phase II report by comparing the CSLF proposed methodologies with those employed by other national or international groups producing high level capacity estimates, in particular the Capacity and Fairways Subgroup of the US DOE Regional Carbon Sequestration Partnership Program. The Phase III report concluded that the CSLF and US DOE methodologies were virtually identical, differences being confined to computational formulation and for deep saline formations, the inclusion or otherwise of theoretical capacity outside the influence of structural traps.

Both the CSLF and US DOE methodologies included the concept of storage coefficients within capacity calculations. The coefficients allow for technical factors (e.g. geological heterogeneity) which reduce the capacity for CO₂ storage – with regard to the resource pyramid illustrated above, the coefficients as applied move capacity estimates from ‘theoretical’ to ‘effective’.

Scope of Study

The specification required a desk-based study to:

1. Summarise CSLF, US DOE and other comparable methodologies employed for large scale resource estimation for deep saline formations and oil and gas reservoirs. It was envisaged that the study would be based on the CSLF work, but a high level summary of differences with other approaches would be useful. Similarly, the contractor would review differences between proposed CSLF and other nomenclatures (e.g. US DOE, Australia’s CO₂CRC, and EC Geocapacity) published in relation to capacity estimation and resource pyramids, with a clear recommendation regarding terminology to be employed.
2. Review readily available and published, site-specific modelling results and associated data suitable for use in the study.
3. Identification of, and approaches to, industrial and academic CCS stakeholders for provision of additional storage capacity calculations resulting from detailed modelling assessments. The contractor needed to understand the trapping mechanisms, modelling assumptions/basis of calculations and the volume and geological characteristics of the utilised portion of the storage formation, to enable comparison between theoretical and effective capacity for each case.
4. Compile a database of key parameters and results from modelling studies at the various sites.
5. Calculate storage coefficients based on the methodologies and data derived from in the steps above. The coefficients should reflect the complexity and uncertainty inherent in all capacity estimation and so could be presented as, for example, lower bound, most likely and upper bound values for the main storage scenarios.
6. The contractor was asked to place the coefficients in the context of the relevant resource pyramid, so that their application to estimation of defined levels (e.g. ‘effective’ or ‘practical’) is unambiguous.

During the early stages of the study, the limited amount of data available from real-world CO₂ injection projects became obvious and the focus of the study switched to the use of modelling simulations to derive storage coefficients.

Storage Resource Classification and Methodologies

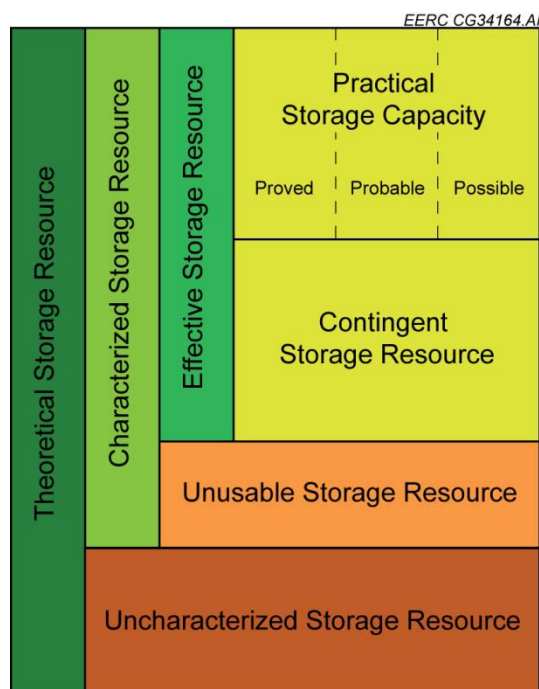
Resource Classification

The study considered 4 existing CO₂ storage resource classification schemes:

- The CSLF Techno-Economic Resource-Reserve Pyramid;
- The US DOE classification scheme developed for use in the Carbon Sequestration Atlas of the United States and Canada;
- The probabilistic assessment methodology being developed by the United States Geological Survey;
- The classification system proposed by CO₂CRC of Australia.

The study considered that the CSLF and US DOE classification schemes, with associated assessment methodologies being computationally very similar, as the most appropriate basis for development of storage capacity coefficients. However, elements of the CO₂CRC scheme were also incorporated into a new proposal for storage resource classification, as depicted in Figure 2 below.

Figure 2: *Proposed CO₂ Storage Classification Framework*



Full definitions of the terms used in Figure 1 are given in the main report. In relation to the storage coefficients developed by the study, the key definitions are:

Theoretical Storage Resource – Is the upper limit of storage resource and includes pore volume that can be used to store CO₂ in separate phase, dissolved phase, and mineral phase. In practice for any given area, this is an unrealistically high number because physical, technical, regulatory, and economic restrictions will always limit the full utilization of available pore space (modified from IEA GHG, 2008).



Effective Storage Resource – A resource that can be estimated after technical (geological and engineering) constraints have been applied to characterized storage resource. Effective storage resource is the pore volume in known (i.e., well-characterized) storage sites into which it is technically feasible to inject and store CO₂.

Depleted Hydrocarbon Fields

Depleted oil and gas reservoirs offer significant potential for CO₂ storage, being generally well characterised from exploration/production data and having proven capacity to retain buoyant fluids over geological timescales. Methodologies for CO₂ storage resource estimation in depleted hydrocarbon fields, developed by the CSLF and US DOE, were reviewed by the authors.

Both methodologies include volumetric approaches, whereby the volume of an oil or gas trap is equated to a theoretical storage resource by the application of an efficiency factor. This approach is ideal for ‘open’ reservoirs, where pressure and fluid communication from surrounding formation(s) is strong.

The CSLF methodology also includes an alternative approach, based on mass balance considerations from the recoverable reserves of oil and gas, plus any other produced fluids and compressibility considerations. This approach is suited to ‘closed’ reservoirs, where there is limited connectivity to surrounding formations and hydrocarbon extraction has resulted in depletion of pressure.

The study did not give further consideration to depleted hydrocarbon fields or develop storage capacity coefficients for these scenarios. Principally, this was because storage resources can be readily assessed using mass balance considerations rather than through coefficients; and also because project resources could be most beneficially applied to deep saline formations (DSF), with their associated larger potential storage capacity but greater technical uncertainty.

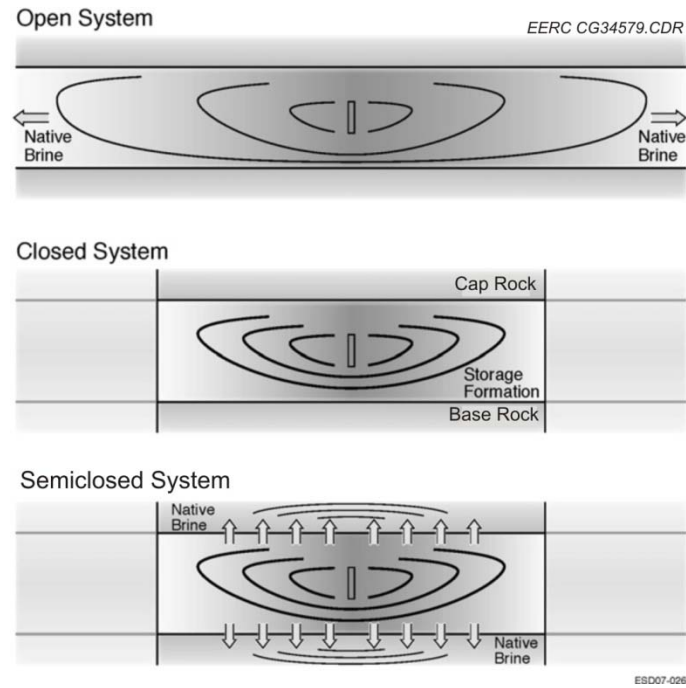
Deep Saline Formations

Development of reliable CO₂ storage capacity estimates for DSF can be problematic, especially as the results from site-specific modelling assessments cannot always be easily extrapolated to formation or regional scales, depending on whether systems are ‘open’ or ‘closed’ (Figure 3).

The authors suggest that ‘open’ systems form the majority cases for DSF storage, in which fluid and pressure communication across the formation is strong. However, ‘closed’ or ‘semi-closed’ systems may also exist, where lateral flow boundaries such as faults can restrict fluid movement. For modelling of CO₂ storage, understanding which of these boundary conditions pertains is critical; the study examined both ‘open’ and ‘closed’ systems for the development of storage capacity coefficients.

For closed systems, CO₂ injection would result in pressure increase, limiting effective storage capacity to the volume created by both the compressibility of the formation and existing pore fluids, and the limit of pressure increase before physical damage to the system. The study presents a series of equations derived from US DOE methodology, which enable the storage coefficient to be defined as the fraction of total pore volume that will be accessible to CO₂, based on volumetric changes caused by compressibility.

Figure 3: Diagram representing 3 potential systems (from Zhou et al, 2008)



The study states that open systems can be anticipated in many sedimentary basins around the world, where DSF will have relatively consistent geological properties and may be largely unfaulted. The two most commonly applied methodologies for assessment of storage resource in these scenarios are again, those published by the CSLF and the US DOE. The study presents a detailed mathematical review of the two approaches and confirms that from a computational standpoint, the methods are essentially equivalent and importantly, derived capacities can be easily related.

The basic equation for the US DOE approach is:

$$G_{CO_2} = A * h * \phi * \rho_{CO_2} * E$$

Where, the mass of stored CO₂ is (G_{CO_2}) based on investigational area (A), formation thickness (h), porosity (ϕ), CO₂ density (ρ_{CO_2}) and the application of a storage coefficient (E)

The CSLF main equation is:

$$V_{CO_2T} = V_{trap} * \phi * (1 - S_{wirr}) = A * h * \phi * (1 - S_{wirr})$$

Where the theoretical volume of stored CO₂ (V_{CO_2T}) is based on a geometric volume of a trap (V_{trap}), the area of the storage trap (A), average thickness of the trap (h), porosity (ϕ), the irreducible water saturation (S_{wirr}). The CSLF capacity coefficient C_C , which incorporates the cumulative effects of trap heterogeneity, CO₂ buoyancy, and sweep efficiency, is then multiplied by (V_{CO_2T}) to derive an effective storage capacity.



The storage coefficients used by the two methodologies can be related by the following equation, provided that the same assumptions concerning storage conditions are applied:

$$E_E = C_C * (1 - S_{wirr})$$

where E_E is the DOE effective storage coefficient, C_C is the CSLF effective storage coefficient, and S_{wirr} is the irreducible water saturation in the presence of CO_2 under reservoir conditions. When these coefficients are applied to their respective methodologies, the effective storage resources calculated will then be equal.

Development of Coefficients for Effective Storage Capacity

Methodology

Whilst preliminary coefficients based on generalised simulations have been utilised in the assessments of storage capacity in the US and Canadian national atlas, no coefficients have yet been published for the CSLF methodology. The study set out to create a set of broadly applicable storage coefficients for DSF that could be applied to both methodologies.

Since determination of coefficients relies on field based data and/or numerical modelling, the first step undertaken was a literature review of actual CO_2 storage projects, and it was immediately evident that these are of insufficient number to adequately representative all possible DSF scenarios. Therefore, a simulation approach was adopted, whereby a significant range of representative 3D models were used to generate values for storage coefficients.

The construction of these models required the development of a database containing representative values for DSF properties, lithologies, depositional environments and structures. Since there is a general paucity of data available for DSF, the authors constructed the Average Global Database (AGD) by using hydrocarbon reservoir properties as a proxy for DSF characteristics. The AGD was compiled through use of existing US databases and an extensive literature review for other regions. With details of over 20,000 reservoirs, analysis of the AGD allows parameters to be defined as a statistical dataset. Table 1 below lists examples of general formation properties derived from the AGD.

Table 1. General Formation Properties from the AGD

Percentile Value	Depth, m	Salinity, ppm	Temp Grad, °C/m	Reservoir Thickness, m
10	900	8,200	0.020	3.4
50	2,300	53,000	0.025	26
90	3,800	170,000	0.033	190

All figures shown to 2 significant figures

Reservoirs in the AGD could also be classified according to 3 lithologies (clastics/limestone/dolomite), ten depositional environments, and five different structures.



A uniform injection and evaluation scheme was developed as a base for all of the modelling runs undertaken:

- Coefficients were calculated at the projected time when injection stopped;
- CO₂ injection volumes were set at 1Mt over 1 year for homogeneous models and 1Mt over 5 years for heterogeneous models;
- Areal dimensions of the models were set at 3.2km by 3.2km, thickness at 26m, whilst models were divided into 204,000 grid cells;
- Trapping was dominated by physical containment, but solution and residual trapping were also accounted for even though they were relatively minor contributors to trapping over the projected timescales of injection;
- Plumes were defined by the extent of free-phase CO₂.

Parameter Evaluation Using Homogeneous Models

The first stage of the modelling process involved running a series of simulations using homogeneous models, constructed with average properties derived from the AGD. This enabled an assessment of the sensitivity of calculated coefficients to various key input parameters.

The results of this assessment showed that tightly closed structures, increased depth, lower temperatures, low ratios of vertical to horizontal permeability and high injection rates, all increased storage efficiency and the value of the calculated coefficient. Effects of relative permeability and irreducible water saturation appeared to be much less pronounced.

The insights gained from the modelling using homogeneous conditions, served as a basis for the design and execution of heterogeneous models subsequently used for calculation of the coefficients.

Calculation of Storage Coefficients

Heterogeneous models were developed for the various lithologies, depositional environments and structures, to derive ranges of storage capacity coefficients. Statistical distributions from the AGD were employed for key input parameters including porosity and permeability.

The issue of scale was considered in detail by the report, in particular whether calculation of coefficients and storage resource at localised scales can be applied to entire formations. The study first developed site-specific storage coefficients from 195 simulations using heterogeneous models, before attempting to extrapolate these results to the formation level. The resulting values for storage coefficient (E_E , US DOE method) ranged from 4% to 17% with an 80% confidence interval. Structural setting was found to exert the largest influence of any parameter on the results, with storage coefficients for effective resource exceeding 25% in some cases.



The site-specific results were then extrapolated to the formation scale. Table 2 below summarises the statistical distribution of coefficient values according to lithological type.

Table 2. Storage Coefficients Calculated at Formation Level by Lithology

Lithology	P10, %	P50, %	P90, %
Clastics	1.86	2.70	6.00
Dolomite	2.58	3.26	5.54
Limestone	1.41	2.04	3.27
All	1.66	2.63	5.13

Results quoted as US DOE methodology coefficients, equivalent to $Cc(1-S_{wirr})$ for the CSLF method.*

The authors stress that in order to assess effective storage resource at the basin level, resources in individual DSF units should be assessed using the methodology outlined, and then results aggregated.

Comparison of Open and Closed Systems

Where formations are closed, extrapolation of storage coefficients from site-specific assessment to formation level is problematic and instead, compartments within the formation require individual assessment. Note also that the storage coefficients presented above would not be applicable; storage coefficients for closed systems are likely to be at least an order of magnitude lower than those presented in Table 2 for open systems.

One possible solution to the problem of pressure increase in closed systems would be the production of brine, however this would option presents economic issues that are beyond the scope of this study.

Applicability and Limitations

The methodologies and storage coefficients presented in the report can be used as a guide for developing estimates of effective storage resources at the site-specific to the formation level and can further be expanded to cover other assessment areas.

The tables of site-specific storage coefficients presented in the report (Appendix E) represent a range of values based on data collected in the AGD. They are not specific to any site but can be useful as a generalized comparison tool as well as an illustration of the expected ranges under different conditions.

It is important to understand that the methodology and coefficients presented in the report can never be regarded as a substitute for detailed assessments at the site-specific level required during the design and implementation of CO₂ storage projects.



Expert Review Comments

Comments on the draft report were received from 11 expert reviewers. Overall feedback was positive; many comments related to specific technical issues and assumptions made in the modelling work, reflecting the broad, generic nature of the work and also emphasising that the study results do not reduce the requirement for detailed, site-specific modelling at the appropriate stages of actual storage projects. Nevertheless, the final report included numerous adjustments and caveats as a result of the expert review process.

Some of the more significant or recurrent comments are summarised below:

- The executive summary required further refinement, to deliver the main aspects and findings of the study in a clear and concise format which can be readily understood by non-technical specialists;
- In either the executive summary or the conclusions, a simplified tabular or graphical summary of the ranges of coefficients derived was suggested, clearly linked to the proposed storage classification scheme;
- Linked to the above bullet point, the authors questioned whether the draft report clearly conveyed how these coefficients could be applied to storage capacity estimation;
- The report stated that the coefficients are applicable at all scales. Whilst this may be true, it seems that the real benefit may be for regional studies, whereas at a site specific level, the numbers may have little value beyond initial rapid estimates or as checks for the results of detailed, site-specific assessment. Further emphasis of this point was requested in the report;
- Reviewers queried if there was appropriate discussion of onshore versus offshore storage capacity;
- The question was raised of how sensitive are coefficients derived from the study, to the assumptions concerning injection rate?
- Reviewers requested that the basis of the proposed classification scheme (SPE/CO₂CRC) should be appropriately acknowledged.

Conclusions

The study has successfully built upon earlier work by both the CSLF and US DOE, confirming the similarities of the two methodologies and more importantly, establishing an ease of comparison of storage coefficients employed and resources calculated for deep saline formations.

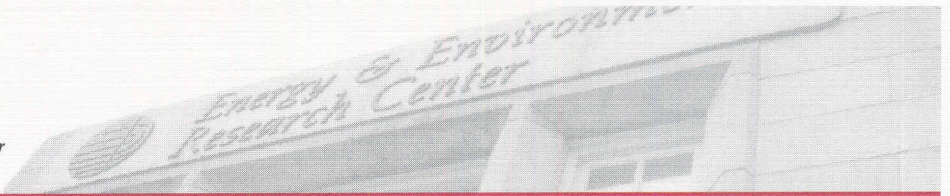
As there was insufficient real-world CO₂ injection data to derive a representative range of coefficients, an alternative numerical modelling approach was employed with input parameters derived from global hydrocarbon reservoir data. The modelling work showed the relative influence of various parameters on the efficiency of storage, and allowed the derivation of probabilistic ranges of storage coefficients for calculation of effective storage resource at both site-specific and formation levels, the overall mean value for all lithologies being 2.6% at the formation level.

The report has provided a series of storage coefficients that can be used for assessment of CO₂ storage resources in deep saline formations, in association with the published methodologies of the US DOE and CSLF.



Recommendations

The analysis and conclusions presented by the study are based on theoretical modelling. As experience and data is gained from increasing numbers of actual injection projects, the results of this study and the storage coefficients derived should be re-assessed at an appropriate point in the future using real-world data. This could form the basis of a future IEA GHG study.



DEVELOPMENT OF STORAGE COEFFICIENTS FOR CARBON DIOXIDE STORAGE IN DEEP SALINE FORMATIONS

Final Report

(for the period August 25, 2008, through June 30, 2009)

Prepared for:

Neil Wildgust

IEA Greenhouse Gas R&D Programme
The Orchard Business Centre
Stoke Orchard
Cheltenham GLOS, GL52, 7RZ
UNITED KINGDOM

Prepared by:

Charles D. Gorecki
James A. Sorensen
Jordan M. Bremer
Scott C. Ayash
Damion J. Knudsen
Yevhen I. Holubnyak
Steve A. Smith
Edward N. Steadman
John A. Harju

Energy & Environmental Research Center
University of North Dakota
15 North 23rd Street, Stop 9018
Grand Forks, ND 58202-9018

2009-EERC-07-06

July 2009

EERC DISCLAIMER

LEGAL NOTICE This research report was prepared by the Energy & Environmental Research Center (EERC), an agency of the University of North Dakota, as an account of work sponsored by IEA Greenhouse Gas R&D Programme (IEA-GHG) and the U.S. Department of Energy (DOE). Because of the research nature of the work performed, neither the EERC nor any of its employees makes any warranty, express or implied, or assumes any legal liability or responsibility for the accuracy, completeness, or usefulness of any information, apparatus, product, or process disclosed or represents that its use would not infringe privately owned rights. Reference herein to any specific commercial product, process, or service by trade name, trademark, manufacturer, or otherwise does not necessarily constitute or imply its endorsement or recommendation by the EERC.

ACKNOWLEDGMENTS

This report was prepared with support of the IEA Greenhouse Gas R&D Programme (IEA-GHG) and the U.S. Department of Energy (DOE) National Energy Technology Laboratory Cooperative Agreement No. DE-FC26-08NT43291. However, any opinions, findings, conclusions, or recommendations expressed herein are those of the author(s) and do not necessarily reflect the views of IEA-GHG and DOE.

The authors would like to acknowledge the hard work and dedication of several individuals and organizations, without whose help and support this report would not have been possible. We want to extend a special thanks to the following individuals: Dr. Scott Frailey for his contributions, insight, and critique of some of the critical elements of the this report, in particular, a variety of aspects related to the DOE methods for estimating CO₂ storage; Dr. Stefan Bachu for his invaluable guidance and insight in the development of the final report; and Mr. Steve Melzer for his unique perspective on carbon capture and storage in general and, specifically, his insight with regard to CO₂ storage in hydrocarbon reservoirs. We also want to acknowledge the guidance and support of Neil Wildgust of IEA-GHG, Dawn Marie Deel of DOE, and John Litynski of DOE. We want to thank Schlumberger and the Computer Modeling Group for the use of their software packages in the development and execution of the modeling and simulation portions of this project. The authors would like to thank the staff of the Energy & Environmental Research Center (EERC) for their hard work helping to prepare this report and the students and interns behind the scenes, in particular, Johannes Mendgen. Finally, we would also like to acknowledge the Plains CO₂ Reduction (PCOR) Partnership, under which many of the ideas and philosophy used in this report were first formulated.

TABLE OF CONTENTS

LIST OF FIGURES	iii
LIST OF TABLES	iv
EXECUTIVE SUMMARY	v
INTRODUCTION	1
APPROACH	2
Key Concepts and Terminology.....	3
Processes and Timescale for CO ₂ Storage	3
CO ₂ Storage Targets	3
CO ₂ Storage Mechanisms in Geologic Formations.....	5
Physical Trapping	5
Residual Gas Trapping	5
Solubility Trapping.....	6
Mineral Trapping.....	6
Hydrodynamic Trapping.....	6
Resource/Capacity Concept	9
CO ₂ Storage Resource Classification and Estimation Systems	10
CSLF	10
DOE	11
Proposed New Classification System	12
Definitions	15
 CO ₂ STORAGE RESOURCE ESTIMATION IN DEPLETED HYDROCARBON RESERVOIRS	18
DOE and CSLF Methodologies for Depleted Hydrocarbon Reservoirs	18
Discussion of the Application of Storage Coefficients to Depleted Hydrocarbon Reservoirs.....	19
 CO ₂ STORAGE RESOURCE ESTIMATION IN DEEP SALINE FORMATIONS	20
Closed System	21
Open System	23
CSLF Methodology	23
DOE Methodology.....	24
Equivalence of the DOE Method and the CSLF Method, Related to the Proposed Resource Classification System	25
 DEVELOPMENT OF EFFECTIVE STORAGE COEFFICIENTS.....	29
Lithologies and Depositional Environments	30

Continued...

TABLE OF CONTENTS (continued)

Model Structures and Traps	30
Determining Storage Coefficients Through Numerical Simulation.....	33
Development of Uniform Injection and Evaluation Scheme.....	33
Evaluation of Parameters Affecting CO ₂ Storage Coefficients Using Homogeneous Models.....	37
Structure.....	39
Depth and Temperature	39
Relative Permeability and Irreducible Water Saturation (S_{wirr}).....	40
Permeability Anisotropy (k_v/k_h)	41
Injection Rate/Fluid Velocity	43
Homogeneous Model Summary.....	44
Heterogeneous Model Development.....	45
Calculation of Broadly Applicable Storage Coefficients.....	50
Issue of Scale	50
Site-Specific Storage Coefficients.....	51
Formation-Based Storage Coefficients.....	53
Comparison of Open-System Effective Storage Resource Estimation to Closed- System Compressibility Storage Resource Estimation	54
Applicability and Limitations.....	56
 SUMMARY AND CONCLUSIONS	 57
 REFERENCES	 59
 REFERENCES FOR THE AVERAGE GLOBAL DATABASE	 Appendix A
 REVIEW OF DEPOSITIONAL ENVIRONMENTS	 Appendix B
 CLASTIC AND CARBONATE TYPE LOGS	 Appendix C
 POROSITY DISTRIBUTION FOR EACH LITHOLOGY AND DEPOSITIONAL ENVIRONMENT	 Appendix D
 SITE-SPECIFIC STORAGE COEFFICIENTS FOR DIFFERENT LITHOLOGIES, DEPOSITIONAL ENVIRONMENTS, STRUCTURES, AND PROBABILITY LEVELS.....	 Appendix E

LIST OF FIGURES

1	General outline of the major sedimentary basins around the world.....	4
2	The operating time of the physical and geochemical processes which trap CO ₂ in geologic formations.....	8
3	Storage security of the different trapping mechanisms and their relationship with time.....	8
4	CSLF Techno-Economic Resource-Reserve pyramid	11
5	Proposed CO ₂ storage classification framework.....	13
6	Political/geographical, physical/geological pyramid, illustrating differences between assessment area types	14
7	Diagram representing the three potential storage systems.....	21
8	Depositional environments modeled in this project, from AGD	30
9	Depositional environments from the AGD	31
10	Flat deltaic stratigraphic porosity model.....	31
11	Dome deltaic porosity model	32
12	Trap types from AGD	32
13	Four concepts for the accessible area considered in this project.....	36
14	k_v/k_h ratio of 0.01	42
15	k_v/k_h ratio of 0.1	42
16	k_v/k_h ratio of 1	43
17	Sandstone relative permeability curve	46
18	Carbonate relative permeability curve	47
19	Examples showing the sandstone type log (A) translated to the alluvial fan total porosity log.....	47
20	Relationship between the site of the assessment and the resulting storage coefficient.....	50

LIST OF TABLES

1	DOE Efficiency Factor Terms.....	25
2	List of P10, P50, and P90 General Formation Properties from the AGD	30
3	List of Homogeneous Models	38
4	Properties of Clastic Reservoirs in Homogeneous Models.....	39
5	Structure Models Tested.....	39
6	Effects of Depth and Temperature on Storage Coefficients.....	40
7	Relative Permeability Models Tested Along with Resulting Storage Efficiency and Storage Coefficients, from Bennion and Bachu (2008).....	41
8	Vertical to Horizontal Permeability Models Tested.....	41
9	Injection Rate/Fluid Velocity Models Tested Are Listed Below	44
10	Basic Model Parameters for a Reservoir Depth of 2336 m and a Salinity of 53,080	48
11	Basic Model Parameters for a Temperature of 75°C and a Reference Pressure at 2336 m of 23,900 kPa Produced from the AGD and Deutsch	49
12	Ranges of Variables Used to Calculate Storage Coefficients for Different Lithologies and Depositional Environments.....	52
13	P10, P50, and P90 Storage Coefficients E_E and $C_C * (1 - S_{wirr})$ Calculated for the Site-Specific Scale for Different Lithologies (A_n/A_t is fixed at 0.8)	52
14	Formation-Based Storage Coefficients and the P50 Values for Each Variable Used to Calculate the Coefficients	53
15	P10, P50, and P90 Storage Coefficients Calculated E_E and $C_C * (1 - S_{wirr})$ for the Formation Level for Different Lithologies	54
16	Assessment Area Properties for the Comparison of the Open and Closed Systems Effective Storage Resource.....	55

DEVELOPMENT OF STORAGE COEFFICIENTS FOR CARBON DIOXIDE STORAGE IN DEEP SALINE FORMATIONS

EXECUTIVE SUMMARY

Storage resource/capacity estimates are critical for stakeholders to make informed decisions regarding the potential implementation of large-scale carbon dioxide (CO₂) storage. Previous methodologies based solely on fundamental geologic data grossly overestimate the storage resource/capacity of a given area, and for this reason, the concept of storage efficiency was introduced. One approach to developing more realistic estimates of storage resource/capacity is to use knowledge about a wider variety of the physical properties of a rock formation as a basis for an assumption that only a certain percentage of that rock formation will be amenable to CO₂ storage. The value of that percentage is referred to as a “storage coefficient.” The development of technically robust storage coefficients is critical to the advancement of broadly applicable and comparable storage resource/capacity estimates at all scales. With this in mind, activities were conducted that 1) identified and evaluated previously developed methods for calculating storage resource/capacity, with an emphasis on those presented by the Carbon Sequestration Leadership Forum (CSLF) and the U.S. Department of Energy (DOE) and then 2) developed a methodology and a set of storage coefficients that could be applied to deep saline formations in a variety of settings at both the site-specific and formation scales. The primary purpose of the work herein is to allow decision makers, scientists, and engineers to utilize the equations and concepts necessary to move estimates forward from “theoretical” to “effective” storage resources, thereby providing a more realistic view of the CO₂ resource/capacity of a given assessment area.

The two most promising types of storage formations for CO₂ capture and storage (CCS) are depleted hydrocarbon reservoirs and deep saline formations. Depleted hydrocarbon reservoirs are, for the most part, portions of saline formations which have proven trapping mechanisms and competent sealing units made apparent by the accumulation of hydrocarbons which have remained in place for millions of years. Also, as a result of exploration and production activities, most depleted hydrocarbon reservoirs have a higher degree of characterization than deep saline formations. As a result, depleted hydrocarbon reservoirs and the methods used to calculate storage resource/capacity were examined in this study; however, no new storage coefficients were developed for these systems because of the site-specific nature of the formation fluids and the production history of depleted hydrocarbon reservoirs and the fact that material balance equations will generally result in more accurate estimates of storage resource/capacity. Deep saline formations occur over large regions of every continent and are often less well characterized than depleted hydrocarbon reservoirs. However, because of their large volume and wide distribution, deep saline formations have the greatest potential storage resource/capacity, and most of the efforts of this report went into the refinement of storage coefficients for these formations.

A clear and applicable resource/capacity classification system with consistent terms and definitions will be of great benefit for the advancement of CCS, particularly with respect to refining storage resource/capacity estimates. Previous classification systems developed for hydrocarbon and mining resources and commodities have limited applicability to CCS because

their intent is to classify material removed from the ground as opposed to CO₂ storage within the material beneath the surface. Another issue to address is the notion of “undiscovered” resources, which doesn't really apply to saline formations since, for the most part, their location is known, however poorly they may be characterized. To address this, a classification system is proposed that combines concepts heralded by the CSLF technoeconomic resource pyramid (CSLF, 2005) as well as the industry standard Petroleum Resource Management System (Society of Petroleum Engineers and others, 2007). Also included are definitions from the DOE Carbon Sequestration Atlas of the United States and Canada (DOE, 2008), and concepts and definitions proposed by the CO₂CRC in the report prepared for the IEA Greenhouse Gas Research & Development Programme entitled “Aquifer Storage” (IEA-GHG, 2008). In addition, terminology was developed regarding the “area of assessment”—previously a combination of geological and geographical jurisdictions, which made comparison between assessment terms difficult. The geological/physical and geographical/political terminology concepts were split, and terms were developed for both hierarchies.

Through the examination of the published methodologies used to estimate storage resource/capacity in deep saline formations, a critical difference in storage resource/capacity results from the behavior of boundary conditions and whether the dominant process is the result of mobilization (as seen within open boundaries) or compression (as seen within closed boundaries). These two mechanisms represent two end points, as both processes will be present in a given storage scenario; however, the boundaries of the formation will cause one process to dominate over the other. Calculation of storage coefficients for both processes are described and addressed. Deterministic examination of the interplay of the two processes has not been developed, however. In the case of compression, efficiency is limited by an increase of pressure and the resulting compression of fluids and particles as well as the dilation of pore spaces. In the case of mobilization, the storage process involves the movement of natural formation fluids away from the injection site. Because of the relatively straightforward nature of the compressibility, closed-system method, the focus of this report has been on developing effective storage coefficients for open systems using both the DOE and CSLF methods.

Since previous work by the CSLF has demonstrated that the DOE and CSLF methods for calculating CO₂ storage in open saline formations are nearly equivalent (CSLF, 2008), the two methods were related to each other through a series of factors and equations so that storage estimates made with one system can be easily compared to the other. In the end, if the assumptions are made in a similar manner, the resulting effective storage coefficients and estimates of effective storage resource made with one method can be easily related to the other through the following relationship:

$$E_E = C_C * (1 - S_{wirr})$$

where E_E is the DOE effective storage coefficient, C_C is the CSLF effective storage coefficient, and S_{wirr} is the irreducible water saturation in the presence of CO₂ under reservoir conditions. Then when the storage coefficients are applied to their respective methodologies, the resulting effective storage resource calculated with each method will be equal:

$$V_{CO_2,CSLF_E} = V_{CO_2,DOE_E}$$

where $V_{CO_2,CSLF_E}$ is the effective volume of CO₂ that can be stored under reservoir conditions as calculated using the CSLF methodology, and V_{CO_2,DOE_E} is the effective volume of CO₂ that can be stored under reservoir conditions as calculated using the DOE methodology. With this relationship in mind, a methodology was developed to determine the range of values for the effective storage coefficients at the site-specific and formation scales. This work was completed through a two-part effort, by first developing homogeneous models to test the relative strength of single variables on the effective storage coefficients and then by developing a series of heterogeneous models to develop a range for the effective storage coefficients for different lithologies, depositional environments, and structures. Ideally, the models would have been populated with properties from real-world CO₂ storage projects; however, since there are only a few large-scale CO₂ storage projects currently under way, a dataset was developed based on hydrocarbon reservoirs. Considering that hydrocarbon reservoirs may reasonably be considered to be subsets of larger saline formations, the applicability of these hydrocarbon reservoir properties is appropriate. The dataset, referred to as the Average Global Database (AGD), contains fluid and geologic properties from over 20,000 hydrocarbon reservoirs representing a wide variety of reservoir types from all over the world.

The strength and effect of five parameters (structure, relative permeability and irreducible water saturation, depth and temperature, vertical to horizontal permeability anisotropy, and injection rate/fluid velocity) were tested using homogeneous models, built based on the average properties from the AGD, to examine the effect of each parameter on storage efficiency and the resulting storage coefficients. In general, tightly closed structures, increased depth and lower temperatures, low ratios of vertical to horizontal permeability, and high injection rates/fluid velocity all increased the storage efficiency and the value of the storage coefficient. The effects of relative permeability and irreducible water saturation were much more subtle, with no large difference in the value of the storage coefficients with the relative permeability curves and irreducible water saturation values that were tested.

Values for the effective storage coefficients were developed for application to deep saline formations at the site-specific level using 195 different heterogeneous models based on the properties in the AGD for three different lithologies, ten depositional environments, and five structural settings. The resulting values for E_E and $C_C * (1 - S_{wirr})$ for the site-specific scenarios ranged from about 4% to about 17% with a 80% confidence interval, depending on the lithology, depositional environment, and structure. In each case, the structure played the largest role, with several of the dome structures having an effective storage coefficient greater than 25%. The values developed for the site-specific level were extrapolated out to the formation scale for the three different lithologies, and values were determined for both the E_E and $C_C * (1 - S_{wirr})$ at the P10, P50, and P90 probability levels (Table ES-1 below).

Table ES-1. P10, P50, and P90 Storage Coefficients E_E and $C_C * (1 - S_{wirr})$ Calculated at the Formation Level for Different Lithologies

Lithology	P10, %	P50, %	P90, %
Clastics	1.86	2.70	6.00
Dolomite	2.58	3.26	5.54
Limestone	1.41	2.04	3.27
All	1.66	2.63	5.13

The values for storage coefficients and methodology developed over the course of this work can be applied at scales from the site-specific to the formation-level for both the DOE and CSLF open-system methodologies, and a technique is also presented which can be applied to closed systems. When performing an evaluation to determine the effective storage resource, there are two important issues that must be addressed: 1) the scale of assessment, and 2) whether the majority of the storage come from mechanisms associated with closed- or open-formation boundaries. If the evaluation is to be performed on an entire basin, then the effective storage resource should be calculated for each saline formation that has properties that make it amenable to CO₂ storage when the appropriate assessment methodology is applied. The resulting values should be added together to develop an effective storage resource for the entire basin. Similarly, an assessment made over geographical/political areas should be estimated by evaluating the storage formations or portions of the storage formations separately, then adding the resulting effective storage resource estimates together to come up with the effective storage resource for the entire country, region, or state/province. This must be done since, in many cases, there are multiple stacked deep saline formations, each with its own unique properties, which could be used individually to effectively store CO₂ on a geologic time scale. Storage coefficients and resulting storage resource/capacity estimates calculated by any of the methods presented in this document may be used to compare assessment areas in order to identify areas that may be suitable for further, more detailed studies. Storage coefficients calculated using any of the methods presented in this document are not a replacement for the site-specific work required before the commencement of a large-scale storage project but are appropriate for first-order evaluations of the effective storage resource.

REFERENCES

- Carbon Sequestration Leadership Forum, 2005, A task force for review and development of standards with regards to storage capacity measurement—Phase I: CSLF-T-2005-9 15, August 2005, 16 p., www.cslforum.org/publications/documents/PhaseIReportStorageCapacityMeasurementTaskForce.pdf (accessed June 2009).
- Carbon Sequestration Leadership Forum, 2008, Comparison between methodologies recommended for estimation of CO₂ storage capacity in geologic media—Phase III report: April 21, 2008, www.cslforum.org/publications/documents/PhaseIIIReportStorageCapacityEstimationTaskForce0408.pdf (accessed June 2009).

IEA Greenhouse Gas R&D Programme (IEA-GHG), 2008, Aquifer storage—development issues: November 2008/12.

Society of Petroleum Engineers, World Petroleum Council, American Association of Petroleum Geologists, and Society of Petroleum Evaluation Engineers, 2007, Petroleum resources management system.

U.S. Department of Energy National Energy Technology Laboratory Office of Fossil Energy, 2008, Carbon sequestration atlas of the United States and Canada.

DEVELOPMENT OF STORAGE COEFFICIENTS FOR CARBON DIOXIDE STORAGE IN DEEP SALINE FORMATIONS

INTRODUCTION

In recent years, the concept of mitigating global climate change through large-scale carbon capture and storage (CCS) into geologic media (saline formations, depleted hydrocarbon reservoirs, and unminable coal seams) has gained worldwide attention. Identifying potential geologic sinks for carbon dioxide (CO₂) storage and developing reliable estimates of their storage resource/capacity is a critical component of determining the efficacy of CCS. While numerous evaluations have been conducted to develop storage resource/capacity estimates for geologic formations throughout the world, they are the product of several different methodologies, and comparison of the results of one evaluation to another is often difficult and misleading. The IEA Greenhouse Gas Research & Development (R&D) Programme (IEA-GHG) has been working closely with a wide variety of international organizations, including the U. S. Department of Energy (DOE) to develop approaches and methods for developing CO₂ storage resource/capacity estimates that can be applied to assessments at the site-specific, local, regional, basin, and country scales. Recently IEA-GHG and DOE have identified the development of technically robust “storage coefficients” as being crucial to the advancement of broadly applicable and comparable storage resource/capacity estimates at all scales.

The concept of applying storage coefficients to CO₂ resource/capacity estimates for geological media has been described and applied in a variety of published reports and papers. Perhaps the most influential and notable of such documents include the series of three reports presented by the Carbon Sequestration Leadership Forum (CSLF) from 2005 to 2008 and the methodology presented by DOE Capacity and Fairways Subgroup for the development of the Carbon Sequestration Atlas of the United States and Canada, 2007 and 2008 (DOE, 2007, 2008). These documents present the means by which theoretical maximum storage resource can be refined by mathematically considering the real-world characteristics of a geologic formation (e.g., formation dimensions and porosity distribution, etc.) that limit its storage resource, thereby allowing evaluators to develop more accurate storage resource/capacity estimates. At the heart of the matter is the fact that only a fraction of the pore space within any given geological formation will be available or amenable to CO₂ storage. The purpose of a storage coefficient is to assign a value to that fraction of a given formation in which CO₂ can be effectively stored. The concept is derived and applied in much the same way that the concept of “sweep efficiency” has been for secondary and tertiary enhanced oil recovery (EOR) operations.

The Energy & Environmental Research Center (EERC) has conducted a number of activities that have resulted in a series of storage coefficients that can be applied to the estimation of CO₂ storage resource/capacity for a variety of geological formations. Specifically, storage coefficients have been developed for saline formations at scales ranging from site-specific locations to entire formations. These coefficients can be used to estimate storage resource for large sedimentary basins and, ultimately, entire nations and continents.

To develop realistic, broadly applicable storage coefficients, several key issues have been addressed, including the various trapping mechanisms, the temporal nature of those mechanisms,

and the effects of scale on data density and, therefore, assessment strategies. The development of storage coefficients has considered each of the key trapping mechanisms (dissolution, mineralization, and physical trapping of the gas phase) at assessment scales ranging from the local to the continental. The application of coefficients will provide stakeholders and decision makers with a means by which key technical factors that will affect the capacity of a geologic formation to store CO₂ can be considered on a defensible, mathematically consistent basis.

Storage resource/capacity estimates are critical components of the myriads of information that are required for stakeholders and policy makers to make informed decisions regarding the potential implementation of large-scale CO₂ storage as a means of reducing GHGs. As previously mentioned, a tremendous amount of work has been focused in recent years on developing classification systems and methods for developing estimates of CO₂ storage resource/capacity. In particular, work done under the auspices of the CSLF, DOE, and the Intergovernmental Panel on Climate Change (IPCC), to name a few, offers significant insight regarding a wide variety of technical and nontechnical issues affecting the large-scale storage of CO₂. While previous efforts to qualitatively and quantitatively describe the storage resource/capacity of geological formations have limitations, these works have provided solid foundations upon which the development of broadly applicable storage coefficients can be achieved.

APPROACH

The EERC efforts first focused on identifying the key elements of previous relevant work that could be brought to bear on achieving the goal of developing broadly and consistently applicable storage coefficients. Storage resource classification and estimation schemes historically used by the U.S. Geological Survey (USGS), Petroleum Resource Management System (PRMS), and mining industry to assess the existence of hydrocarbon and mineral resources, as well as CO₂-specific storage classification and estimation schemes proposed by the CSLF, DOE, USGS, and the Cooperative Research Centre for Greenhouse Gas Technologies (CO₂CRC) were examined and evaluated. These classification and estimation schemes were considered with respect to their applicability to both hydrocarbon reservoirs and saline formations. The next step was to determine the parameters and factors that would affect the storage coefficient and, as a result, the estimation of the potential storage of any given assessment area. To determine the effect of different parameters, the EERC drew upon the previous literature and ran a series of numerical simulations using models of different types of sedimentary rock formations under several types of structural settings. These examinations and subsequent computer modeling and simulation work led to clarifications of the effects of different key parameters on CO₂ storage under a broad range of geological conditions. The ultimate culmination of these efforts was 1) the identification and refinement of equations for estimating CO₂ storage resources for hydrocarbon reservoirs and saline formations; 2) the development of coefficient values for such systems, representing a wide variety of geological features at scales ranging from small to very large; and 3) an approach for utilizing those equations and coefficients toward the development of technically defensible and consistent storage resource/capacity estimates.

Key Concepts and Terminology

The description and application of key concepts and terminology often differ from discipline to discipline and sometimes even from paper to paper within the same discipline. Since CCS is by its nature a cross-disciplinary subject of study, it is important to carefully define the meanings and applications of the key terms used throughout this paper.

Processes and Timescale for CO₂ Storage

CO₂ Storage Targets

There are three primary geologic CO₂ storage targets: deep saline formations (sometimes referred to as “brine formations”), hydrocarbon reservoirs (often referred to as “oil and gas fields”), and unminable coal seams.

Deep Saline Formations

Deep saline formations are defined as porous and permeable sedimentary rock formations which are 1) located at a depth where injected CO₂ would be a dense liquid or supercritical fluid, 2) the formation water total dissolved solids (TDS) are above a level where the local regulations consider the water as nonpotable (brine), and 3) the formation is overlain by a thick regionally extensive impermeable cap rock that will prevent migration of injected CO₂ into potential underground sources of drinking water. CO₂ storage in saline formations is generally limited to depths greater than 800 meters (2625 ft), since it is assumed under most thermal and pressure gradients that the CO₂ will exist in either the dense liquid or supercritical fluid phase (DOE, 2008). This cutoff is not designed to preclude any potential storage projects shallower than 800 meters but is rather a recognition that because of the low density of the injected CO₂, likely in gas phase, that it would not contribute significantly to overall storage mass of CO₂. Deep saline formations exist around the world in sedimentary basins and have the largest potential for storage of anthropogenic CO₂ because of their large pore volume and spatial distribution (Figure 1).

Hydrocarbon Reservoirs

Generally speaking, from a geologic standpoint, hydrocarbon reservoirs may be considered to be a subset of deep saline formations. Hydrocarbon reservoirs are areas of porosity and permeability within a sedimentary rock formation where petroleum and/or natural gas have naturally accumulated. These accumulations are typically caused by migration of the hydrocarbons into a structural, stratigraphic, or hydrodynamic trap. Hydrocarbon reservoirs are most often found within sedimentary basins or on their margins, and the reservoirs themselves occur within many of the same rock units that are considered to be deep saline formations. Hydrocarbon reservoirs are excellent candidate locations for large-scale storage of CO₂ for several reasons. Because of the historical systematic collection of a wide variety of geological, geochemical, geomechanical, and geophysical data over the course of hydrocarbon exploration and production operations, there is typically a very good understanding of the geologic properties

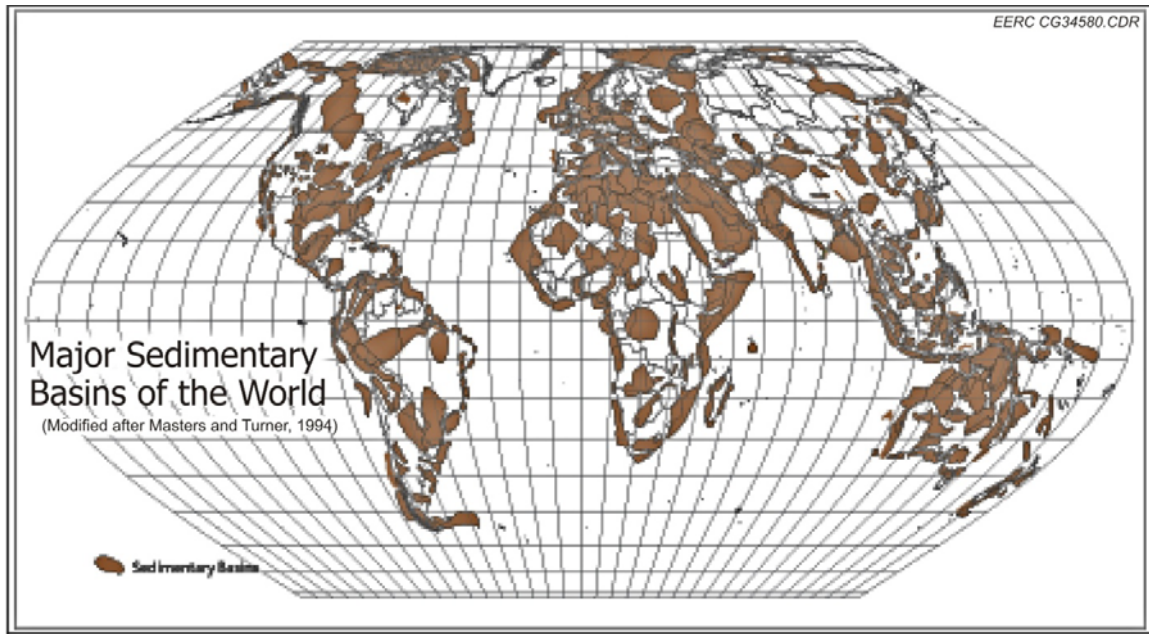


Figure 1. General outline of the major sedimentary basins around the world (from USGS, 2009).

of individual petroleum reservoir systems, leading to greater certainty of storage potential. In short, the primary basis for the current understanding of the geology of the world’s sedimentary basins, including most of what is known about deep saline formations, is the data generated by the search for and extraction of oil and gas over the last century. The presence of hydrocarbons in these rock units is a strong indicator of competent seals and suggests the potential for secure CO₂ storage over geological time periods. Depleted hydrocarbon reservoirs may be particularly effective and attractive locations for large-scale CO₂ storage because of lower reservoir pressure as a result of decades of production and may yield increased storage potential compared to deep saline formations in compartmentalized reservoirs. Perhaps most significantly from an economic point of view, the production of some residual oil and gas through EOR or enhanced gas recovery (EGR) can be used to offset the costs of CO₂ capture, compression, and transportation infrastructure. In hydrocarbon reservoirs, the primary trapping mechanisms are structural and/or stratigraphic, and there could also be significant solubility trapping in both the hydrocarbon phase and the water phase. Mineral trapping and residual gas trapping may take place, but these won’t likely become significant until after the end of injection.

Unminable Coal Seams

An unminable coal seam is a coal seam that is considered to be too thin, too deep, of too low quality, or a combination of all three of these factors, to be economically mined by today’s standards. Because of the wide variety of site-specific variables that may go into determining what is “economical” with respect to mining, the depth and thickness of what is considered to be unminable may vary significantly from location to location. With respect to CO₂, the primary trapping mechanism in unminable coal seams is adsorption. In relation to hydrocarbon reservoirs and saline formations, coal seams are unique targets for geologic storage of CO₂. In addition to

the adsorptive qualities of coal with respect to CO₂, coal seams are typically too shallow to allow for the injection of supercritical CO₂, which dramatically limits the efficiency of injection. Coal seams also often contain water that is less than 10,000 ppm TDS and are therefore considered in some jurisdictions to be potential underground sources of drinking water. Because of these factors, any efforts to develop storage coefficients for coal would have to focus on entirely different sets of geological, geochemical, and engineering parameters than for deep saline formations and hydrocarbon reservoirs. With this in mind, it was decided very early on in the development of this study to exclude coal seams from the scope of work.

CO₂ Storage Mechanisms in Geologic Formations

CO₂ storage in geologic formations is achieved through injection into a permeable formation, where it is trapped by a number of physical and geochemical processes (IPCC, 2005). Injected CO₂ can be physically trapped in a structural or stratigraphic closure or as residual gas due to relative permeability hysteresis. Geochemically, CO₂ can be trapped by adsorption onto organic material or through dissolution into the formation brine (solubility trapping), where it can interact with the rock matrix and eventually precipitate into stable carbonate minerals (mineral trapping) (IPCC, 2005). Hydrodynamic trapping of CO₂ is a process that is affected by a complex combination of the physical and geochemical trapping mechanisms. Each of the trapping mechanisms and processes takes place on a different timescale and, as such, has a different degree of importance at different scales.

Physical Trapping

Physical trapping occurs when CO₂ is injected below a regionally extensive low-permeability or impermeable cap rock, such as a shale or evaporite unit, and is contained within a structural or stratigraphic enclosure. Structural features that may act as traps include folded, fractured, or faulted rock that prevents lateral movement of buoyant CO₂ plumes. Some of the more common structural traps include domes, anticlines, and faults. Stratigraphic traps are physical traps that occur in sedimentary formations that are characterized by changes in depositional environment that affect the porosity and/or permeability of the formation. Examples of stratigraphic traps include formation pinch outs, transitional areas between facies within a formation, and postdepositional remineralization of a formation (e.g., dolomitization of carbonates, secondary cementation of clastics).

Residual Gas Trapping

Residual gas trapping occurs when free-phase CO₂ becomes physically trapped in pore spaces because of relative permeability hysteresis. Hysteresis is a two-part process whereby in the first part, as the CO₂ is injected, it displaces the formation fluid (brine or hydrocarbon). After the injection operation ends, the brine that was displaced during the active injection (a process referred to as “drainage”) is able to move back in (a process referred to as “imbibition”) and traps a portion of the retreating gas. This trapped gas is referred to as residual gas. This process occurs as long as the free-phase CO₂ is moving away from the initial injection point. Therefore, residual gas trapping does not play a major role in the trapping process until after the injection ends.

Solubility Trapping

Solubility trapping occurs as soon as the CO₂ starts mixing with the formation brine, and the amount of CO₂ that is dissolved is a function of the formation pressure, temperature, and water salinity. Solubility trapping is a time-dependent process, and the rate at which CO₂ mixes with unsaturated formation brine is a function of the contact surface between the free-phase CO₂ and the unsaturated formation brine. When CO₂ dissolves into and saturates the formation brine, it becomes approximately 1% denser than the unsaturated brine. This creates a density inversion, and over time, a convective mixing process may develop, moving the saturated formation brine down and away from the free-phase CO₂ and bringing unsaturated brine in contact with free-phase CO₂ (Ennis-King and Paterson, 2005). On the mid- to long-term timescale, solubility trapping can become one of the most important trapping mechanisms; however, on a short-term timescale, particularly during the injection period, the effects of solubility trapping are usually rather small.

Mineral Trapping

Mineral trapping is the process by which geochemical interactions between injected CO₂, formation fluids, and rock matrix result in the precipitation of stable minerals. Mineral precipitation is the most secure trapping mechanism but is also the least understood. While there is a fairly good understanding of the mineral interactions in the laboratory, the effects of the complex mineralogy and mixing conditions in situ are poorly known, and it is believed that mineral trapping will only become important on a long-term timescale, on the order of tens to perhaps many thousands of years (CSLF, 2005; IPCC, 2005).

Hydrodynamic Trapping

CO₂ can also be trapped hydrodynamically; in this case, CO₂ is injected into a formation where there are no large structural or stratigraphic closures to contain it laterally (IPCC, 2005). The injected CO₂ moves away from the source, both upwards until it contacts the cap rock and laterally until natural formation hydrostatic pressure or fluid flow outweighs the pressure required to keep CO₂ mobile. At this point, the CO₂ has very low to zero velocity, effectively kept immobile by the lateral pressure confinement and overlying sealing formation, where it is eventually trapped by the previously mentioned processes (Bradshaw and others, 2007).

During the injection period and immediately thereafter, the primary trapping mechanism is physical trapping either in stratigraphic or structural traps. In the absence of a significant trap, hydrodynamic trapping will be the primary trapping process.

All of these mechanisms, and the complex interactions they have with each other over the lifespan of a CCS project and beyond, must be carefully taken into consideration when developing storage coefficients. Each of the different trapping mechanisms plays a different role depending on the type of hydrogeologic system and/or trap into which the CO₂ is injected. For instance, in a stratigraphic or structural closure underlain by an open hydrogeologic system (such as may occur in large intracratonic basins), the primary mechanisms for storage over the short-term early phase of storage will be physical trapping, while solubility and mineral trapping can

become more important over the long-term as convective mixing begins to take place. Also, in the case of structural or stratigraphic trapping, where the CO₂ was injected directly into the closure, residual gas trapping may never become a major trapping mechanism, as the brine may never imbibe back into the zones that were drained of brine as the CO₂ was injected. If the structural or stratigraphic trap is a sealed compartment that is a closed hydrogeological system, such as may be found in a fault-bounded area within an intermontane basin, then physical trapping will be the primary storage mechanism over both the short- and the long-term time frames. This is because most of the injected CO₂ will stay in the free phase as the brine that is in the closure will reach saturation relatively quickly because of a lack of new, unsaturated brine moving in to replace the more dense, saturated brine. Formations which contain these compartmentalized closed systems will likely have limited storage, as there will be limited displacement of formation fluids and the maximum injection pressures will limit the injected volume very quickly. Ideally, the best locations within closed systems for large-scale CO₂ storage may be depleted hydrocarbon reservoirs, which have extra storage volume in the form of reduced formation pressure caused by decades of oil and/or gas production. If the injection takes place in an open system, then hydrodynamic and residual trapping becomes very important in the short to long term as the free-phase CO₂ moves through the formation. Solubility and mineral trapping will also play a larger role in open systems as the free-phase CO₂ will contact more unsaturated formation brine, creating more mixing, sooner after injection. In an open hydrogeologic system, there will also be some degree of structural and stratigraphic trapping as the free-phase CO₂ moves along the cap rock and gets caught in small, local closures.

When it comes to determining CO₂ storage resource/capacity, of primary importance are the processes that take place on the short- to midterm time frames, particularly during the active injection period. These processes vary depending on the target, but in most cases, the primary short-term trapping mechanisms are physical and hydrodynamic. In the cases where hydrodynamic trapping prevails, solubility trapping increases as a result of the free-phase CO₂ contacting more unsaturated brine; however, solubility trapping will in most cases represent only a small portion of the trapped gas and, as such, will not significantly contribute to storage resource/capacity. Residual gas trapping and mineral trapping also do not significantly add to the overall storage resource/capacity of a target formation but rather increase the security of the trapping. Figures 2 and 3 graphically illustrate the relative contribution that each mechanism makes to CO₂ storage and the relative time frames within which each generally occurs. The storage coefficients that were developed as a result of this project take into account physical, hydrodynamic, solubility, and residual gas trapping. However, because of the complex nature of mineral trapping and the unknowns associated with it, mineral trapping was not considered as part of the development of the storage coefficients.

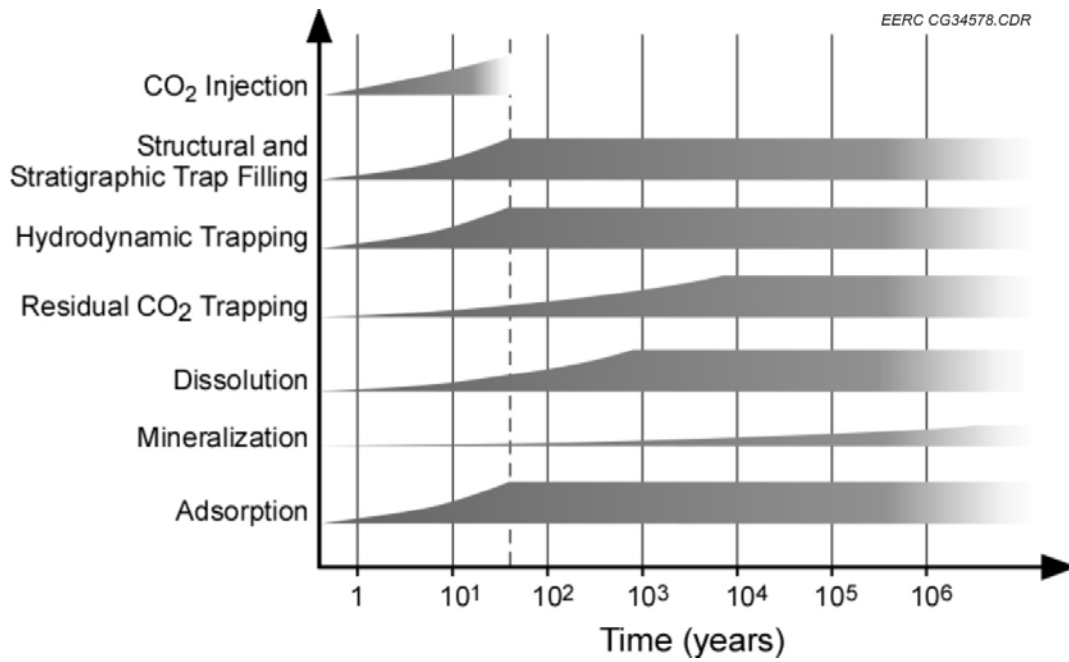


Figure 2. The operating time of the physical and geochemical processes which trap CO₂ in geologic formations (IPCC, 2005).

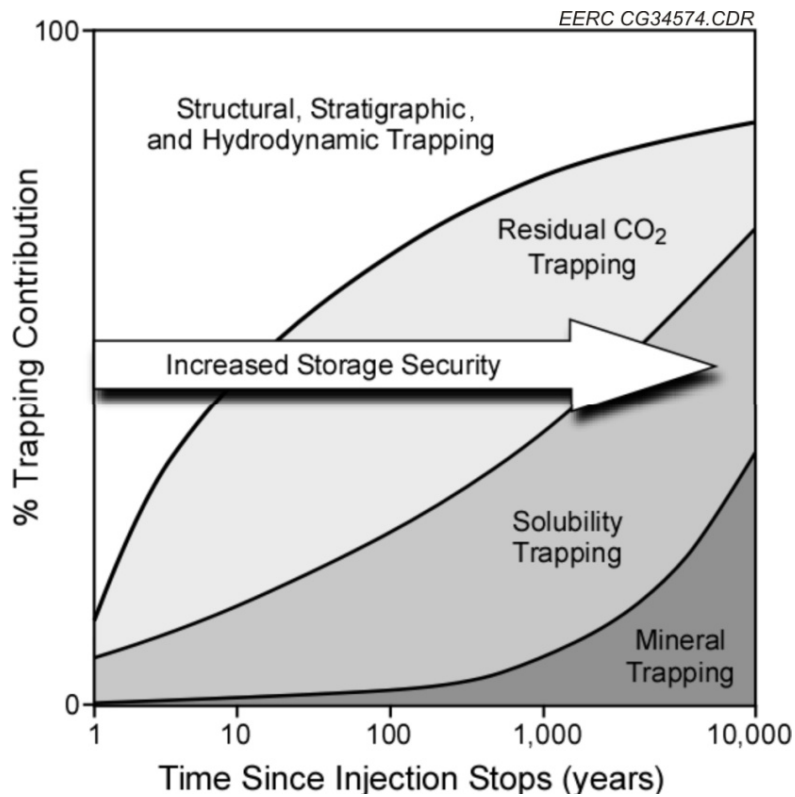


Figure 3. Storage security of the different trapping mechanisms and their relationship with time (IPCC, 2005).

Resource/Capacity Concept

To date, the classification of resources and commodities has been used almost exclusively for valuable materials that can be economically extracted from the subsurface, e.g., hydrocarbons, metal ore, coal, etc. These industries have benefited from the establishment of classification systems with consistent terms and definitions that have gained international acceptance. As the CCS industry grows, there is increasing need for an accepted classification system that describes the available CO₂ storage resource. As described above, three types of storage sites are considered technically suitable: saline formations, hydrocarbon reservoirs, and unminable coal seams. Two of these types of geological media have been exploited for resources for centuries, i.e., by the petroleum and mining industries. These industries have well-established resource classification systems that allow for systematic accounting and comparison of resources across geological, geographical, and jurisdictional boundaries. The use of similar reservoir types, as well as the wide acceptance of the previously mentioned classification systems, has led to several attempts to adapt them for use in CO₂ storage. Some of the more prominently referenced resource classification systems that were evaluated as part of this study include 1) the PRMS, which is a resource classification system and joint terminology set shared between the Society of Petroleum Engineers (SPE), American Association of Petroleum Geologists (AAPG), World Petroleum Council (WPC), and Society of Petroleum Evaluation Engineers (SPEE) and which has been widely accepted internationally and has been used for many years by the petroleum industry (SPE and others, 2007); 2) the USGS series of Oil and Gas Resource Assessments for geological provinces, which are based on a system of definitions for resource and reserve estimations along with a conceptual model which is similar to the PRMS; 3) the USGS Coal Resource Classification System, which is designed to quantify the total amounts of coal in the ground before mining began (original resources), that which remains after any mining (remaining resources), the amounts of coal that are known (identified resources), and the amounts of coal that remain to be discovered (undiscovered resources). While each of these classification systems had elements that were instructive and sometimes indirectly applicable with respect to CO₂, the direct application of those systems is largely insufficient. This is because, in the context of geological CO₂ storage, the desired resource is not something to be removed from a subsurface reservoir but rather the accessible pore volume of the reservoir itself.

There are two major aspects of the general resource classification systems defined by the PRMS, the USGS, and the mining industry that prevent them from being directly useful in describing CO₂ storage resources and capacity. The first difference is noticed when considering economics and commerciality of the project in question. The resource classification systems of the PRMS, USGS, and mining industries are implemented by industries where it is not only economically feasible but profitable to extract the resources described, e.g., hydrocarbons, metal ore, etc. The early nature of the CO₂ storage industry and the lack of a carbon market make it difficult to consider the economic feasibility and profitability of such projects.

The second area where the general resource classification systems fall short in their applicability to the CCS industry is observed when discussing “undiscovered” resources. For instance, the PRMS explicitly defines undiscovered resources, indicating oil and gas reservoirs that could exist but have yet to be discovered (SPE and others, 2007). In the case of CCS, undiscovered storage resource becomes ambiguous. While it could be argued that undiscovered

oil and gas reservoirs as defined by the PRMS could be potential storage sites for CO₂, the same cannot be said about saline formations. Thus a classification system designed specifically for CO₂ storage is desirable.

With that in mind, four different CO₂ storage classification systems that have been developed in recent years were examined as part of this study: 1) the Techno-Economic Resource-Reserve pyramid developed by the CSLF, based on an approach that is hereby referred to as the CSLF method for estimating CO₂ storage potential; 2) the DOE classification system developed for use in the Carbon Sequestration Atlas of the United States and Canada published by DOE, using an approach that will be referred to in this report as the DOE method; 3) a probabilistic assessment methodology developed by the USGS; and 4) a classification system proposed by the CO₂CRC. Each of these systems is described in detail in published or soon-to-be published reports. With respect to the USGS and CO₂CRC approaches, a detailed description of each was determined to be not necessarily constructive in the context of the goals of this report. However, over the course of this project, it was decided that the CSLF and DOE methods were most amenable to the development and application of storage coefficients, and therefore, further description and discussion of those classification systems in the context of storage coefficients are warranted and presented below. Finally, based on the results of examining and evaluating the various existing classification systems and on the identification of elements considered to be critical to the development of broadly applicable storage coefficients, a new classification system was developed, which is also presented in the next section.

CO₂ Storage Resource Classification and Estimation Systems

CSLF

The Techno-Economic Resource-Reserve pyramid defined and adapted by the CSLF has strong applications in CCS terminology and to the direction of future developments. The pyramid itself is a graphical representation of terms that shows the trend from broad-based capacity estimations to small-scale site-specific characterizations. The CSLF Techno-Economic Resource-Reserve pyramid shows how storage capacity can be divided into a number of subsets. Moving up the pyramid requires applying increasing constraints (e.g., technical) to the CO₂ storage capacity, as defined by the CSLF. Figure 4 shows the CSLF Resource-Reserve pyramid.

The CSLF provides definitions for resources and reserves in its CO₂ storage capacity classification system; however, these are generic definitions similar to those used by the petroleum industry and are not specific to CO₂ storage (CSLF, 2007).

Theoretical capacity makes up the whole resource pyramid and represents the upper limit of storage capacity. Theoretical storage capacity assumes the entire pore volume can be utilized to its maximum capability. In practice, theoretical capacity is unrealistic because of technical and economic factors. The CSLF defines a capacity coefficient that is a combination of the technical factors that could limit the storage capacity. By applying this coefficient to the theoretical capacity, effective storage capacity can be estimated. Moving further up the pyramid, i.e., from effective to practical and practical to matched, involves the consideration of economic factors

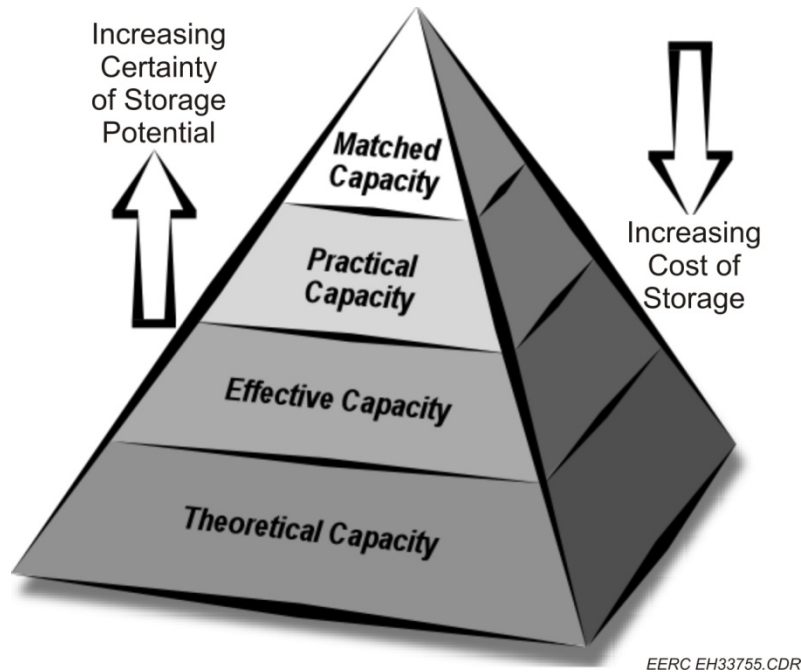


Figure 4. CSLF Techno-Economic Resource-Reserve pyramid (CSLF, 2007).

and the matching of CO₂ sources with storage sites respectively. Because of the early nature of the CCS industry and the lack of a well-established carbon market, the application of economics to storage capacity estimates is impractical on a broad level. As a result, the practical and matched capacities cannot be estimated except on a case-by-case basis.

In addition to the Techno-Economic Resource-Reserve pyramid, the CSLF presents a list of definitions representing the size of the geographical area in an assessment project. These definitions explain the amount of information required to perform a capacity estimate at that scale. The five terms defined by the CSLF in its Phase 2 Final Report are country, basin, region, local, and site (CSLF, 2007).

DOE

In 2007, DOE released the first edition of the Carbon Sequestration Atlas of the United States and Canada (DOE, 2007). This document provides an overview of CO₂ storage as a climate change mitigation technique and examines the national and regional perspectives for implementing CCS. An appendix presents a discussion of developing storage capacity estimates for CO₂, but no classification system or definitions are given.

An updated Atlas was released in 2008, along with an updated appendix on storage resource (DOE, 2008). In this second edition, DOE defines some terms useful for CO₂ resource classification. Although there are only a few general terms (e.g., resource, capacity), they are advantageous in that they are defined specifically for use within the CCS industry.

Resource is defined as the pore volume of sedimentary rocks available for CO₂ storage. Resource estimates consider only physical and chemical constraints; while *capacity* is considered to be a resource with economic and regulatory constraints, applied (DOE, 2008). These definitions are useful; however, additional terms need to be developed by the CCS industry to capture the complexity involved in estimating the CO₂ storage resource or capacity in a geological formation, and DOE does not make any further refinements, leaving that to the CCS industry (DOE, 2008). There are several technical limitations, including engineering capabilities, physical processes, etc., which limit the actual storage resource or capacity available. Although the technical constraints are considered in the DOE definition of storage resource, it is useful to have definitions which reflect refinement in estimated resource after applying these constraints. In addition, although the early nature of the CCS industry limits the applicability of economic factors to resource and capacity estimations, they will eventually become necessary considerations, and classifications that reflect these limitations will be useful.

Proposed New Classification System

Several groups have defined CO₂ storage resource and capacity terminology by utilizing terminology already established in the petroleum industry and by developing unique expressions (IEA-GHG, 2008). Although much work has been accomplished, inconsistencies in definitions related to CCS exist between groups, and a widely accepted set of definitions for discussing CO₂ storage resource and capacity has not yet been established. Thus to move the CCS industry toward a useful set of definitions and provide a consistent set of terms for use within this document, the authors suggest an improved classification system by building on the work already accomplished by DOE (2008), CSLF (2007), SPE and others (2007), and CO₂CRC (IEA-GHG, 2008).

It is important to understand the difference between resource and reserve as used by the petroleum industry and the CO₂ storage industry. As stated earlier, a major difference is the commercial and economic aspects of the respective industries. Resources, as defined by the petroleum industry, have a historically established commercial incentive, whereas the storage resource for the young CCS industry does not. Therefore, explicit definitions for resource and capacity are given which relate specifically to CO₂ storage; these definitions are equivalent to those presented by DOE (2008). Following the example of CSLF, several subsets of storage resources are created by applying various constraints (e.g., physical, technical, economic) to the theoretical storage resource. The subdivisions of theoretical storage resources include characterized, effective, unusable, uncharacterized and contingent resources and practical storage capacities. Figure 5 shows the proposed CO₂ storage classification framework.

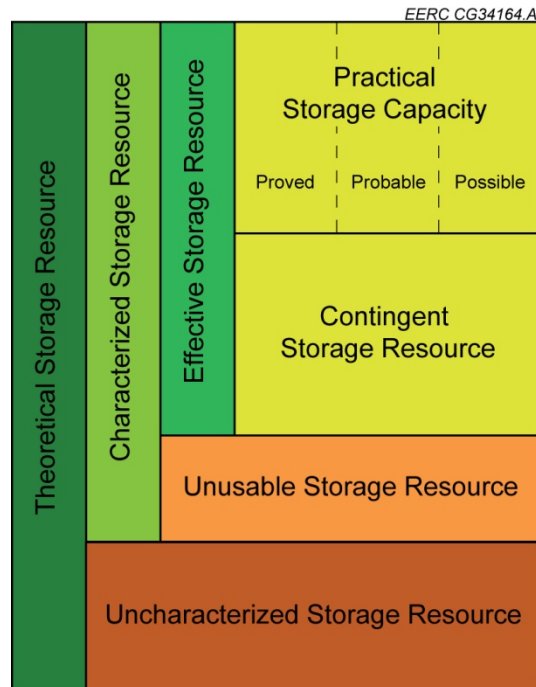


Figure 5. Proposed CO₂ storage classification framework.

The proposed CO₂ storage classification framework begins with theoretical storage resource. This represents the absolute total pore volume within a rock formation or geologic storage target after fundamental formation characteristics are taken into account. There are no restrictions or constraints put on this estimate, and as a result, this level of resource is a theoretical maximum that is an unrealistically high value. The first division of theoretical storage resource (characterized) considers only the pore volume in known (i.e., well-characterized) reservoirs and formations. CSLF accounts for these two definitions in their theoretical storage capacity. This is accomplished by using two equations, one which takes into account spatial variability of porosity and irreducible water saturation proposed (i.e., knowledge obtained by characterizing the site), and one neglecting this variability. This division improves on the CSLF pyramid by explicitly accounting for resources that are in characterized reservoirs and subsequently those that are uncharacterized. The next level of resource estimate (effective storage resource) further refines the estimate by considering the technical (geological and engineering) limitations. This is equivalent to CSLF’s definition of effective storage capacity, although here it is defined as a resource and not a capacity since economic considerations have not been implemented. Once technical constraints have been observed, a further refinement can be made by considering economic limitations. This is defined as practical storage capacity and is equivalent to the practical storage capacity of CSLF. It should be noted that in the proposed classification system, the storage resource becomes a storage capacity once economic conditions have been considered. An important distinction is made between storage resource that is viable under current economic conditions (practical) versus future economic conditions (contingent). The authors acknowledge that the early nature of CCS and absence of a well-established carbon market make the estimation of storage capacities that consider economics (i.e., practical and

contingent) impractical; however, it is useful to define such classifications since economic and commercial implications can be considered as the industry matures.

When performing CO₂ storage resource/capacity estimates, it is useful to begin on a large scale, such as a basin or region, and refine the estimate to a specific formation or site. This reflects the fact that in the early stages of a project, the level of detail of available information may be low and will increase as a project matures. To account for this, it is necessary to have multiple scales of assessment that can be considered. This requires a spatial distribution to be established for each level of assessment. CSLF states that the methodology to be applied in estimating the storage capacity, as well as the required level of detail for the necessary data, will vary depending on the scale of the assessment (CSLF, 2007). CSLF goes on to define five levels of assessment: country, basin, regional, local, and site (in increasing level of detail). The CSLF scale definitions are a valuable approach; however, they may be difficult to use in some situations, such as in the case where a basin extends into multiple countries. As a result, the authors seek to resolve the potential confusion by proposing two categories for the scale of assessment. The pyramid in Figure 6 illustrates the two proposed categories. One face represents the *political* and *geographical* boundaries, and the other represents *physical* and *geological* boundaries. This division is meant to show the difference in types of assessment areas and not necessarily the relationship of scale between them. Figure 6 also shows how the boundaries, if not considered in separate categories, can sometimes be ambiguous, e.g., a basin can encompass a country, region, and state. As the assessment area becomes smaller (i.e., the scale of the assessment becomes smaller), both sides of the pyramid share the same boundary terms, local and site. Another thing to notice is that as the spatial area of assessment becomes smaller, the confidence in the resource or capacity estimate increases. This is due largely to the increasing quality and quantity of data that can be acquired through geological characterization of a smaller area.

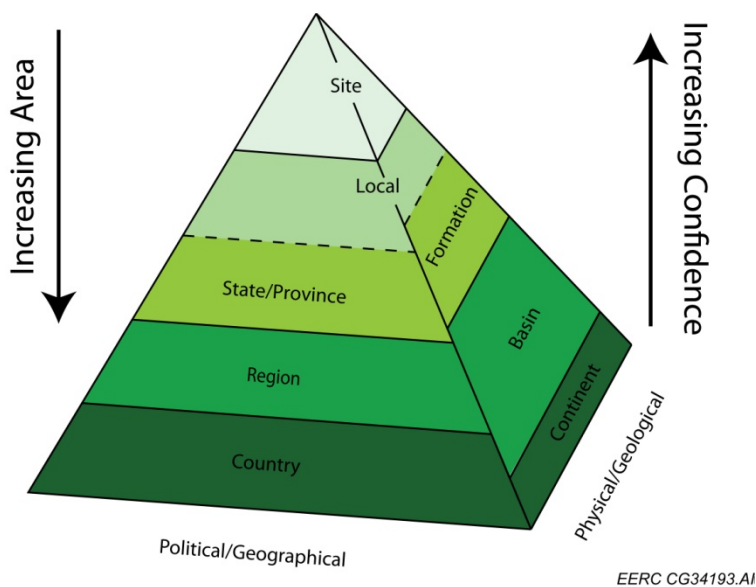


Figure 6. Political/geographical, physical/geological pyramid, illustrating differences between assessment area types.

Definitions

The terms and classifications for the proposed CO₂ resource and capacity classification system are shown in Figure 5 and the descriptions of the spatial boundary terms in Figure 6.

General Terms with Respect to the Proposed Classification System

Resource – Is used to describe the available pore volume of a rock formation being considered for CO₂ storage which is accessible to injected CO₂ via drilled and completed wellbores. Because of uncertainties inherent in subsurface evaluation, exact quantification of geological properties is not possible, and therefore, storage resource is always at best an approximation (modified from DOE, 2008, and IEA-GHG, 2008).

Capacity – Is the volume of CO₂ that can be stored in a given formation once technical and economic constraints have been applied to the storage resource. This is a subset of the theoretical resource of subsurface geologic reservoirs.

Specific Terms with Respect to the Proposed Classification System

Theoretical Storage Resource – Is the upper limit of storage resource and includes pore volume that can be used to store CO₂ in separate phase, dissolved phase, and mineral phase. In practice for any given area, this is an unrealistically high number because physical, technical, regulatory, and economic restrictions will always limit the full utilization of available pore space (modified from IEA-GHG, 2008).

Characterized Storage Resource – A subset of theoretical storage resource, characterized storage resource includes only known (i.e., well-characterized) storage sites.

Effective Storage Resource – A resource that can be estimated after technical (geological and engineering) constraints have been applied to characterized storage resource. Effective storage resource is the pore volume in known (i.e., well-characterized) storage sites into which it is technically feasible to inject and store CO₂.

Practical Storage Capacity – The storage capacity that can be estimated by applying economic constraints to the effective storage resource. The practical storage capacity is an estimate of that volume of CO₂ which could be technically and commercially injected and sustainably stored in known (i.e., well-characterized) storage sites from a given date forward. Practical storage capacity can be separated into proved, proved plus probable, and proved plus probable plus possible categories following petroleum industry standards. In general, storage capacity should not be classified as practical unless there is an expectation that the CO₂ will be injected into a developed storage site within a “reasonable time frame.” The definitions of “commercial” and “technically feasible” for a storage site will vary according to local conditions and circumstances and is left to the discretion of the operator or jurisdictional (country/state) authority concerned. The early nature of CCS and the absence of a carbon market make the estimation of practical storage capacity difficult to apply on a uniform basis. As the industry

matures, however, economic and commercial implications can be considered (modified from IEA-GHG, 2008).

Proved Storage Capacity – The volume of CO₂ that can be estimated with reasonable certainty to be commercially feasible to inject into known (i.e., well-characterized) storage sites. Estimates of proved storage capacity incorporate analysis of geosciences and engineering data from under defined economic conditions, operating methods, and government regulations; they are limited to that which is commercial under current technoeconomic conditions. In general, proved practical storage capacity is the subset of storage capacity applicable to bankable storage projects. The early nature of CCS and the absence of a carbon market make the estimation of proved practical storage capacity difficult to apply on a uniform basis. As the industry matures, however, economic and commercial implications can be considered (modified from IEA-GHG, 2008).

Probable and Possible Storage Capacity – Capacity based on anticipated future economic conditions; expected to be injected within a “reasonable time frame” (IEA-GHG, 2008).

Contingent Storage Resource – A subset of effective storage resource. Volume of CO₂ which is estimated to be technically feasible for injection into known (i.e., well-characterized) storage sites; however, it is only economically feasible based on anticipated future economic conditions. It is recognized that some ambiguity may exist between the definitions of contingent storage resource and probable and possible practical storage capacity. It is recommended that if the storage site is not expected to be developed and have CO₂ injection within a “reasonable time frame,” then the estimated injectable CO₂ volume for the site should be classified as contingent storage resource (modified from IEA-GHG, 2008).

Unusable Storage Resource – A subset of characterized storage resource. Unusable storage resource is the pore volume that exists in known (i.e., well-characterized) storage sites but is unavailable for injection of CO₂ because of current technical conditions.

Uncharacterized Storage Resource – Pore volume that is a subset of theoretical; unknown pore volume in a package of rocks that are known to exist and are assumed to have some level of injectivity although little or no rock property data exist. Injection will occur at some future date “after characterization.” While it is recognized that storage resource may exist within uncharacterized storage sites, it is difficult to assign a value to the estimate of CO₂ that could be stored in these sites. As such, it is recommended that uncharacterized storage resource not be included in resource estimates, with the understanding that those estimates may be conservative pending the characterization of the pore volume (modified from CO₂CRC, 2008, and IEA-GHG, 2008).

Storage Coefficients – The multiplicative combination of volumetric parameters that reflect the portion of a basin’s or region’s total pore volume that CO₂ is expected to actually contact (DOE, 2008). The storage coefficient, referred to as the storage efficiency factor (E) in the Carbon Sequestration Atlas of the United States and Canada (DOE, 2007, 2008) and the capacity coefficient (C_C) by CSLF (CSLF, 2007), represents the fraction of the accessible pore

space that can be contacted by injected CO₂. For the purposes of this paper, both DOE's storage efficiency factor and CSLF's capacity coefficient will be referred to as storage coefficients.

Political/Geographical Terms

Country – A contiguous geographic area defined by national jurisdiction which can encompass several sedimentary basins and/or parts thereof if a basin is shared between two or more jurisdictions (CSLF, 2007).

Region – A large, geographically contiguous portion of a sedimentary basin, usually defined by the presence of large CO₂ sources and/or by its known large potential for CO₂ storage (CSLF, 2007).

State/Province – Subset of a region, with unique borders and a smaller-scale jurisdiction; territory, parish, district, or some other equivalent can also be used.

Local – A locality is an area that encompasses a manageable collection of injection wells that share a common geological feature and/or injection scheme. This is similar to a unitized oil field.

Site – A geographically contiguous entity comprising leased or owned land, buildings, and other structures required to perform CO₂ storage activities (modified from DOE Glossary, 2009). In many cases, a site is considered to be a single injection well.

Physical/Geological Terms

Continent – One of the seven large divisions of land on the earth, e.g., North America (Merriam-Webster, 2009).

Basin – A geologic structure of tectonic origin containing a unique sequence of sedimentary rocks that are dissimilar to those outside the basin (Hyne, 2006).

Formation – A mappable layer of sedimentary rocks. A formation has a sharp top and bottom boundary and is often the unit of rock shown on a geologic map (Hyne, 2006).

Local – A locality is a manageable collection of injection wells that share a common injection scheme. This is similar to a unitized oil field.

Site – A geographically contiguous entity comprising leased or owned land, buildings, and other structures required to perform CO₂ storage activities (modified from the DOE Glossary, 2009). In many cases, a site is considered to be a single injection well.

CO₂ STORAGE RESOURCE ESTIMATION IN DEPLETED HYDROCARBON RESERVOIRS

Oil and gas reservoirs are naturally the first consideration for large-scale CO₂ storage. Because most hydrocarbon reservoirs have a long history of exploration and production, it is likely that information regarding site characterization and infrastructure (wells, roads, pipelines, etc.) are already likely to be in place. In addition, the accumulation of hydrocarbons suggests the presence of a sufficient cap rock and trap conditions that are proven to prevent flow for millions of years. As a result, as long as the historic field data are available, these depleted hydrocarbon reservoirs should be considered a characterized resource. A depleted hydrocarbon reservoir is an accumulation of oil and gas in the subsurface where production has declined to the point that it has become no longer economical to produce using primary or secondary production techniques. Depleted reservoirs are at, near, or past the end of their productive lives and are then candidates for the application of tertiary production operations or CO₂ storage. Methodologies for resource estimation in depleted oil and gas reservoirs have been developed by several entities, most notably DOE and CSLF in their respective publications (DOE, 2008; CLSF, 2007).

DOE and CSLF Methodologies for Depleted Hydrocarbon Reservoirs

The DOE methodology for estimation of storage resources in oil and gas fields is based on a volumetric equation, which states:

$$G_{CO_2} = A * h_n * \phi_e * (1 - S_w) * \rho_{CO_2} * E$$

Where G_{CO_2} is the effective mass estimate of the CO₂ resource, A is the area of assessment for the storage calculation, h_n is the oil and gas column height of the formation, ϕ_e is the average porosity of the formation within the net thickness, S_w is the average water saturation within the volume defined by the area and height, ρ_{CO_2} is the density of CO₂ at formation conditions, and E is the storage efficiency factor, which also includes the recovery factor. In essence, this equation delineates the volume of a trap, then develops a mass of CO₂ which is the theoretical resource. This value is then multiplied by E to produce an effective resource.

Similarly, the CSLF methodology reports a volumetric equation which states:

$$M_{CO_2T} = \rho_{CO_2r} * [R_f * A * h * \phi * (1 - S_{wirr}) - V_{iw} + V_{pw}]$$

Where M_{CO_2T} is the theoretical, characterized mass of the resource, ρ_{CO_2r} is the density of CO₂ at reservoir conditions, R_f is the recovery factor of the formation, A is the areal extent of the reservoir, h is the thickness of the reservoir, ϕ is the average reservoir porosity, S_w is the average water saturation, V_{iw} is the volume of injected water, and V_{pw} is the volume of produced water. To increase the resource level from theoretical to effective, a capacity coefficient is introduced:

$$M_{CO_2E} = M_{CO_2T} * C_C$$

The two equations are similar, where each calculates the CO₂ storage resource mass by delineating a trap volume, then calculating and converting the mass of CO₂ which can be stored

within that volume. It differs, however, by the inclusion of the recovery factor in the CSLF method, which accounts for the volume of produced or producible hydrocarbons from the reservoir, as well as the injected and produced water terms, which account for pore space that has been freed by fluid removal or may have been saturated through water flooding techniques.

CSLF also reports a separate mass balance equation for gas reservoirs:

$$M_{CO_2T} = \rho_{CO_2r} * R_f * (1 - F_{IG} * OGIP * [(P_s * Z_r * T_r) / (P_r * Z_s * T_s)])$$

And for oil reservoirs:

$$M_{CO_2T} = \rho_{CO_2r} * [R_f * OOIP - V_{iw} + V_{pw}]$$

Where F_{IG} is the fraction of injected gas; the original gas in place is $OGIP$, and P , Z , and T are the pressure, compressibility factors, and temperature, respectively, at the reservoir, r , and surface conditions, s . The original oil in place is $OOIP$ and is represented in reservoir oil volume.

This equation differs from the one proposed by DOE because it is not concerned with the volume of the reservoir, rather relying only on the quantity of the fluids injected and produced, implying a simple reservoir mass balance calculation.

Discussion of the Application of Storage Coefficients to Depleted Hydrocarbon Reservoirs

Fundamentally, there are two approaches to estimating the storage resource for oil and gas reservoirs depending on open or closed boundary conditions. A closed reservoir has become compartmentalized and the flow dynamic has been heavily decreased or completely cut off from the surrounding formation. An open reservoir experiences normal to strong water drive, and fluid flow is unhindered into or out of the trap; this is because it is directly connected to a large saline formation.

A closed reservoir experiences little pressure influence from the surrounding formation, and depletion mechanisms are evident. Therefore, the reservoir will have storage limited to the volume of produced hydrocarbons, and the compressibility of the formation and remaining fluids in response to the pressure increase. For this situation, a mass balance or closed system equation should be used that focuses on the storage space created through these processes.

An open reservoir experiences direct pressure response from the surrounding formation, and water drive processes are evident. These types of reservoirs will have storage limited to the efficiency of the injected CO_2 to displace the pore fluids. A volumetric equation is sufficient for this boundary condition.

Specific estimation of storage coefficients in oil and gas reservoirs becomes extremely complex to apply on a broad scale. This is because many factors are based on site-specific variables such as hydrocarbon chemistry, production history, drive mechanism, and field operation and management. The degree of success experienced through enhanced oil production,

the extreme variability of fluids, and the dynamic nature of the reservoir, as well as the fact that several storage mechanisms are working simultaneously, further complicate the development of broadly applicable storage coefficients for hydrocarbon reservoirs. Regardless of these issues, depleted hydrocarbon reservoirs should still be considered excellent storage targets that will fundamentally behave in a similar fashion to saline formations. Because depleted hydrocarbon reservoirs may be considered a subset of saline formations, it is likely the values and distribution of the storage coefficients used for these reservoirs will approach, but do not directly translate to, those estimated for saline formations with equivalent boundary conditions.

CO₂ STORAGE RESOURCE ESTIMATION IN DEEP SALINE FORMATIONS

Globally, deep saline formations have the largest potential to store anthropogenic CO₂ because of their large pore volume and spatial distribution (See Figure 1 showing world sedimentary basins). However, developing reliable estimates of storage resource/capacity that can be applied to assessments at the site-specific, local, formation, basin, and continent scales is not always straightforward. In some cases, site-specific assessments can be reasonably extrapolated to local- and formation-scale estimates of resource/capacity. An example of such a case may be a large, relatively unfaulted formation with fairly consistent geologic and fluid properties. Such formations may be found in large intracratonic basins that have seen relatively little tectonic activity. In other cases, site-specific assessments cannot be extrapolated to larger scales, but rather, each case must be assessed individually and added together to come up with a cumulative storage resource for the larger assessment area. An example of this may be a formation in a basin that is highly faulted and compartmentalized, such as many intermontane basins. At the heart of this issue is the degree to which the fluids within a formation can communicate between assessment areas inside of the formation.

In most cases, the saline formations have a large extent and for all practical purposes are open or “infinite acting” systems. However, in some cases, the saline formations are compartmentalized by lateral flow boundaries such as low-permeability zones created by changes in pore structure or sealing faults. In these cases, the saline formation would act in a closed or semiclosed manner, as suggested by Zhou and others (2008). One of the first issues to address is what type of boundary conditions exist in the assessment area. This will have a large impact on the injection strategy and dictate what type of resource/capacity estimation technique will be utilized. For the purposes of this work, two scenarios have been considered: 1) a closed system with compartmentalized units in a formation which do not allow any movement of formation fluids out of the assessment area and 2) an open system, where the injection takes place in a large regional system in which formation brine is able to migrate away from the injection point in an infinite acting way, with no formation pressure buildup due to compartmentalization (Zhou and others, 2008) (Figure 7). It is worth noting that semiclosed systems do exist, the characteristics of which may have significant consequences to CO₂ storage security. However, because of the complex nature of these systems, they have not been included in the development of the storage coefficients described in this report.

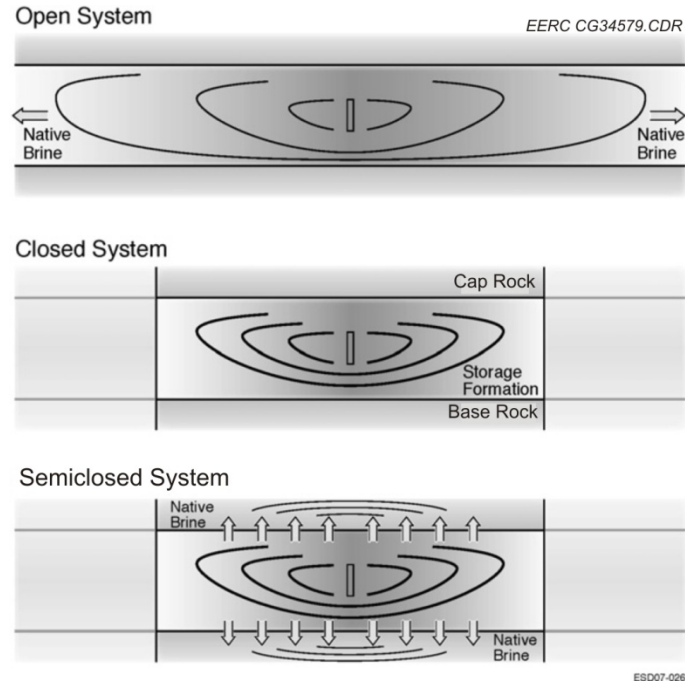


Figure 7. Diagram representing the three potential storage systems (from Zhou and others, 2008).

Closed System

In some regions, the sedimentary basins contain deep saline formations that are highly faulted and compartmentalized, allowing for very little or no formation fluid communication with the surrounding formations. The injection volume in such compartmentalized hydrogeologic systems would be limited by the pressure buildup in the reservoir. This pressure buildup could greatly reduce the total CO₂ storage resource/capacity. The effective storage resource would be limited to the volume created by the compressibility of the pores and formation fluids and the maximum pressure buildup that the formation could sustain without damage. The volume that would be available to store CO₂ in this case could be expressed with the following mathematical expressions developed independently by both Zhou and others (2008) and DOE in the Carbon Sequestration Atlas II of the United States and Canada (2008).

Mathematically, compressibility (c) is defined as:

$$c = -\frac{1}{V_o} * \frac{\partial V}{\partial p}$$

Where V_o is the reference or initial volume and the $\partial V/\partial p$ is the change in the reference volume over some pressure change. The negative sign is to reflect that, in most instances, volume decreases (∂V) with an increase in pressure (∂p). Moreover, the formula is only valid if the rock remains intact; i.e., the rock does not fail mechanically.

The compressibility equation can be written in finite difference form as follows:

$$c = -\frac{1}{V_o} * \frac{\Delta V}{\Delta p}$$

Rearranging and solving for the change in volume (ΔV):

$$\Delta V = -c * V_o * \Delta p$$

In a saline formation consisting of saline water and consolidated rock, water (c_w) and pore compressibility (c_p) are generally the two contributing components to the volumetric change in the formation as a result of a change in pressure. At this point, water volume (V_w) and pore volume (V_p) are separated from the volume term.

$$\begin{aligned}\Delta V_w &= c_w * V_{wo} * \Delta p_w \\ \Delta V_p &= c_p * V_{po} * \Delta p_p\end{aligned}$$

The total change in volume (ΔV_t) is experienced with a consistent pressure increase to the pore and fluid system, which is the sum of the water and pore volume changes.

$$\Delta V_t = \Delta V_{wo} + \Delta V_{po}$$

The volume of water will decrease, and the volume of the pores will increase, with an increase in pressure. If the initial conditions are considered and the changes are then subtracted from the initial case, the negative sign is removed from the compressibility equation.

$$\Delta V_t = c_w * V_{wo} * \Delta p_w + c_p * V_{po} * \Delta p_p$$

In a saline formation, the geologic unit begins at or near 100% water saturation, so the pore volume and water volume begin equal. Likewise, the pore pressure and water pressure are equal. This simplifies the equation to:

$$\Delta V_t = (c_w + c_p) * V_{po} * \Delta p$$

In application in porous media, this pore volume is the effective, connected pore volume.

The storage coefficient, E , is defined as the fraction of the total pore volume most likely accessible to CO_2 . The compressibility concept can be related to E by considering the terms in the equation. If V_{po} is defined as the effective pore volume and ΔV_t is defined as the effective pore volume accessible to CO_2 , E_{comp} can be defined using the compressibility equation as follows:

$$E_{comp} = \frac{\Delta V_t}{V_{po}} = (c_w + c_p) \Delta p$$

$$V_{CO_2comp} = V_{po} * E_{comp}$$

This method is only valid as long as the water flux out of the formation is negligible and the change in pressure does not cause the formation to fail or open a conduit for fluid migration. The storage resource in this case could be increased by producing formation fluids from the saline formation to relieve pressure in the reservoir and create additional storage space.

Open System

In some regions, the sedimentary basins contain deep saline formations that are relatively unfaulted with fairly consistent geologic and fluid properties over a large area. In these areas, the hydrogeologic communication over large areas is such that injection into the formation does not cause a noticeable increase in the formation pressure, and pressure buildup is limited to the near wellbore environment. These are considered to be infinite acting or open systems. Two methods were introduced nearly simultaneously and have been applied by many workers in the CCS field. While other methods have been introduced, the two most often applied systems are the DOE and CSLF methodologies for estimating storage resource in open systems (DOE, 2007, 2008; CSLF, 2007; Bachu and others, 2007). While the CSLF and DOE methods are similar, differences do exist, and in 2008, CSLF released a document which compared the two methods (CSLF, 2008). DOE released an updated version of its methodology document in 2008 (DOE, 2008). A discussion comparing the CSLF and DOE methods is presented below.

CSLF Methodology

The CSLF method is a volumetric approach which calculates a volume of stored CO₂ (V_{CO_2T}) based on a geometric volume of a trap (V_{trap}), porosity (ϕ), the irreducible water saturation (S_{wirr}), and the application of a capacity coefficient (C_c). The CSLF capacity coefficient incorporates the cumulative effects of trap heterogeneity, CO₂ buoyancy, and sweep efficiency. Currently there are no values in the literature for this capacity coefficient (CSLF, 2007).

The CSLF method for calculating theoretical storage resource as follows:

$$V_{CO_2T} = V_{trap} * \phi * (1 - S_{wirr}) = A * h * \phi * (1 - S_{wirr})$$

Where A is the area of the storage trap and h is the average thickness of the trap. If the spatial variability is known, then the trap geometry can be defined with the use of a triple integral such as:

$$V_{CO_2T} = \iiint [\phi * (1 - S_{wirr})] dx dy dz$$

With either equation, the effective storage resource can be defined as the trap's pore volume multiplied by a storage coefficient, which represents the fraction of the trap's pore space that can be filled by injected CO₂.

$$V_{CO_2E} = V_{CO_2T} * C_C$$

The calculation of stored mass of CO₂ depends on the pressure in the trap once it is filled with CO₂. Since the final formation pressure (P_f) is not known until after the injection operations have ended, the density of the CO₂ (ρ_{CO_2}) and therefore the storage mass (M_{CO_2}) cannot be directly calculated. As a result, CSLF proposes a range of CO₂ storage mass where the minimum mass is based on the density of the CO₂ at the initial formation pressure, and the maximum stored volume is calculated based on the density of CO₂ at the maximum allowable formation pressure.

$$\min M_{CO_2} = \rho_{CO_2}(P_i, T) * V_{CO_2E} \leq M_{CO_2} \leq \max M_{CO_2} = \rho_{CO_2}(P_f, T) * V_{CO_2E}$$

DOE Methodology

The DOE method is a volumetric approach which calculates a mass of stored CO₂ (G_{CO_2}) based on investigational area (A), formation thickness (h), porosity (ϕ), and CO₂ density (ρ_{CO_2}) with the application of a storage coefficient (E) shown below. The DOE efficiency factor considers a series of variables that may limit the ability of injected CO₂ to occupy 100% of the pore space in a given formation, including geologic heterogeneity, gravity or buoyancy effects, and sweep efficiency. Monte Carlo simulations were conducted to determine a range of values for efficiency, giving a range from 1% to 4% for formations at the subregional to regional scales with a 15% to 85% confidence range. A description of the variables according to DOE is presented in Table 1.

$$G_{CO_2} = A * h * \phi * \rho_{CO_2} * E$$

The DOE method's storage coefficient "E" is broken into seven multiplicative terms. The first three terms relate to the geologic heterogeneity which limits the accessible portions of 1) the formation area, 2) thickness, and 3) porosity. The last four terms relate to displacement efficiency, specifically 4) areal displacement, 5) vertical displacement, 6) gravity effects, and 7) microscopic displacement. Table 1 is a chart explaining the different efficiency factor terms.

The DOE method assumes that all seven terms used to calculate the storage coefficient can be rolled into a single term that can be applied to the entire pore volume of a given formation to come up with an effective storage resource. This assumes that CO₂ injection wells can be placed regularly throughout the formation to maximize storage and that the saline formation is an open system. The CSLF method can also be applied to an open system by applying a storage coefficient using a series of variables similar to the ones used in the DOE method.

Table 1. DOE Efficiency Factor Terms

Term	Symbol (range)	Description
Terms Used to Define the Entire Basin/Region Pore Volume		
Net to Total Area	A_n/A_t (0.2–0.8)	Fraction of total basin/region area that has a suitable formation present.
Net to Gross Thickness	h_n/h_g (0.25–0.75)	Fraction of total geologic unit that meets minimum porosity and permeability requirements for injection.
Effective to Total Porosity Ratio	ϕ_{eff}/ϕ_{tot} (0.6–0.95)	Fraction of total porosity that is effective, i.e., interconnected.
Terms Used to Define the Pore Volume Immediately Surrounding a Single-Well CO₂ Injector		
Areal Displacement Efficiency	E_A (0.5–0.8)	Fraction of immediate area surrounding an injection well that can be contacted by CO ₂ ; most likely influenced by areal geologic heterogeneity, such as faults or permeability anisotropy.
Vertical Displacement Efficiency	E_I (0.6–0.9)	Fraction of vertical cross section with the volume defined by the area (A) that can be contacted by the CO ₂ plume from a single well; most likely influenced by variations in porosity and permeability between sublayers in the same geologic unit. If one zone has higher permeability than others, the CO ₂ will fill this zone quickly and leave the other zones with less CO ₂ or no CO ₂ in them.
Gravity	E_g (0.2–0.6)	Fraction of net thickness that is contacted by CO ₂ as a consequence of the density difference between CO ₂ and in situ brine.
Microscopic Displacement Efficiency	E_d (0.5–0.8)	Portion of the CO ₂ contacted, brine-filled pore volume that can be replaced by CO ₂ .

Equivalence of the DOE Method and the CSLF Method, Related to the Proposed Resource Classification System

The two most commonly used methods for estimating CO₂ storage capacity/resource around the world are the DOE and CSLF methods. In the CSLF Phase III report, the major differences between the two methods were described, and the equivalency of the two methods was also established (CSLF, 2008). The major differences are that the CSLF method only considers storage in traps while the DOE method considers storage across entire saline formations at the regional scale. Though not specified in the CSLF report, the CSLF method could also be applied to entire formations instead of just known physical traps. The other differences are basically the arrangement of the equations, which in the end makes the methods virtually equivalent.

The purpose of the following section is to relate the two methods to the proposed classification resource/capacity system proposed in this report (see Figure 5) and to each other. To more easily compare the DOE and CSLF methods, the calculation of mass was left out until the end of the comparison. Also, all volumes are at reservoir conditions (reservoir pressure and temperature).

The *theoretical storage resource*, as related to the DOE and CSLF methods, is the total pore space of the assessed area that can be accessed by injected CO₂. This is obviously an overestimation since it would be technically impossible to access all the pore space in the reservoir. The two methods only differ at this point by the inclusion of irreducible water saturation. The CSLF method states that the theoretical storage resource is the pore space minus the irreducible water saturation.

$$V_{CO_2,DOE_T} = A * h * \phi$$

$$V_{CO_2,CSLF_T} = A * h * \phi * (1 - S_{wirr})$$

Where

- V_{CO_2} = Volume of CO₂ stored under reservoir conditions
- A = Geographic area that defines the basin or region being assessed
- h = Gross thickness of the formation CO₂ is assessed within the basin or region defined by A
- ϕ = Average porosity of the entire formation over the gross thickness h
- S_{wirr} = Maximum irreducible water saturation under injection conditions

$$V_{CO_2,DOE_T} * (1 - S_{wirr}) = V_{CO_2,CSLF_T}$$

The *characterized storage resource* is a subset of the theoretical storage resource, which excludes the portions of the pore space in the assessed area that cannot be accessed by CO₂ because of unconnected pores, high shale content, or missing portions of the reservoir. In the DOE method, this is taken into consideration by the inclusion of three geological terms which discount the total pore volume. In the CSLF method, this is accounted for with the use of a triple integral which considers the spatial variation of the porosity and the irreducible water saturation in the assessment area. It is not clear from the CSLF Phase II or III documents if the porosity in the equation is effective (interconnected) or total (CSLF, 2007, 2008). For the purposes of this document, we have assumed that it is total porosity and, as such, needs to be adjusted with an effective porosity multiplier.

$$V_{CO_2,DOE_C} = A * h * \phi * E_{Geol}$$

$$V_{CO_2,CSLF_C} = \left(\iiint \phi * (1 - S_{wirr}) * \frac{\phi_{eff}}{\phi_{tot}} dx dy dz \right)$$

Where

- $E_{Geol} = A_n/A_t * h_n/h_g * \phi_{eff}/\phi_{tot}$ = Geologic terms which define the fraction of the pore space that has properties that make it amenable to CO₂ storage in the assessment region
- A_n/A_t = Fraction of the total basin or region area that has a suitable formation present
- h_n/h_g = Fraction of the total geologic unit that meets minimum porosity and permeability requirements for injection
- ϕ_{eff}/ϕ_{tot} = Fraction of total porosity that is effective (interconnected)

$$V_{CO_2,DOE_C} * (1 - S_{wirr}) = V_{CO_2,CSLF_C}$$

The *effective storage resource* is a subset of the characterized storage resource, which includes the storage efficiency. This represents how efficiently the injected CO₂ is able to access the pore space directly surrounding the injection well. DOE breaks the efficiency into four parts: areal displacement efficiency, vertical displacement efficiency, gravity, and microscopic displacement efficiency. The first three variables can be very difficult to separate and, as such, have been grouped together into a single volumetric displacement efficiency term. CSLF does not attempt to quantify the storage coefficient, C_C but rather states that it incorporates the cumulative effects of trap heterogeneity, CO₂ buoyancy, and sweep efficiency (CSLF, 2007), which is the equivalent of the volumetric displacement efficiency in the DOE method. The two methods are related as follows.

$$V_{CO_2,DOE_E} = A * h * \phi * E_E$$

$$V_{CO_2,CSLF_E} = \left(\int \int \int \phi * (1 - S_{wirr}) * \frac{\phi_{eff}}{\phi_{tot}} dx dy dz \right) * E_V * \frac{(1 - S_{wave})}{(1 - S_{wirr})}$$

$$V_{CO_2,CSLF_E} = A * h * \phi * (1 - S_{wirr}) * C_C$$

$$C_C = E_V * E_{Geol} * \frac{(1 - S_{wave})}{(1 - S_{wirr})}$$

$$E_E = C_C * (1 - S_{wirr})$$

Where

- $E_V = E_A * E_I * E_g$ = Volumetric displacement efficiency – The fraction of the pore space immediately around the injection well that is contacted by injection CO₂.

- $E_E = E_{Geol} * E_V * E_d = \frac{A_n}{A_t} * \frac{h_n}{h_g} * \frac{\phi_{eff}}{\phi_{tot}} * E_A * E_I * E_g * E_d =$ This is the DOE storage coefficient from the DOE Atlas (DOE, 2007, 2008).
- E_A = Areal displacement efficiency – The fraction of the immediate area surrounding an injection well that can be contacted by CO₂; most likely influenced by areal geologic heterogeneity such as faults or permeability anisotropy.
- E_I = Vertical displacement efficiency – The fraction of the vertical cross section (thickness), with the volume defined by the CO₂ plume from a single well, most likely influenced by variations in porosity and permeability between sublayers in the same geologic unit.
- E_g = Gravity – The fraction of the net thickness that is contacted by CO₂ as a consequence of density difference between CO₂ and in situ brine. In other words, (1-E_g) is that portion of the net thickness NOT contacted by CO₂, because CO₂ rises within the geologic unit.
- $E_d = (1 - S_{wirr})$ = Microscopic displacement efficiency – The fraction of CO₂ contacted pore volume that can be replaced by CO₂. E_d is directly related to irreducible water saturation in the presence of CO₂.
- S_{wave} = The average water saturation in the pore spaces that have been contacted by CO₂.
- $\frac{(1 - S_{wave})}{(1 - S_{wirr})}$ = This modifier must be used in the CSLF method, because during the injection of CO₂, the irreducible water saturation can change based on the reservoir pressure. Also, in many cases, it is not possible to reach irreducible water saturation, and, as such, the average water saturation should be used instead of the irreducible water saturation.

The CSLF Phase III document (CSLF, 2008), in its conclusions, states the two methods are computationally equivalent if $E_E = C_C * (1 - S_{wirr})$ and if an average CO₂ density at in situ conditions is used rather than the minimum and maximum values of CO₂ density related to reservoir pressures and temperatures. Therefore:

$$V_{CO_2,DOE_E} = V_{CO_2,CSLF_E}$$

$$G_{CO_2,DOE_E} = \rho_{CO_2} * V_{CO_2,DOE_E} = V_{CO_2,CSLF_E} * \rho_{CO_2} = M_{CO_2,DOE_E}$$

By equating the two methods in this way, it allows for comparison between estimations of storage resources by different groups in different areas using one or the other method. This also means that any storage coefficients that are developed for one method can be easily modified and applied to the other method.

DEVELOPMENT OF EFFECTIVE STORAGE COEFFICIENTS

Storage resource estimates are critical for stakeholders to make informed decisions regarding the potential implementation of large-scale CO₂ storage. As previously described, simple estimations of resources that are based solely on the readily available fundamental reservoir properties data (referred to as theoretical storage resource) will grossly overestimate storage resource. In order to develop more realistic resource estimates, storage coefficients that account for the key variables described in the DOE and CSLF methods must be applied to the theoretical storage resource estimates. While DOE has come up with storage coefficients that have been applied in its series of Carbon Sequestration Atlases of the United States and Canada, the simulations are the product of Monte Carlo simulations in which the input variables represented broad ranges of geologic and efficiency terms in which “no rigor was given to the selection of the distribution or the parameters that describe them” (DOE, 2007, 2008). These early storage coefficients should be considered to provide preliminary, reconnaissance-level estimates of effective storage resource. CSLF has not yet established any values for effective storage coefficients and states that “these values must be determined through numerical simulations and/or field work” (CSLF, 2007). With this in mind, this project set out to use both numerical simulations and available field-based data to build upon the storage coefficients developed by DOE and create a new set of broadly applicable effective storage coefficients, for both the DOE and CSLF methods.

The first step in the process of refining and developing new effective storage coefficients was to examine the body of literature related to field-based projects all over the world in which CO₂ had been or was being injected into saline formations. The examination of the literature on field-based studies of CO₂ storage in deep saline formations resulted in the conclusion that there are currently not enough projects and available data from the existing projects to adequately assess the storage resource in these types of formations. The lack of representative real-world CO₂ storage projects led to the development of a database of hydrocarbon reservoir properties which could serve as a proxy for saline formation properties. Assuming that hydrocarbon reservoirs may reasonably be considered to be subsets of larger saline formations, the applicability of these hydrocarbon reservoir data sets to saline formations is appropriate. The database, hereby referred to as the Average Global Database (AGD), contains fluid and geologic properties for over 20,000 hydrocarbon reservoirs representing a wide variety of reservoir types from all over the world. The AGD was formed as a compilation of data from smaller databases, published tables, and case studies. The two main databases that formed the AGD were the Gas Information System or GASIS (1999) and the Tertiary Oil Recovery Information System or TORIS (1995). Both databases only contain U.S. reservoirs, and as a result, case studies and tables of reservoirs and reservoir properties from previously published books, papers, and reports were added to the AGD so the database would be representative of the entire world (Appendix A). To produce a saline formation model, there are a few basic parameters that define its characteristics and physical properties: these are listed in Table 2. For the modeling portion of this project, the goal was to produce three-dimensional generic models that were representative on a global scale for different lithologies, depositional environments, and structures. All models used probabilistic P10, P50, and P90 geologic and fluid property values derived from the AGD for selected structures and depositional environments. Through the use of extensive numerical modeling and simulation, a set of effective storage coefficients was developed.

Table 2. List of P10, P50, and P90 General Formation Properties from the AGD

P Value	Depth, m	Salinity, ppm	Temp Grad, °C/m	Reservoir Thickness, m
10	895	8,226	0.020	3.35
50	2,338	53,000	0.025	25.9
90	3,802	174,000	0.033	190

Lithologies and Depositional Environments

The reservoirs in the AGD were first grouped into three lithologies: clastics (sands), limestone, and dolomite. Of the 21,086 reservoirs in the AGD, about 88% were classified as clastics, 9% were limestones, and 3% were dolomite. Depositional environment data were available for 8462 of the AGD reservoirs, which were then further classified according to ten depositional environments (Figures 8 and 9; Appendix B).

Model Structures and Traps

Five different structures were constructed defining vertical reservoir boundaries. These structures were a dome, anticline, flat stratigraphy, and 5°- and 10°-inclined formations with a sealing fault. Figures 10 and 11 show examples of each of the structural cases imposed upon the deltaic depositional environment. These structures were selected based on the known trap types from the AGD, a majority of which were domes and anticlines, with a smaller portion from fault traps (Figure 12).

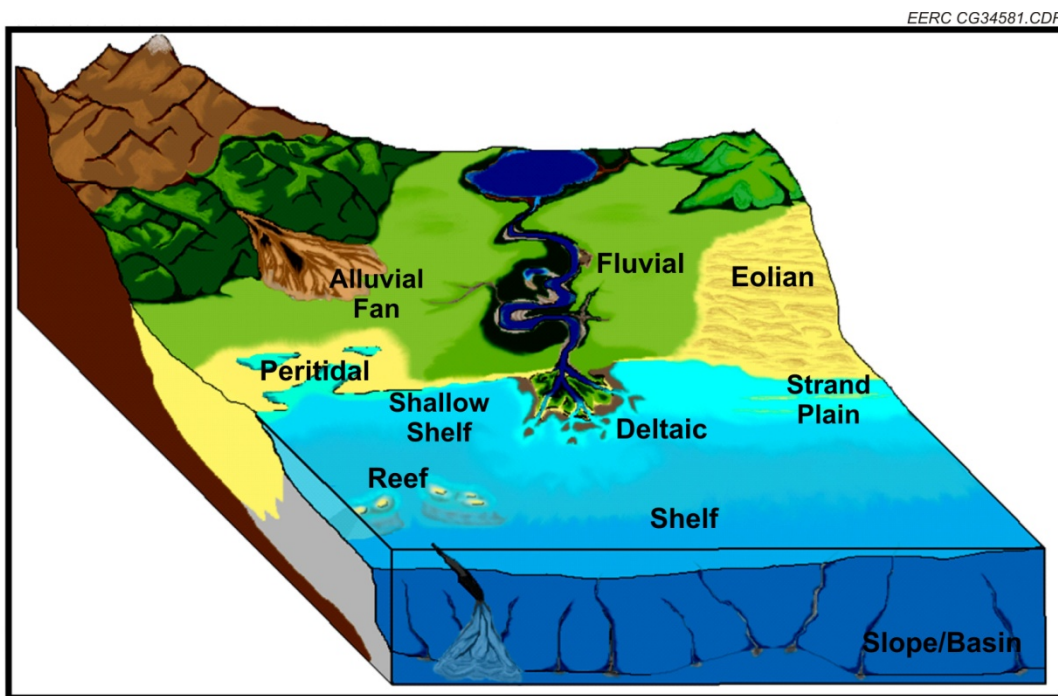


Figure 8. Depositional environments modeled in this project, from AGD.

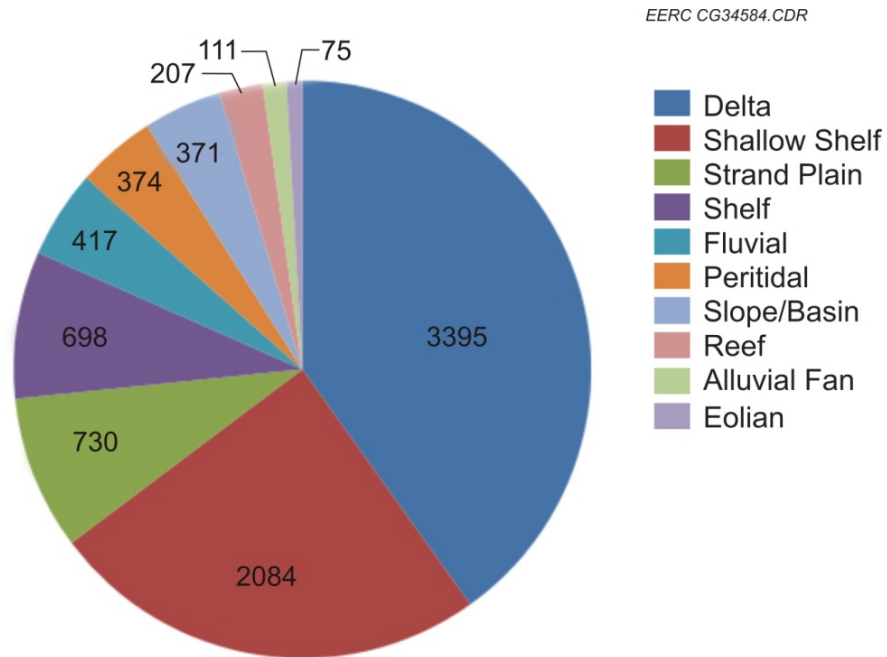


Figure 9. Depositional environments from the AGD.

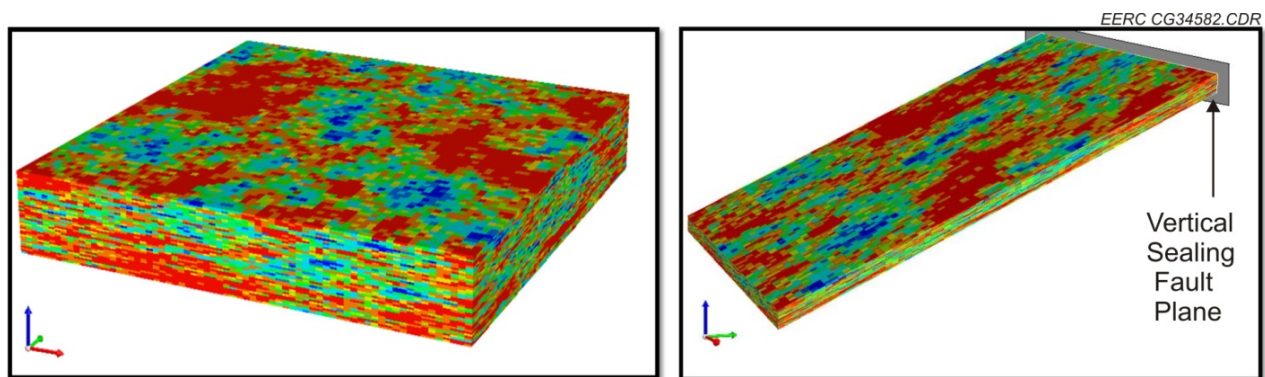


Figure 10. Flat deltaic stratigraphic porosity model (20x vertical exaggeration) is shown on the left and the deltaic fault barrier porosity model with 5° inclination (5x vertical exaggeration) shown on the right.

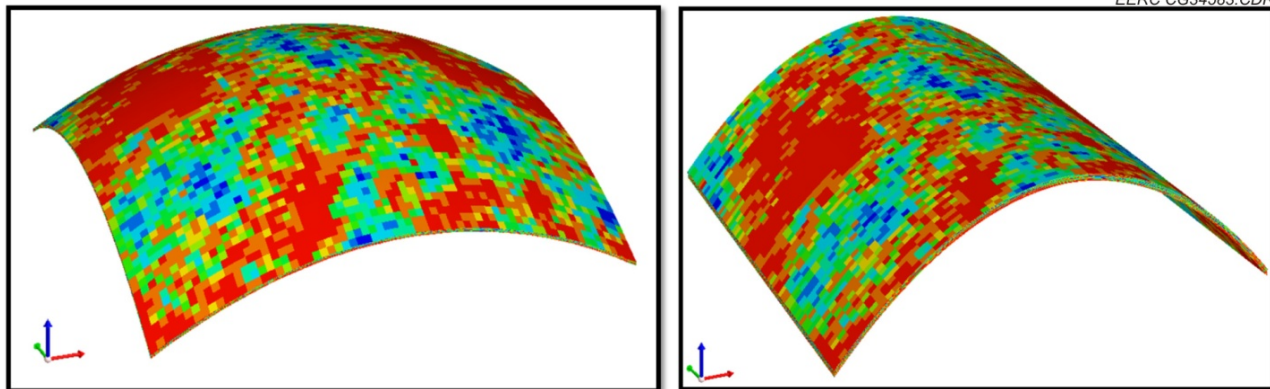


Figure 11. Dome deltaic porosity model (1x vertical exaggeration) is shown on the left, and the anticline deltaic porosity model (2x vertical exaggeration) is shown on the right.

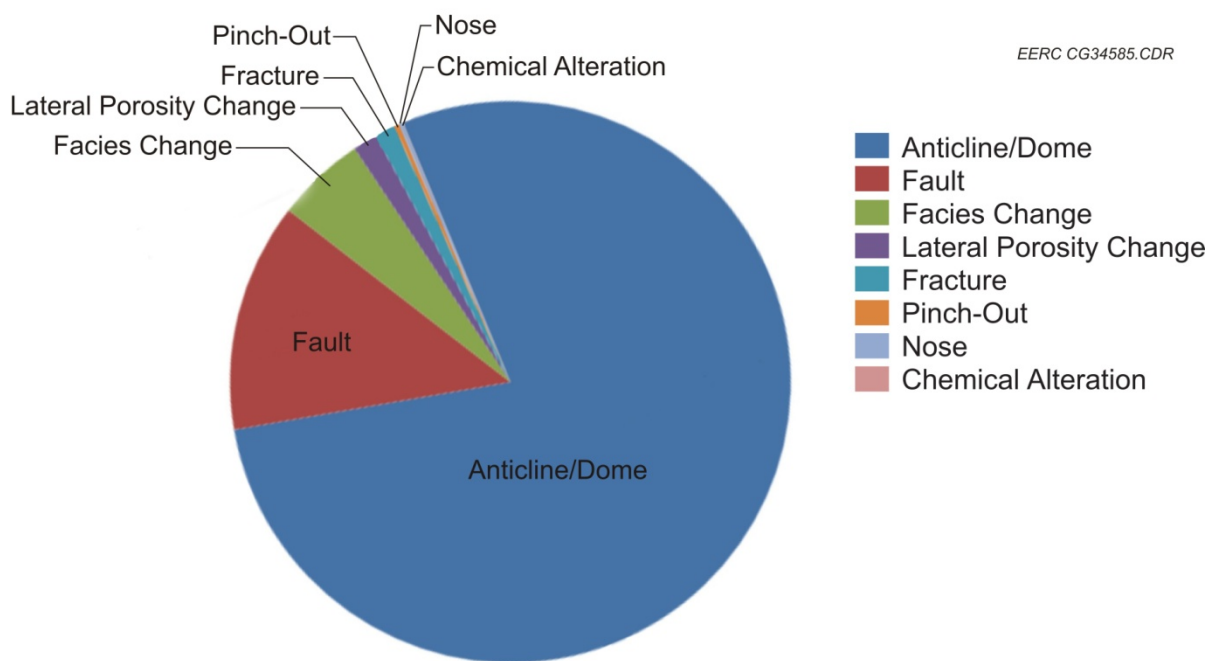


Figure 12. Trap types from AGD. To expedite the project, only anticline, dome, fault seal, and flat structures were used.

Determining Storage Coefficients Through Numerical Simulation

Development of Uniform Injection and Evaluation Scheme

The approach used by the EERC in this study to determine storage coefficients for a large number of different scenarios was to run numerical simulations and calculate those coefficients from the models. The numerical simulations were run using the Computer Modeling Group (CMG) General Equation of State Modeling (GEM) reservoir simulation package, and the models were built using CMG, Schlumberger's Petrel software, and Geostatistical Software Library (GSLIB). The properties, interaction, and behaviors of the brine and CO₂ were modeled using a Peng-Robinson EOS in CMG's Winprop application. No tuning of the equation of state to laboratory data was done since these models and simulations are all generic cases.

In order to test the strength of different parameters on the storage coefficients, a uniform injection and evaluation scheme first had to be developed. The first element of the scheme was to determine the point in time in the injection/storage scheme at which the storage coefficient would be calculated. Three points were identified as possible evaluation times: 1) at the end of injection, 2) when the free-phase CO₂ plume stops moving or nearly stops moving, or 3) dynamically through injection and postinjection. For the purposes of this project, it was decided that the storage coefficient would be calculated at the end of injection.

The second element of the scheme was the determination of the injection volumes and rates for both the homogeneous and heterogeneous models. An injectivity study was conducted using the homogeneous models attempting to inject 0.91 million tonnes (1 million tons) of CO₂ over different time periods, those being 3 months, 6 months, 1 year, 2.5 years, 5 years, and 10 years. The injection of 1 million tons over 1 year was determined to be optimal because it was the highest injection rate that all of the homogeneous scenarios could handle without exceeding the maximum allowable bottomhole pressure. Maximum allowable bottomhole pressure is generally determined on a case-by-case basis, however, because these are generic cases, the bottom-hole pressure limit was set at 0.6 of the lithostatic pressure gradient (22.6 kPa/m or 1 psi/ft) based on depth where:

$$P_{Max} = 13.57(kPa / m) * Depth(m) + 101.35(kPa)$$

When applied in the real world, as when used by many petroleum regulatory agencies, this limitation would ensure that injection does not induce fracturing of the reservoir or cap rock. In the heterogeneous cases, the optimal injection rate was 1 million tons over 5 years (200,000 tons/yr). This is because the heterogeneous distribution of porosity and permeability created higher pressure buildups near the wellbore, which in some cases approached the bottom-hole pressure limit. The use of higher rates of injection and/or longer periods of injection would also limit the number of simulations that could have been performed over the study period.

The third element of the scheme was the selection of model size and grid configuration. The model areal dimensions were approximately 3.22 km by 3.22 km (2 miles by 2 miles). The model thickness was determined from the AGD for the P50 cases to be approximately 26 m (85 feet). The reservoir model was divided into 204,723 cells, which was (69, 69, 43) in the

(X, Y, Z) direction. This setup yielded the smallest possible model that could contain all of the injected CO₂. The model was also broken up into the largest number of cells possible that would allow for reasonably short simulation run times without oversimplifying the porosity and permeability distribution among the different lithologies and depositional environments. The cell size was also tested to ensure that the gridding applied did not affect the results of any of the simulation runs. It was determined that the gridding selected did not, in any case, change the storage coefficient by more than a percent from cases with very small cubic cells.

The fourth element of the scheme was to determine what trapping processes would be allowed in the simulation runs. As discussed earlier, physical trapping would be the most important trapping mechanism when determining the storage resource, especially if the storage coefficients are determined at the end of injection. However, CO₂ does go into solution as soon as it mixes with the formation brine. Also, it is possible for some CO₂ trapping to occur before the injection ends, as a result of residual gas trapping, and it is likely that there are mineral reactions and some mineral trapping occurring before the injection ends. As a result, it was determined that residual gas trapping and solution gas trapping would be allowed in the simulations; however, no mineral trapping was allowed as a result of the composition-specific nature of this trapping mechanism. It is worth noting that at the end of the active injection period, in the following simulation runs, that only about 3% of the injected CO₂ had gone into solution, and less than 1% was trapped as residual gas. It was determined that even though only a small percentage of the overall injected CO₂ was trapped by these processes, it was important to include them, as they do slightly reduce the size of the free-phase plume.

The final element of the injection and evaluation scheme was to determine how the CO₂ plume would be defined. To estimate the storage coefficient and its components, a quantitative means of identifying the plume is necessary. Defining the plume is not trivial, and there are several possible options. The plume can be defined as 1) pressure plume, 2) a free-phase CO₂ saturation plume, 3) mobile-phase CO₂ saturation plume, or 4) all-phase CO₂ plume.

The pressure plume is defined by a pressure increase above the initial pressure that is a result of CO₂ injection. In this case, a minimum pressure increase would need to be defined, most likely based on pressures that would adversely interfere with other CO₂ injection wells in the area. In a closed system, the pressure plume will grow as long as the injection continues and will stay elevated until some of the formation fluids are produced or “leak” out of the formation. In an open system, the pressure plume will grow with time and will slowly recede after the injection operations end and will eventually disappear.

The free-phase CO₂ saturation plume is defined by a plume that includes all of the mobile CO₂ and the CO₂ trapped as residual gas. It does not include the CO₂ that is dissolved in the formation brine, CO₂ that is mineralized, or CO₂ that has adsorbed onto the rock fabric. This is the definition which is traditionally used to define the plume. This plume will grow with time and then decrease as the mobile phase slows and dissolution and mineralization start to dominate.

The mobile-phase CO₂ saturation plume is similar to free-phase CO₂ saturation; however, it does not contain the CO₂ trapped as residual gas. With this definition, it is possible to have a

leading and trailing edge of the CO₂ plume. If the CO₂ is injected into a formation with a regional dip, after the injection stops, the CO₂ will move up dip, and the mobile CO₂ plume will get smaller in size as it is trapped as residual gas, dissolves into solution, and is converted into stable minerals.

All-phase CO₂ plume includes all of the free-phase CO₂ plus the dissolved and mineralized CO₂. Unless the dissolved CO₂ moves because of the movement of formation brine or a regional dip, the plume will grow with time and then remain somewhat static after the injection period ends.

For the purposes of this project, the free-phase CO₂ saturation plume was used to define the plume, since it will contain most of the CO₂ at the end of the active injection period.

Approach to the Calculation of Storage Coefficients

Storage coefficients were calculated for both DOE E and CSLF C_c using data from the DOE Atlas (2007, 2008), the AGD, and the numerical simulations. As stated before, the storage coefficients are a multiplicative combination of three geologic variables and four displacement efficiency variables. In all cases, wherever possible, the three geologic variables should be based on real-world site-specific or formation-specific data. That being said, for the purposes of this study, values have been assigned or calculated for net-to-gross area (assigned from the DOE Atlas), net-to-gross thickness (calculated from AGD at the site-specific level), and effective-to-total porosity (calculated from the AGD). The four displacement efficiency terms were all calculated based on numerical simulations. Of the four displacement efficiency variables, three of them have been multiplicatively combined (E_A , E_I , E_g) into a single term, E_V , or volumetric displacement efficiency. This was done because of the difficulties in separating the variables in a heterogeneous case, where it was found to be easier to determine them in a 3-dimensional volume. This method also eliminates double-counting of areas that could be considered to overlap between multiple variables. With respect to the fourth displacement efficiency term, different terms were used for the calculation of storage coefficients for DOE E and CSLF C_c, respectively. In the DOE E, the fourth term is microscopic displacement efficiency (E_d), and for the CSLF C_c, it is $(1 - S_{wave})/(1 - S_{wirr})$. Each of these displacement efficiency terms (E_V , E_d , and $(1 - S_{wave})/(1 - S_{wirr})$) represents the fraction of the pore volume immediately surrounding the wellbore that could be filled by CO₂, termed the accessible volume.

Accessible volume can be determined in a number of ways. Figure 13 graphically illustrates four concepts by which accessible volume can be considered. Ideally, the estimation of accessible volume is a representative unit volume that can be extrapolated out from the small, site-specific scale to larger regional or formation scales.

The four concepts considered over the course of this study included the following:

- The first concept considers a right cylinder defined areally by a circle with radius defined by the maximum radial distance of the plume from the injection well. This

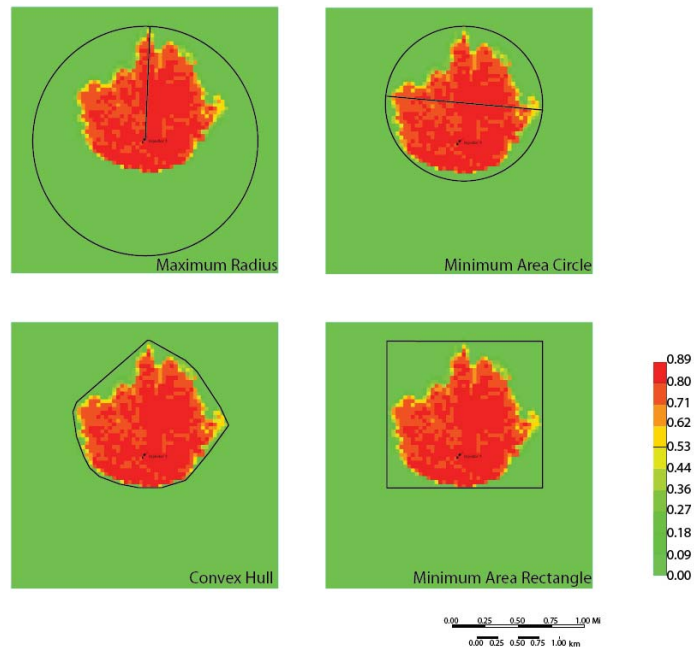


Figure 13. Four concepts for the accessible area considered in this project.

method is effective when applied to homogeneous flat model but falls woefully short in any type of nonflat structure and in most heterogeneous models.

- The second concept was a right cylinder defined areally by a “minimum area circle” whose diameter is defined by the maximum length of the plume. This works well for heterogeneous cases but still does not account for structures such as anticlines or tilted formations where the areal nature of the plume is not, and never will be, circular.
- The third concept is the application of a “convex hull.” For this project, a convex hull is defined areally by a polygon, typically of irregular size and shape, based on the connection of the outermost points on all lobes of a given plume. At the local scale, application of the convex hull method fits the expected storage coefficient distribution of different structures very closely. However, since each polygon is of nonuniform shape, it is very difficult to extrapolate the storage coefficient values generated by the convex hull approach out to the larger scale because of their inherent irregularity.
- The fourth concept is the use of a “minimum area rectangle.” The minimum area rectangle is defined areally by a rectangle whose long axis is defined by the maximum width of the plume, while the short axis is defined by the maximum width of the plume offset 90° from the long axis. Application of this method fits the expected distribution of storage coefficients for different structures and complex heterogeneity nearly as closely as the convex hull method, but it results in unit volumes that can be easily extrapolated to a variety of scales. It also fits the concept of well spacing that is used by oil and gas regulatory agencies to maximize hydrocarbon production within a field or larger region.

The minimum area rectangle is transformed into a “minimum volume block” by translating the bounding rectangle along the height of the plume. The volume of the block represents the denominator of the volumetric efficiency calculation, where E_{VOL} becomes the comparative ratio of plume volume to block volume. The minimum volume block approach to determining accessible volume was selected as the basis for calculating the effective storage coefficients. This method was chosen because it fits the distribution of the effective storage coefficients and can also represent a unit volume which can be extrapolated to a larger region or formation. This approach also seems to be the most practical with respect to actual implementation for large-scale assessments of storage resource.

Evaluation of Parameters Affecting CO₂ Storage Coefficients Using Homogeneous Models

To develop reliable, broadly applicable storage coefficients, it is necessary to first identify and test the key parameters that most strongly affect the storage coefficient. The approach described above was used to test single parameters using a series of homogeneous models to determine how much each parameter affected the storage coefficient (Table 3). The homogeneous models were created using average properties of clastic reservoirs derived from the AGD (Table 4). Parameters that were considered likely to be the most influential were tested and included depth, temperature, vertical to horizontal permeability ratio (k_v/k_h), relative permeability/irreducible water saturation, injection rate/fluid velocity, and structure. In each case the parameters tested were listed along with the resulting volumetric efficiency (E_V), microscopic displacement efficiency (E_d), and storage coefficient (E_E), which in this case is the multiplicative combination of E_V and E_d , since the geologic variables (E_{geol}) are equal to one in a homogeneous case ($E_E = E_{geol} * E_V * E_d$).

Table 3. List of Homogeneous Models

Homogeneous Models	Ref	Depth, m	P, MPa	T, °C	S_{wirr}	kr _{CO2} at S_{wirr}	Structure	k_v/k_h	Q, ton/yr
Median – (1 ton/yr) (Median Case)	2338	23.9	75	0.197	0.5265	Flat	0.108	1	
Median – (4 ton/yr)	2338	23.9	75	0.197	0.5265	Flat	0.108	4	
Median – (2 ton/yr)	2338	23.9	75	0.197	0.5265	Flat	0.108	2	
Median – (0.4 ton/yr)	2338	23.9	75	0.197	0.5265	Flat	0.108	0.4	
Median – (0.2 ton/yr)	2338	23.9	75	0.197	0.5265	Flat	0.108	0.2	
Median – (0.1 ton/yr)	2338	23.9	75	0.197	0.5265	Flat	0.108	0.1	
Median – Dome	2338	23.9	75	0.197	0.5265	Dome	0.108	1	
Median – Anticline	2338	23.9	75	0.197	0.5265	Anticline	0.108	1	
Median – 5° Incline	2338	23.9	75	0.197	0.5265	5° incline	0.108	1	
Median – 10° Incline	2338	23.9	75	0.197	0.5265	10° incline	0.108	1	
Median – Quarter Dome	2338	23.9	75	0.197	0.5265	1/4 Dome	0.108	1	
Median – Half Dome	2338	23.9	75	0.197	0.5265	1/2 Dome	0.108	1	
Median – Three- Quarter Dome	2338	23.9	75	0.197	0.5265	3/4 Dome	0.108	1	
Shallow – High Temp.	895	9.2	45	0.197	0.5265	Flat	0.108	1	
Shallow – Mid Temp.	895	9.2	38	0.197	0.5265	Flat	0.108	1	
Shallow – Low Temp.	895	9.2	33	0.197	0.5265	Flat	0.108	1	
Median – High Temp.	2338	23.9	92	0.197	0.5265	Flat	0.108	1	
Median – Low Temp.	2338	23.9	62	0.197	0.5265	Flat	0.108	1	
Deep – High Temp.	3802	38.8	141	0.197	0.5265	Flat	0.108	1	
Deep – Mid Temp.	3802	38.8	113	0.197	0.5265	Flat	0.108	1	
Deep – Low Temp.	3802	38.8	92	0.197	0.5265	Flat	0.108	1	
Median – k_v/k_h 0.01	2338	23.9	75	0.197	0.5265	Flat	0.01	1	
Median – k_v/k_h 0.05	2338	23.9	75	0.197	0.5265	Flat	0.05	1	
Median – k_v/k_h 0.1	2338	23.9	75	0.197	0.5265	Flat	0.1	1	
Median – k_v/k_h 0.25	2338	23.9	75	0.197	0.5265	Flat	0.25	1	
Median – k_v/k_h 0.5	2338	23.9	75	0.197	0.5265	Flat	0.5	1	
Median – k_v/k_h 1	2338	23.9	75	0.197	0.5265	Flat	1	1	
Median – k_v/k_h 2	2338	23.9	75	0.197	0.5265	Flat	2	1	
Median – k_v/k_h 4	2338	23.9	75	0.197	0.5265	Flat	4	1	
Median – Basal Sandstone	2338	23.9	75	0.294	0.5446	Flat	0.1	1	
Median – Calmar	2338	23.9	75	0.638	0.1871	Flat	0.1	1	
Median – Cardium 1	2338	23.9	75	0.379	0.2978	Flat	0.1	1	
Median – Cardium 2	2338	23.9	75	0.197	0.5265	Flat	0.1	1	
Median – Ellerslie	2338	23.9	75	0.659	0.1156	Flat	0.1	1	
Median – Viking 2	2338	23.9	75	0.423	0.2638	Flat	0.1	1	
Median – Viking 1	2338	23.9	75	0.558	0.3319	Flat	0.1	1	

Table 4. Properties of Clastic Reservoirs in Homogeneous Models

Model Area, km ² (mi ²)	10.36 (4)
Model Thickness, m (ft)	25.9 (85)
Cell Area, m ² (ft ²)	2175 (23,412)
Cell Thickness, m (ft)	0.61 (2)
Number of Cells	204,723
Effective Porosity, %	15
Permeability, m ² (mD)	$2.27 * 10^{-13}$ (230)
Salinity, ppm	53,000
Formation Compressibility, 1/kPa (1/psi)	$3.48 * 10^{-13}$ ($2.4 * 10^{-6}$)
Brine Compressibility, 1/kPa (1/psi)	$3.93 * 10^{-13}$ ($2.71 * 10^{-6}$)
Pressure Gradient, kPa/m (psi/ft)	10.17 (0.45)
Maximum Pressure Gradient, kPa/m (psi/ft)	13.57 (0.6)

Structure

The relationship between structure and storage efficiency is quite strong: the more confined the structure is, the higher the storage efficiency will be given the same reservoir conditions. To test the effects of structure, a flat model was compared to four dome models with differing degrees of curvature. The models tested are listed in Table 5. In the presence of a closure such as the domes that were tested, the more tightly curved formations yielded higher volumetric and microscopic displacement efficiencies, as well as higher storage coefficient values. In these cases, the gravity effects are not as important and the structure forces the CO₂ to access the pore volume in the structure and, at the same time, promotes better microscopic displacement.

Table 5. Structure Models Tested

		Curvature, %	E _V	E _d	E _E
Median – Flat	Flat	0	0.26	0.58	0.15
Median – Quarter Dome	1/4 dome	25	0.28	0.60	0.17
Median – Half Dome	1/2 dome	50	0.29	0.61	0.18
Median – Three-Quarter Dome	3/4 dome	75	0.38	0.62	0.24
Median – Dome	Dome	1	0.39	0.64	0.25

Depth and Temperature

In equal temperature gradients, values of both E_V and E_d increase with depth, as does the storage coefficient E (Table 6). This is a result of increasing CO₂ density, as the ratio of CO₂ density to brine density ($\rho_{\text{CO}_2}/\rho_{\text{brine}}$) approaches 1, the gravity effects go down, increasing both E_V and E_d because of greater gravity effects. However, in the shallow, low-temperature case, E_V, E_d, and E were significantly lower than the other shallow cases. This is because under the shallow, low-temperature conditions as described in Table 6, the CO₂ is in the dense liquid phase. By definition, the molecules of CO₂ in the liquid phase are less tightly packed than those

in the supercritical phase; therefore, storage in the liquid phase is less efficient, resulting in a lower storage coefficient E.

Table 6. Effects of Depth and Temperature on Storage Coefficients

Homogeneous Models	Ref Depth, m	P, MPa	T, °C	Temp grad, °C/m	E_V	E_d	E_E
Shallow – Low Temp.	895	9.2	33	0.020	0.14	0.52	0.07
Shallow – Mid Temp.	895	9.2	38	0.025	0.19	0.54	0.10
Shallow – High Temp.	895	9.2	45	0.033	0.15	0.60	0.09
Median – Low Temp.	2338	24	62	0.020	0.23	0.52	0.12
Median – Mid Temp.	2338	24	75	0.025	0.22	0.58	0.13
Median – High Temp.	2338	24	92	0.033	0.21	0.63	0.13
Deep – Low Temp.	3802	38.8	92	0.020	0.28	0.54	0.15
Deep – Mid Temp.	3802	38.8	113	0.025	0.27	0.60	0.16
Deep – High Temp.	3802	38.8	141	0.033	0.26	0.64	0.17

Relative Permeability and Irreducible Water Saturation (S_{wirr})

There is a fundamental lack of relative permeability curves for CO₂ and brine in the databases and literature that were available for this project. To date, Bennion and Bachu have published the majority of data regarding CO₂-to-brine relative permeability for the Basal, Cooking Lake, Nisku, Wabamun, Ellerslie, Viking, and Cardium Formations within the Alberta Basin (Bennion and Bachu, 2008). Supplemental relative permeability curves for the Frio and Berea Formations in the United States and a database of all available work have been compiled by Benson in her Relative Permeability Explorer (Benson, 2009). Such curves are essential when developing numerical simulations to predict not only the potential storage efficiency of the site but also to accurately predict plume growth and movement.

Four relative permeability curves from clastic formations and one from a carbonate formation were tested and are listed below in Table 7. A key point that must be considered is that, in these cases, the lower the value of S_{wirr} , the higher the microscopic displacement efficiency will be and the higher the gravity response, which in turn will lower the value of E_V . The two displacement efficiencies basically equalized each other so that there is no clear relationship between S_{wirr} and the storage coefficient E in this case. Relative permeability of CO₂ (kr_{CO_2}) at S_{wirr} also exhibited some interesting results, although there is not as direct a correlation between kr_{CO_2} at S_{wirr} and storage efficiency. In general, as kr_{CO_2} at S_{wirr} goes down, microscopic displacement efficiency goes down, and the gravity effect goes down, resulting in an increase in the value of E_V . Again, the effects of the two variables counteract each other, and relative permeability does not have a strong effect on E. From these tests, it appears that a lower value of irreducible water saturation and a higher relative permeability of CO₂ at irreducible water saturation allow for greater gravity effects, thereby lowering the volumetric displacement efficiency because of the CO₂ rising more quickly in these cases.

Table 7. Relative Permeability Models Tested Along with Resulting Storage Efficiency and Storage Coefficients, from Bennion and Bachu (2008)

Relative Permeability Curve	kr_{CO_2} at				
	S_{wirr}	S_{wirr}	E_V	E_d	E_E
Cardium Sandstone Relative Permeability	0.197	0.5265	0.26	0.59	0.16
Basal Sandstone Relative Permeability	0.294	0.5446	0.32	0.56	0.18
Viking Sandstone Relative Permeability	0.558	0.3319	0.50	0.31	0.15
Ellerslie Sandstone Relative Permeability	0.659	0.1156	0.56	0.28	0.16
Wabamun Carbonate Relative Permeability	0.569	0.1883	0.45	0.38	0.17

Permeability Anisotropy (k_v/k_h)

Vertical-to-horizontal permeability (k_v/k_h) anisotropy varies greatly between different lithologies, depositional environments, and even within similar environments. In order to determine the effects of k_v/k_h , six ratios were tested (0.01, 0.05, 0.1, 0.25, 0.5, and 1) (Table 8). At low ratios (less than 0.25), the effect is very strong, preventing the density difference between the CO₂ and the formation brine from causing a strong gravity effect. When k_v/k_h is very low, the result is an increase in the storage coefficient and volumetric efficiency because of low gravity effects; however, there is low microscopic displacement (Figures 14–16). If the ratio is above 0.5, at least in these homogeneous models, the gravity effects dominate, and there is lower volumetric displacement efficiency, as well as the storage coefficient.

Table 8. Vertical-to-Horizontal Permeability Models Tested

	k_v/k_h	E_V	E_d	E_E
Median – k_v/k_h 0.01	0.01	0.48	0.35	0.17
Median – k_v/k_h 0.05	0.05	0.32	0.48	0.15
Median – k_v/k_h 0.1	0.1	0.27	0.58	0.16
Median – k_v/k_h 0.25	0.25	0.19	0.64	0.12
Median – k_v/k_h 0.5	0.5	0.19	0.66	0.12
Median – k_v/k_h 1	1	0.19	0.67	0.12

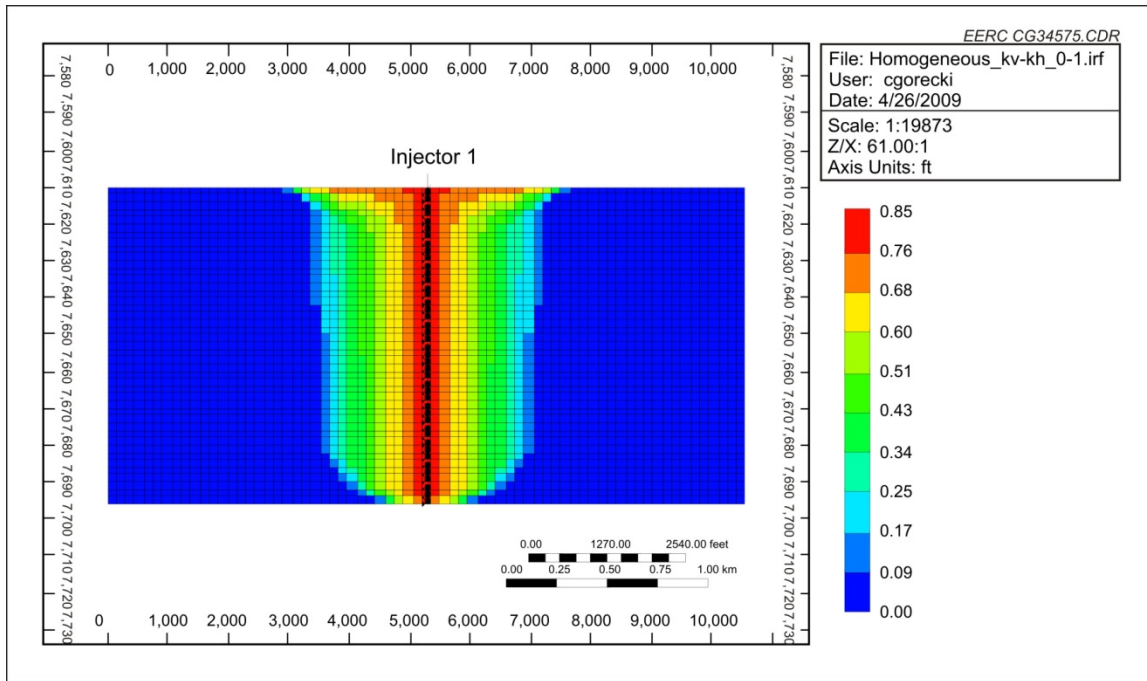


Figure 14. k_v/k_h ratio of 0.01: in this scenario, the CO_2 contacts much of the accessible pore volume; however, the saturation E_d stays relatively low.

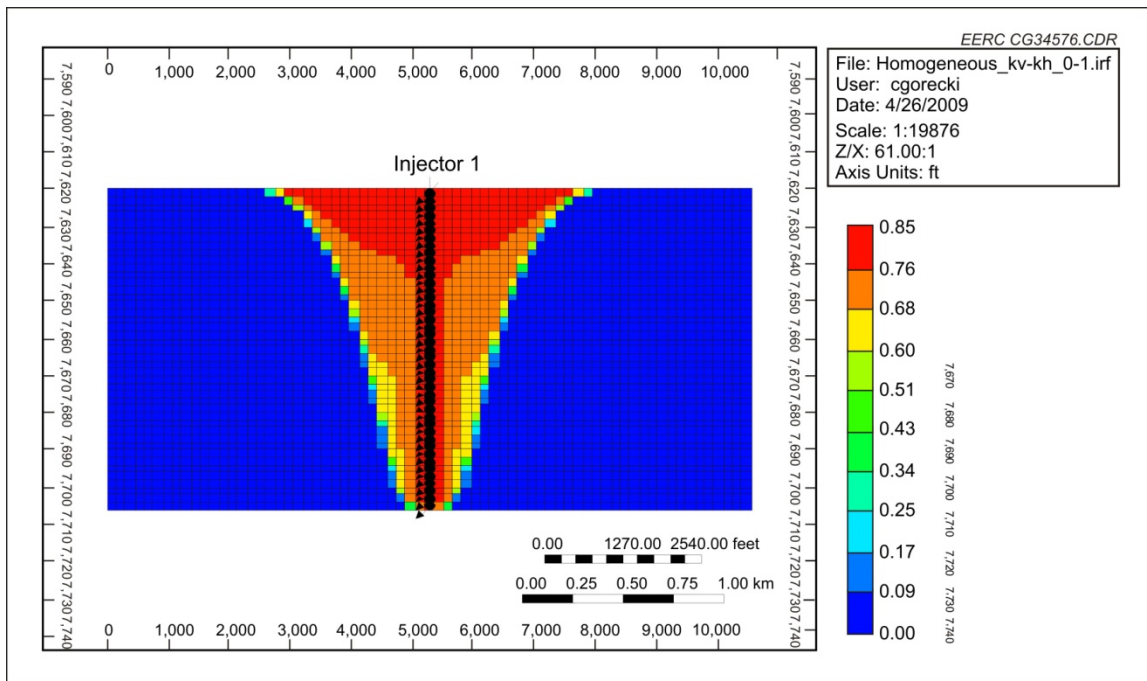


Figure 15. k_v/k_h ratio of 0.1: in this scenario, the CO_2 does not access as much of the accessible pore volume; however, the saturation E_d is much higher than the 0.01 case.

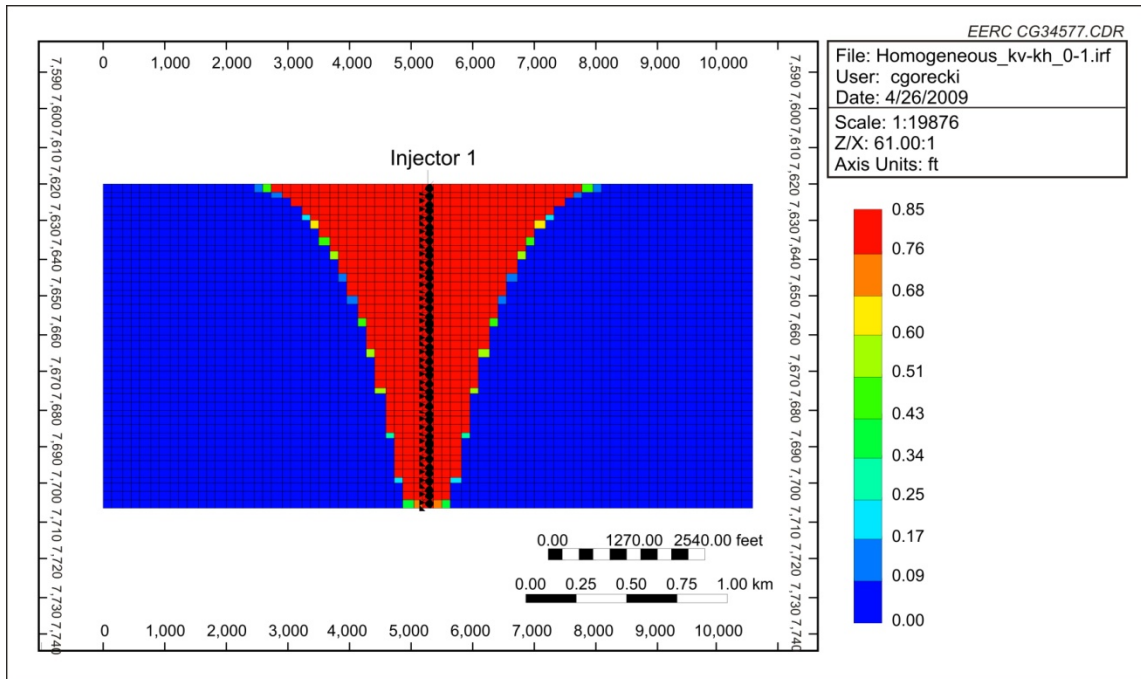


Figure 16. k_v/k_h ratio of 1: in this scenario, the CO_2 does not access nearly as much of the accessible pore volume; however, the saturation E_d is much higher than the previous cases.

Injection Rate/Fluid Velocity

Injection rate can have a significant effect on the storage coefficient E . By injecting at the highest possible rates, the pressure buildup near the wellbore forces the injected CO_2 to access more pore space lower in the injection zone than would have been the case with a lower injection rate. In order to test how much effect this had on the storage coefficient, six scenarios were tested and are listed with the resulting storage efficiency and storage coefficient values (Table 9). In each case, one million tons of CO_2 was injected into the model in different amounts of time. Compared to the vertical-to-horizontal permeability models, the fluid velocity models see a similar effect from gravity. When the CO_2 is injected very slowly at lower injection pressures, the CO_2 rises up more easily, contacting less of the available pore space, but at the same time, the microscopic displacement is much higher in the accessed areas. The faster the CO_2 is injected, the greater the pore space that will be contacted; however, a smaller fraction of the contacted pore space will be filled by the injected CO_2 . While these effects appear to counteract each other to some degree, the resulting storage coefficients indicate that higher injection rates will yield higher storage coefficients.

Table 9. Injection Rate/Fluid Velocity Models Tested Are Listed Below

	Duration, yr	Q, ton/yr	E_V	E_d	E_E
Median – 0.1 tons/yr	10	0.1	0.16	0.70	0.11
Median – 0.2 tons/yr	5	0.2	0.18	0.67	0.12
Median – 0.4 tons/yr	2.5	0.4	0.19	0.65	0.12
Median – 1 tons/yr	1	1	0.26	0.58	0.15
Median – 2 tons/yr	0.5	2	0.33	0.46	0.15
Median – 4 tons/yr	0.25	4	0.49	0.37	0.18

Homogeneous Model Summary

Through the use of homogeneous models, five parameters (structure, relative permeability and irreducible water saturation, depth and temperature, vertical-to-horizontal permeability anisotropy, and injection rate/fluid velocity) were tested to examine the effect of each parameter on the storage efficiency and resulting storage coefficients. In general, tightly closed structures, increased depth and lower temperatures, low ratios of vertical-to-horizontal permeability, and high injection rates/fluid velocity all increased the storage efficiency and the value of the storage coefficient. The effects of relative permeability and irreducible water saturation were much more subtle, with no large difference in the value of the storage coefficients with the relative permeability curves and irreducible water saturation values that were tested. The experiments concluded that:

- Curvature of a structure increases both microscopic and volumetric efficiency by concentrating a larger amount of CO₂ into a smaller area. Gravity is a major contributor to this observation as it is the driving force that concentrates the CO₂ into the trap.
- Depth and the higher pressure associated with increasing depth indicate higher efficiency. This is in agreement with Kopp and others, 2009, who concluded that deep reservoirs are more favorable for storage because of the increased density of CO₂. Properties associated with depth appeared to increase both microscopic and volumetric efficiency factors.
- Higher reservoir temperature also appears to increase overall efficiency because of high relative gains of microscopic displacement efficiency, while losing a small amount of volumetric efficiency. This observation shows that warm CO₂ is both less dense and more mobile than cooler CO₂, in agreement with Kopp and others; however, it more readily displaces pore fluids, leading to higher gas concentrations. Modest gains in E_E were observed in the midcase and deep reservoirs, but conflicting values were apparent in the shallow case because of a subcritical state of CO₂.
- Five different relative permeability curves (Bennion and Bachu, 2008) were isolated, and although the curves themselves are difficult to compare to each other, the comparison of the Viking, Ellerslie, and Basal Sandstones from Alberta, Canada, appear to be in agreement with Kopp and others, 2009. The two additional curves (Cardium Sandstone and Wabamun Carbonate, also from Alberta) are within the range of the

other formations. Large variations in microscopic and volumetric displacement efficiency are noted in the four sandstone units, with values much closer to each other apparent in the carbonate. Relative permeability remains an important but underdeveloped area requiring a greater number of test results from more formations.

- Vertical-to-horizontal permeability anisotropy values show an inverse relationship between microscopic and volumetric displacement efficiency. As k_v/k_h increases, microscopic displacement increases, while volumetric displacement efficiency decreases. These changes occur very quickly at low anisotropy ratios, leveling off at higher values. Volumetric displacement efficiency gets very small in these simulations, indicative of inefficient “coning” of the plume instead of a more favorable cylinderlike shape.
- Injection rate/velocity also shows an inverse relationship of microscopic and volumetric displacement efficiency; however, a modest increase is observed with faster injections, in agreement with Kopp and others, 2009. The cause for increase is most likely the method of calculation chosen for these simulations, which takes place at the end of injection and causes variable interaction with time and, therefore, gravity effects. The results suggest that higher injection velocities do employ a greater extent of the formation, so a greater volume will be captured with residual trapping mechanisms.

Heterogeneous Model Development

Having examined the effects of single parameters under homogeneous conditions, some of the lessons learned through that exercise were applied to the development of the heterogeneous models.

To test lithologies and depositional environments, heterogeneous models were developed in which the above-listed parameters were all varied for different depositional environments in order to develop a range of storage coefficients that could be applied to similar depositional environments around the world. The results of the homogeneous model runs provided valuable insight as to how the heterogeneous models might behave and served as a basis for the design and execution of those models.

Saline formation models were developed using the three lithologies, five structural settings, (dome, anticline, 10° inclined fault, 5° inclined fault, and flat) and ten depositional environments based on the P10, P50, and P90 properties and classifications derived from the AGD. The properties that were assigned a P10, P50, and P90 range for the models are k_v/k_h , porosity, permeability, and variogram range. The variogram range describes the way in which the rock properties are distributed throughout a given lithology for a given depositional environment (Deutsch, 2008). Two type logs (Appendix C), one for clastics and one for carbonates, were used that fit the P50 reservoir thickness for each lithology. The clastic sandstone type log was acquired from the Cretaceous Dakota Sandstone interval in the Foreman Butte oil field of North Dakota, United States. The limestone and dolomite type log was acquired from the Silurian Interlake Formation in the Beaver Lodge oil field of North Dakota. The Interlake Formation is an alternating dolomite and limestone mixture, allowing for the use of this

single type log for both limestone and dolomite lithologies. Consistent relative permeability curves were used for the sandstones and carbonates, Cardium Sandstone (Figure 17) and Wabamun Carbonate (Figure 18) respectively, from Bennion and Bachu (2008). This was done to more easily compare model runs between different depositional environments in the same lithology. Porosity was projected into three-dimensional space by fitting the appropriate single type log to the AGD porosity histogram distribution and using a three-dimensional Monte Carlo conditional simulation algorithm, referred to as sequential Gaussian simulation (SGS) (Deutsch and Journel, 1998), to distribute values to a given formation volume (Figure 19). Through Gaussian transformation using tools in the GSLIB (Deutsch and Journel, 1998) and back transformation, the type log histogram was made to match the AGD porosity histogram for a given depositional environment. Porosity and permeability calibration curves were produced from the AGD. Probability values were calculated from the AGD using the regression method of Hall (2002) and were modified to determine a 80% confidence interval and the P10 and P90 permeability calibration curves. Each of the P10, P50, and P90 cases (Tables 10 and 11; Appendix D), were then applied to the five structural settings, resulting in a total of 195 models and associated simulations. The simulations were the basis for the development of a range of effective storage coefficients for different lithologies and/or depositional environments.

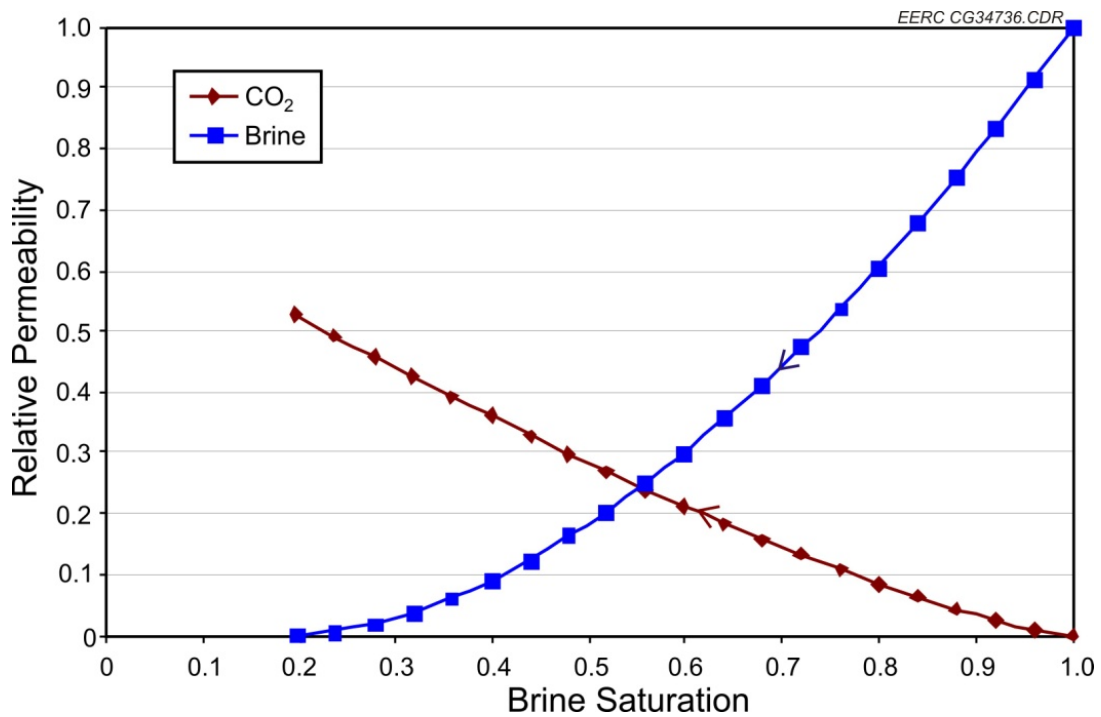


Figure 17. Sandstone relative permeability curve, Cardium Sandstone from Bennion and Bachu (2008).

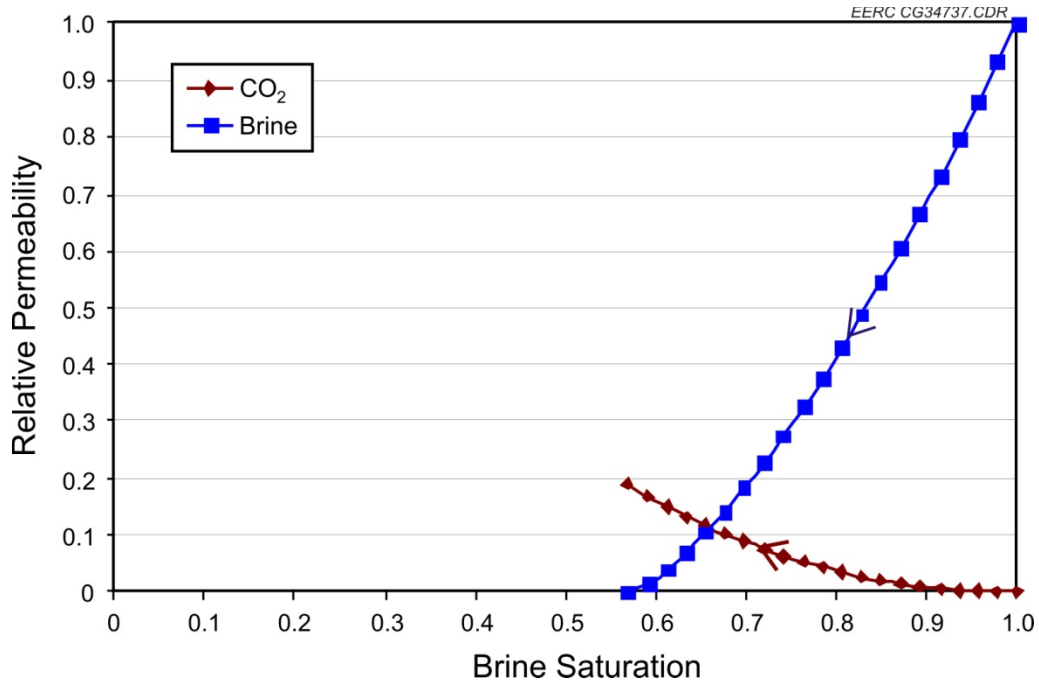


Figure 18. Carbonate relative permeability curve, Wabamun Carbonate from Bennion and Bachu (2008).

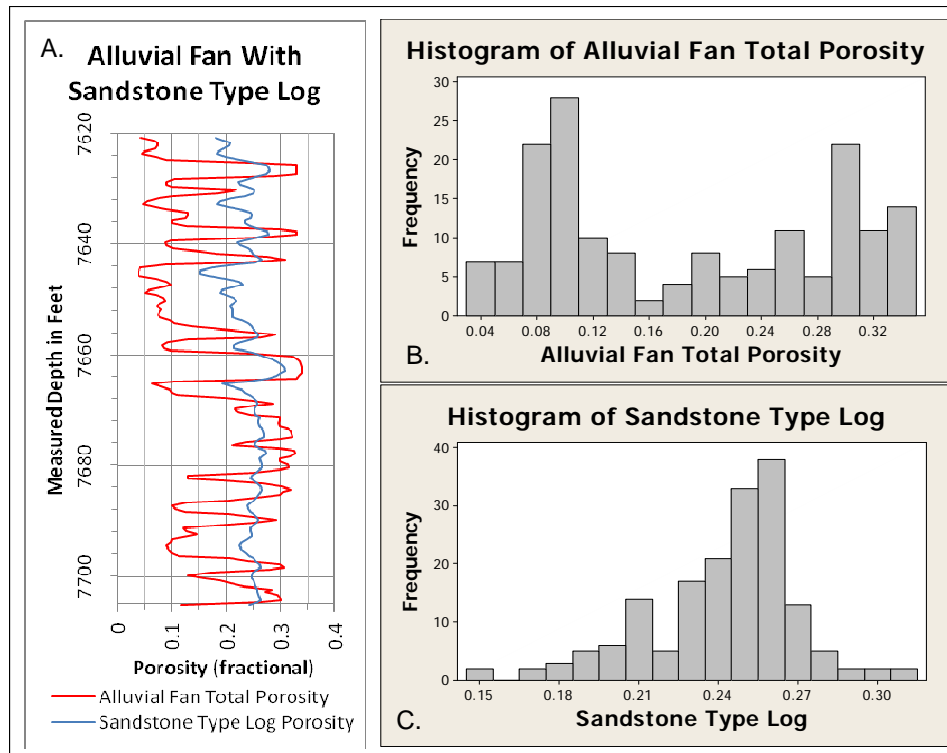


Figure 19. Examples showing the sandstone type log (A) translated to the alluvial fan total porosity log. The histograms for these datasets are shown in graphs (B) and (C).

Table 10. Basic Model Parameters for a Reservoir Depth of 2336 m and a Salinity of 53,080 Produced from the AGD and Deutsch (2008), where SS, LS, and Dol represent sandstone, limestone, and dolomite formations, respectively

Base Model for Traps and Structures	Horizontal Variogram Range Short, m	Horizontal Variogram Range Long, m	Vertical Variogram Range Short, m	Vertical Variogram Range Long, m	Rock Compressibility, 1/kPa
SS_Alluvial_Fan_10	40	145	2	7	4.41E-07
SS_Alluvial_Fan_50	108	398	2	7	4.41E-07
SS_Alluvial_Fan_90	177	650	2	7	4.41E-07
SS_Delta_10	150	550	2	7	3.60E-07
SS_Delta_50	410	1,504	2	7	3.60E-07
SS_Delta_90	671	2,459	2	7	3.60E-07
SS_Slope_Basin_10	134	492	2	7	2.80E-07
SS_Slope_Basin_50	367	1,346	2	7	2.80E-07
SS_Slope_Basin_90	600	2,200	2	7	2.80E-07
SS_Shallow_Shelf_10	681	2,499	2	7	3.18E-07
SS_Shallow_Shelf_50	1,852	6,792	2	7	3.18E-07
SS_Shallow_Shelf_90	3,023	11,085	2	7	3.18E-07
SS_Shelf_10	681	2,499	2	7	3.34E-07
SS_Shelf_50	1,852	6,792	2	7	3.34E-07
SS_Shelf_90	3,023	11,085	2	7	3.34E-07
SS_Fluvial_10	40	145	2	7	4.44E-07
SS_Fluvial_50	108	398	2	7	4.44E-07
SS_Fluvial_90	177	650	2	7	4.44E-07
SS_Eolian_10	54	198	2	7	4.73E-07
SS_Eolian_50	144	529	2	7	4.73E-07
SS_Eolian_90	234	860	2	7	4.73E-07
SS_Peritidal_10	76	279	2	7	4.45E-07
SS_Peritidal_50	206	754	2	7	4.45E-07
SS_Peritidal_90	335	1,230	2	7	4.45E-07
SS_Strand_Plain_10	15	57	2	7	4.22E-07
SS_Strand_Plain_50	27	99	2	7	4.22E-07
SS_Strand_Plain_90	39	142	2	7	4.22E-07
LS_Peritidal_10	44	571	1	14	4.45E-07
LS_Peritidal_50	120	1,543	1	14	4.45E-07
LS_Peritidal_90	196	2,515	1	14	4.45E-07
LS_Reef_10	9	116	1	14	6.87E-07
LS_Reef_50	16	203	1	14	6.87E-07
LS_Reef_90	23	290	1	14	6.87E-07
LS_Shallow_Shelf_10	397	5,111	1	14	6.27E-07
LS_Shallow_Shelf_50	1,081	13,892	1	14	6.27E-07
LS_Shallow_Shelf_90	1764	22,674	1	14	6.27E-07
Dol_Shallow_Shelf_10	397	5,111	1	14	5.26E-07
Dol_Shallow_Shelf_50	1,081	13,892	1	14	5.26E-07
Dol_Shallow_Shelf_90	1,764	22,674	1	14	5.26E-07

Table 11. Basic Model Parameters for a Temperature of 75°C and a Reference Pressure at 2336 m of 23,900 kPa Produced from the AGD and Deutsch (2008)

Base Model for Traps and Structures	Effective Φ , Min %	Effective Φ , Max %	Permeability Min, m ²	Permeability Max, m ²	k _v /k _h Ratio
SS_Alluvial_Fan_10	3	24	4.87E-17	8.71E-13	0.013
SS_Alluvial_Fan_50	3	26	1.17E-16	1.28E-12	0.108
SS_Alluvial_Fan_90	3	27	2.80E-16	1.89E-12	0.876
SS_Delta_10	2	19	8.20E-17	4.35E-13	0.013
SS_Delta_50	2	20	1.29E-16	5.15E-13	0.108
SS_Delta_90	2	21	2.02E-16	6.09E-13	0.876
SS_Slope_Basin_10	5	23	4.04E-15	8.84E-13	0.013
SS_Slope_Basin_50	5	25	6.42E-15	1.10E-12	0.108
SS_Slope_Basin_90	5	27	1.02E-14	1.37E-12	0.876
SS_Shallow_Shelf_10	3	22	2.04E-16	6.15E-13	0.013
SS_Shallow_Shelf_50	4	25	4.92E-16	1.00E-12	0.108
SS_Shallow_Shelf_90	4	28	1.19E-15	1.63E-12	0.876
SS_Shelf_10	2	19	9.36E-17	5.65E-13	0.013
SS_Shelf_50	2	22	2.19E-16	7.78E-13	0.108
SS_Shelf_90	2	25	5.12E-16	1.07E-12	0.876
SS_Fluvial_10	1	21	4.34E-18	5.70E-13	0.013
SS_Fluvial_50	1	24	1.05E-17	8.37E-13	0.108
SS_Fluvial_90	2	26	2.52E-17	1.23E-12	0.876
SS_Eolian_10	4	18	9.56E-16	2.93E-13	0.013
SS_Eolian_50	4	20	1.75E-15	4.19E-13	0.108
SS_Eolian_90	4	22	3.20E-15	5.98E-13	0.876
SS_Peritidal_10	2	20	3.10E-17	4.24E-13	0.013
SS_Peritidal_50	3	23	6.03E-17	7.10E-13	0.108
SS_Peritidal_90	3	25	1.18E-16	1.19E-12	0.876
SS_Strand_Plain_10	2	19	2.98E-17	4.69E-13	0.013
SS_Strand_Plain_50	2	22	5.47E-17	6.63E-13	0.108
SS_Strand_Plain_90	2	24	1.00E-16	9.37E-13	0.876
LS_Peritidal_10	5	22	1.12E-15	6.37E-13	0.031
LS_Peritidal_50	5	24	2.92E-15	8.02E-13	0.314
LS_Peritidal_90	6	25	7.67E-15	1.01E-12	0.596
LS_Reef_10	4	15	5.64E-16	2.04E-13	0.031
LS_Reef_50	4	19	1.31E-15	3.23E-13	0.314
LS_Reef_90	4	21	3.04E-15	5.12E-13	0.596
LS_Shallow_Shelf_10	2	19	9.15E-17	5.17E-13	0.031
LS_Shallow_Shelf_50	2	22	1.59E-16	7.10E-13	0.314
LS_Shallow_Shelf_90	2	25	2.74E-16	9.74E-13	0.596
Dol_Shallow_Shelf_10	1	12	2.87E-16	1.34E-13	0.209
Dol_Shallow_Shelf_50	1	15	9.19E-16	2.18E-13	0.487
Dol_Shallow_Shelf_90	1	18	2.94E-15	3.55E-13	0.835

Calculation of Broadly Applicable Storage Coefficients

Issue of Scale

One of the most important issues to consider when calculating the effective storage resource of a formation under consideration for CO₂ storage is the scale of the assessment. If the assessment of storage resource within a formation is over a small, localized area, then it is likely that the values of the geologic variables (net to total area [A_n/A_t] and net to gross thickness [h_n/h_g]) will be relatively high. This is because it is likely that the location selected has already been the subject of a preliminary, reconnaissance-level evaluation and judged to have geologic properties that make it a good potential storage site for CO₂. If the assessment is over a larger area, such as an entire sedimentary formation across a basin or region, then the values of those geologic variables will likely be lower, as there will be a larger fraction of the target formation that is not amenable to CO₂ storage (Figure 20). One approach to assessing the effective storage resource of a formation over a large area is to base a larger-scale (e.g., regional or basin) assessment on the data generated by smaller-scale or site-specific assessments. Using this approach, the individual site-specific assessments can be assumed to be a unit volume of the total formation and, as such, extrapolated out to the entire formation across the larger study area. This can only be done if the entire formation is open to hydrodynamic flow (noncompartmentalized) and the rock and fluid properties are relatively consistent throughout the formation. If the formation is compartmentalized or has regions with extremely different formation and fluid properties, then the storage potential of each compartment area would have to be assessed and added together to come up with a total storage potential for the entire formation. Because the scale of the assessment does affect the resulting storage coefficient, a series of values was calculated for different scales ranging from site-specific (as small as a few square km) to scales that span an entire formation (as large as thousands of square km).

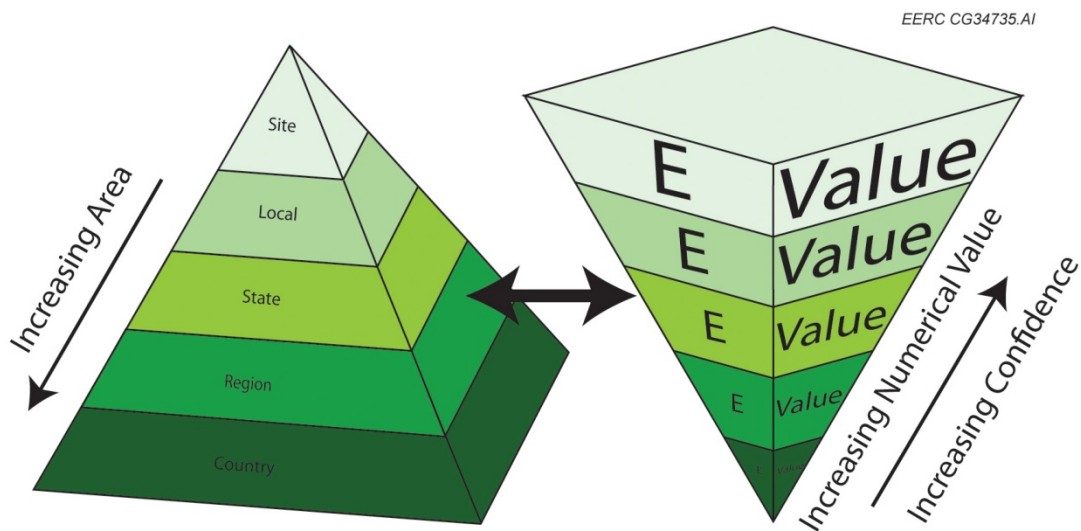


Figure 20. Relationship between the site of the assessment and the resulting storage coefficient.

At the site-specific scale the value of the storage coefficient will increase as well as the confidence in the result, because of increased knowledge of the site.

While geoscientists and engineers will tend to examine geologic storage targets on a formation-by-formation basis, many nontechnical policy makers and stakeholders will often require storage resource to be reported according to geographical conventions such as basins, states/provinces, and entire countries. It is important to remember that these larger geographic areas, which are typically defined by political rather than geologic boundaries, will generally contain several unique and hydrodynamically separate rock formations that may have CO₂ storage resource. These individual formations are often stacked as multiple horizons with variable and sometimes inconsistent areal extent across a given geographical area. Because of this stacked horizontal component, evaluations conducted at the basin, state/province, and country scale must be made by assessing each individual storage formation within that geographical area and summing them to come up with the total effective storage resource of the entire state/province or country.

Site-Specific Storage Coefficients

Site-specific storage coefficients were calculated for three different lithologies, and ten different depositional environments. As stated earlier, the DOE and CSLF methods are basically equivalent, with only minor differences in the storage coefficient (DOE E_E and CSLF C_C) $E_E = C_C * (1 - S_{wirr})$, and as a result, any coefficients developed for one method can quickly and easily be converted to the other method. Because the storage coefficients can be applied to their respective equations and result in the same effective storage resource, they have been listed together for each level of assessment.

In this study, the focus was first to develop site-specific storage coefficients and then to extrapolate those out to the larger regional- and formation-scale storage coefficients. All of the individual values for the variables were determined based on numerical simulations run on models developed from the AGD, except A_n/A_t . Values have not been determined for net to total area because it is very site-specific and requires some knowledge of the geology of the given formation, which is required to calculate an effective storage resource estimate. A value for A_n/A_t was assigned from the Carbon Sequestration Atlas of the United States and Canada (DOE, 2007, 2008). If the actual values of the three geologic variables (A_n/A_t , h_n/h_g , ϕ_{eff}/ϕ_{tot}) are known, they should be used. Alternatively, instead of using a single value for any of the variables, a range could be used, which may be more appropriate if there is a high level of uncertainty in the geologic properties. A range of values for the variables used to calculate the storage coefficients has been presented in Table 12.

For a site-specific assessment, the P10, P50, and P90 values were used for the efficiency variables (E_V , E_d , $\frac{(1 - S_{wave})}{(1 - S_{wirr})}$) determined through numerical simulation and the ϕ_{eff}/ϕ_{tot} value determined from the AGD. For the A_n/A_t and h_n/h_g , it is considered likely that the assessment was conducted over a site that has relatively good formation properties for CO₂ storage. As a result, a value of 80% for A_n/A_t was applied, and the individual P90 values for h_n/h_g within each different lithology or depositional environment were used to calculate the site-specific storage coefficients (Table 13).

Table 12. Ranges of Variables Used to Calculate Storage Coefficients for Different Lithologies and Depositional Environments

Lithology	Depositional Environment	E_{geol}			E_v	E_d	$(1 - S_{\text{wave}})$
		A_n/A_t	h_n/h_g	$\sigma_{\text{eff}}/\sigma_{\text{tot}}$			$(1 - S_{\text{wirr}})$
Clastics	Clastics	0.2–0.8	0.21–0.76	0.64–0.77	0.16–0.39	0.35–0.76	0.44–0.95
Dolomite	Dolomite	0.2–0.8	0.17–0.68	0.53–0.71	0.26–0.43	0.57–0.64	0.71–0.79
Limestone	Limestone	0.2–0.8	0.13–0.62	0.64–0.75	0.33–0.57	0.27–0.42	0.67–0.98
Clastics	Alluvial fan	0.2–0.8	0.21–0.76	0.7–0.82	0.18–0.54	0.32–0.71	0.39–0.89
Clastics	Delta	0.2–0.8	0.21–0.76	0.61–0.71	0.19–0.59	0.39–0.81	0.48–1.00
Clastics	Eolian	0.2–0.8	0.21–0.76	0.69–0.79	0.12–0.54	0.53–0.80	0.66–1.00
Clastics	Fluvial	0.2–0.8	0.21–0.76	0.63–0.77	0.19–0.53	0.34–0.73	0.42–0.90
Clastics	Peritidal	0.2–0.8	0.21–0.76	0.60–0.78	0.14–0.58	0.42–0.80	0.52–0.99
Clastics	Shallow shelf	0.2–0.8	0.21–0.76	0.62–0.78	0.18–0.63	0.39–0.82	0.49–1.00
Clastics	Shelf	0.2–0.8	0.21–0.76	0.62–0.74	0.20–0.59	0.41–0.84	0.51–1.00
Clastics	Slope basin	0.2–0.8	0.21–0.76	0.68–0.77	0.12–0.54	0.53–0.80	0.66–1.00
Clastics	Strand plain	0.2–0.8	0.21–0.76	0.64–0.76	0.19–0.58	0.38–0.74	0.47–0.92
Limestone	Peritidal	0.2–0.8	0.13–0.62	0.61–0.75	0.30–0.67	0.37–0.42	0.87–0.97
Limestone	Reef	0.2–0.8	0.13–0.62	0.62–0.77	0.36–0.63	0.28–0.42	0.66–0.98
Limestone	Shallow shelf	0.2–0.8	0.13–0.62	0.69–0.73	0.44–0.72	0.31–0.42	0.71–0.96

Table 13. P10, P50, and P90 Storage Coefficients E_E and $C_C * (1 - S_{\text{wirr}})$ Calculated for the Site-Specific Scale for Different Lithologies (A_n/A_t is fixed at 0.8)

Lithology	Depositional Environment	P10, %	P50, %	P90, %
Clastics	Not applicable	4.62	6.79	14.92
Dolomite	Not applicable	6.57	7.91	14.92
Limestone	Not applicable	4.24	6.13	9.82
Clastics	Alluvial fan	4.35	6.22	13.97
Clastics	Delta	4.96	6.70	14.03
Clastics	Eolian	5.64	7.44	15.86
Clastics	Fluvial	5.13	6.44	12.50
Clastics	Peritidal	4.12	6.06	15.41
Clastics	Slope basin	4.89	7.39	16.98
Clastics	Shallow shelf	5.41	7.67	15.62
Clastics	Shelf	4.07	6.23	17.23
Clastics	Strand plain	5.40	6.72	12.90
Limestone	Peritidal	4.45	5.61	9.41
Limestone	Reef	4.09	5.31	9.00
Limestone	Shallow shelf	4.70	7.47	10.59

At the site-specific level, the effects of different structures could be quite strong. For example, over the course of the study, it was observed that the storage coefficients calculated for dome structures were found in many cases to be more than twice that of the flat structure, indicating that structural traps are significantly more efficient for storing CO₂. The five generic structures were applied to the heterogeneous models and site-specific values for the storage coefficients for each lithology and depositional environment under each structural setting are reported in Appendix E.

Formation-Based Storage Coefficients

Over an entire formation, it is unlikely that the values of the geologic property variables will be the same as those used to calculate site-specific storage coefficients. This is because it is unlikely that the optimal geologic conditions which typically characterize sites chosen for CO₂ storage will continue to exist over a broader geographic area. This study suggests that a larger portion of the net area and net thickness be excluded to account for the expected variability in geologic properties over the entire formation. For this reason, the P50 values of A_n/A_t (taken from the DOE atlas) and h_n/h_g (calculated from the AGD) were applied in the calculation of formation-level storage coefficients. Table 14 provides the P50-level storage coefficients for formation-scale assessments of CO₂ storage resources and the values of the variables used to generate those coefficients.

Table 14. Formation-Based Storage Coefficients and the P50 Values for Each Variable Used to Calculate the Coefficients

Lithology	A_n/A_t	h_n/h_g	ϕ_{eff}/ϕ_{tot}	E_V	E_d	$\frac{(1 - S_{wave})}{(1 - S_{wirr})}$	E_E and $C_C * (1 - S_{wirr})$, %
Clastics	0.5	0.49	0.71	0.25	0.56	0.7	2.70
Dolomite	0.5	0.43	0.64	0.35	0.6	0.75	3.26
Limestone	0.5	0.33	0.7	0.45	0.35	0.92	2.04
All	0.5	0.42	0.68	0.35	0.50	0.79	2.63

It is recognized that there could be cases where the values for the geologic variables (A_n/A_t , h_n/h_g , ϕ_{eff}/ϕ_{tot}) are extremely over- or underestimated, and it is the responsibility of the investigator to evaluate the formation and ascertain what fraction of the formation or regional pore volume has properties which make it amenable to CO₂ storage and use the appropriate values. It is also worth noting that, in general, the values for the final P50 storage coefficients line up closely with the values reported in the DOE Atlas for formation level E. There is some significant fluctuation in some of the individual efficiency variables. For instance, the results of the single-variable tests indicate that the values for the storage coefficients can fluctuate by as much as double or as little as half of these reported values; however, not all of these variables were tested in the heterogeneous cases, such as depth and temperature. This means E values ranging from less than 1% to more than 4% could be possible even on a large scale, in some settings. A range of P10, P50, and P90 storage coefficients was also calculated and shown in Table 15.

Table 15. P10, P50, and P90 Storage Coefficients Calculated E_E and $C_C * (1 - S_{wirr})$ for the Formation Level for Different Lithologies

Lithology	P10, %	P50, %	P90, %
Clastics	1.86	2.70	6.00
Dolomite	2.58	3.26	5.54
Limestone	1.41	2.04	3.27
All	1.66	2.63	5.13

Only one depositional environment was tested for dolomites, and as such, the high E value may not be representative of all dolomites; however, it gives a starting point. There does seem to be some effect of both depositional environment and lithology on the storage coefficient, but it is important to remember that the heterogeneous models each contained parameters that are specific to different lithologies, such as k_v/k_h , relative permeability curve, porosity distribution, and permeability transform.

Comparison of Open-System Effective Storage Resource Estimation to Closed-System Compressibility Storage Resource Estimation

The effective storage coefficients described in the previous section can be applied at scales from site-specific to formation level to develop estimates of pore volume as long as the system is open. This means that the formation is open to hydrodynamic flow and is relatively free of compartmentalization from faulting or lithology changes. If the formation is not open to hydrodynamic flow and comprises a number of smaller discrete compartments, then each compartment must be assessed individually. Furthermore, the coefficient developed for open systems does not apply to these systems since there is no place to displace the formation brine. In these scenarios, the use of the closed system compressibility coefficient is required.

It is worth noting that the compressibility method is equivalent to the DOE method at both the theoretical and characterized levels of the proposed storage resource classification system as:

$$V_{CO_2,DOE_T} = V_{CO_2,comp_T} = A * h * \phi$$

$$V_{CO_2,DOE_C} = V_{CO_2,comp_C} = A * h * \phi * E_{Geol}$$

$$E_{Geol} = \frac{A_n}{A_t} * \frac{h_n}{h_g} * \frac{\phi_{eff}}{\phi_{tot}}$$

At the effective storage resource level, the two methods are not equivalent and are defined as:

$$V_{CO_2,DOE_E} = A * h * \phi * E_E$$

$$E_E = \frac{A_n}{A_t} * \frac{h_n}{h_g} * \frac{\phi_{eff}}{\phi_{tot}} * E_A * E_I * E_g * E_D$$

$$V_{CO_2,comp_E} = A * h * \phi * E_{Geol} * E_{comp}$$

$$E_{comp} = \frac{\Delta V_t}{V_{po}} = (c_w + c_p) \Delta p$$

In most cases, the effective compressibility storage resource is substantially lower than an open-system effective storage resource estimate. To illustrate this point, the two systems are compared on an equal area example, one with open boundary conditions (representing the open system) and the other with closed-boundary conditions (representing a single compartment in a closed system). For this example, all formation properties are equal except the boundary conditions and are shown in Table 16. Under these conditions, the effective storage resource, as developed under the DOE method, would be 6.28 billion m³, and since it is an open system, the pressure should return to the original pressure after some period of time, and as such, the density of CO₂ would be approximately 685 kg/m³ (Span and Wagner, 1996) resulting in a storage mass of 4.3 billion tonnes CO₂. If the formation is closed, then the storage will be limited to the compressibility of the formation, formation fluids, and the maximum pressure change within the formation, which in this case is:

$$E_{comp} = [(3.93E - 07 + 3.48E - 07) / kPa] * 7,900kPa = 0.00585 = 0.59\%$$

Table 16. Assessment Area Properties for the Comparison of the Open and Closed Systems Effective Storage Resource

Assessment Area/Compartment Area, km ²	2,500
Formation Thickness, m	100
Formation Volume, m ³	2.50 * 10 ¹¹
Total Porosity, %	20
Formation Depth, m	2,336
Initial Pressure, kPa	23,900
Maximum BHP, kPa	31,800
Maximum ΔP, kPa	7,900
Formation Temperature, °C	75
Formation Compressibility, 1/kPa	3.48 * 10 ⁻⁷
Brine Compressibility, 1/kPa	3.93 * 10 ⁻⁷
A _n /A _t	0.5
h _n /h _g	0.42
ø _c /ø _{tot}	0.68
E _{Geol}	0.14
E _E	2.51%
E _{comp}	0.59%
Effective Pore Volume, m ³	3.57 * 10 ¹⁰
V _{CO₂,DOE_E} , m ³	6.28 * 10 ⁹
V _{CO₂,comp_E} , m ³	2.09 * 10 ⁸
M _{CO₂,DOE_E} , tonnes (tons)	4.30 * 10 ⁹ (4.74 * 10 ⁹)
M _{CO₂,comp_E} , tonnes (tons)	1.64 * 10 ⁸ (1.91 * 10 ⁹)

This low value for the compressibility coefficient results in a storage volume of 209 million m³. Since the system is closed, the pressure in the formation would remain at the maximum formation pressure of 31,800 kPa, and as a result, the density of the CO₂ would be approximately 785 kg/m³ (Span and Wagner, 1996), resulting in an effective storage resource mass of 164 million tonnes of CO₂, which is approximately 25 times lower than the open system with equal formation properties. It is also worth noting that the closed-system final pressure is much higher than the open-system final pressure, which may reduce storage security. The storage resource of the closed system could be increased by producing brine from the formation; however, then there will be the issue of brine treatment and disposal, which is economic in nature and beyond the scope of this project.

Applicability and Limitations

The methods presented in this document can serve as a guide for developing estimates of effective storage resources at the site-specific to the formation level and can further be expanded to cover other assessment areas.

Once a formation has been determined to be a target of investigation, the investigator must decide on a scale of assessment, including a formation and a geographical area. In the case that multiple formations are being considered within the same area, each formation must be assessed individually. Data should be gathered pertaining to the formation properties and boundary conditions. If boundary conditions are known, work should be focused on the methodology presented for either open or closed formations. Both equations may be applied if boundary conditions are unknown or unclear, which aids in determining the endpoints defining the range of possible efficiency coefficients.

For closed boundary conditions, storage efficiency and the storage coefficient are defined by the compressibility of water and the dilation of pores in response to an increase in pressure and the difference between the maximum formation pressure and the initial formation pressure. Storage coefficients calculated for closed systems are generally lower than those calculated for open systems by an order of magnitude; however, they may be increased by producing water from the system and reducing the formation pressure buildup. For open systems, storage efficiency is defined by the shape and concentration of the CO₂ plume resulting from injection and how effectively the CO₂ fills the accessible volume. First, the terms representing geological factors should be applied that remove the areas, thicknesses, and porosities that are not amenable to CO₂ storage. Following this step, volumetric plume behavior should be considered by detailed characterization, computer modeling, and simulation, although for a preliminary estimate, values presented in this document may be considered as a good foundation. This, however, is never a substitute for site-specific modeling and is meant only to enable a reasonable first estimate.

At this point in the assessment process, a detailed site-specific effective storage resource has been determined, which represents the technically attainable volume of storage space based on the injection parameters input into the model and simulation. Optimization can occur by preferentially choosing the most efficient areas, most effective injection parameters, or both. If sufficient scalability and adequate sample population exist to quantify the short- and long-range variability of the investigated geologic unit, the efficiency of a formation may be estimated. This

interpolation assumes that wells can be placed regularly throughout the net area of the area of assessment and that each sample is representative of a larger area.

The tables of site-specific storage coefficients presented in Appendix E are meant to represent the range of values based on the data collected in the average global database. They are not specific to any site but can be useful as a generalized comparison tool as well as an illustration of the expected ranges of different conditions and a demonstration of the methodology. One observation made during analysis is that the value for efficiency varies over time. The snapshot at which efficiency was reported was kept constant at the end of injection, which eliminates assigning an arbitrary time period for generic models. This should be taken into account when considering numbers calculated in Appendix E.

SUMMARY AND CONCLUSIONS

Identifying potential geologic sinks for CO₂ storage and developing reliable estimates of their storage resource/capacity are critical components of determining the efficacy of CCS. The development of technically robust storage coefficients has been identified as one of the most crucial aspects in the advancement of broadly applicable and comparable storage resource/capacity estimates at all scales. As such, the EERC has set out to first compare the methods by which storage resources are evaluated. It was determined that the previously published classification systems laid a solid foundation; however, some improvement could be made. As such, a new classification system has been proposed that more accurately represents the different levels of storage resource and capacity estimates. Following this assessment, the methods for calculating storage resource/capacity were evaluated and two general systems were considered, open systems and closed systems. The open system is an appropriate assumption in large broad basins with little tectonic activity. Closed systems are representative of heavily faulted compartmentalized formations and, in general, have a lower potential to store injected CO₂. Two methodologies were considered for open systems, the CSLF methodology and the DOE methodology; these two systems are basically equivalent and, as such, have been related by a series of equations so that storage estimates developed under one system can be accurately compared to estimates made with the other.

The application of storage coefficients to depleted hydrocarbon fields was examined, with an emphasis on the DOE and CSLF methods for estimating CO₂ storage in oil and gas fields. However, no new storage coefficients for depleted hydrocarbon fields were developed. This is because the complex and site-specific nature of the reservoirs and reservoir fluids would require a level of evaluation and modeling that is beyond the scope of this study. Furthermore, it is likely that because hydrocarbon reservoirs have been produced for decades, their characteristics are probably very well known, and the application of storage coefficients is less necessary. Storage capacities of depleted hydrocarbon reservoirs can be fairly accurately estimated through well-documented, accepted methods with little need to apply a storage coefficient that goes beyond those that have already been published by CSLF and DOE.

Effective storage coefficients have been developed for deep saline formations at scales ranging from site-specific to entire formations. For example, storage coefficients which are

calculated at the site-specific scale using real-world data and numerical simulations can be extrapolated to the formation scale as long as the formation is open to hydrodynamic flow and not compartmentalized. To determine storage volumes for entire basins, estimates for each formation being considered within the basin must be added up to develop a total storage resource for the basin. This same methodology would apply for estimating storage resource within state/provincial and national boundaries. In this way, the application of broadly applicable storage coefficients can be used to estimate storage resource at levels ranging from site-specific to formation level, ultimately spanning large sedimentary basins and even entire nations and continents.

The storage coefficients developed over the course of this study and presented in this report advance the estimation of storage resources from the theoretical to characterized to the effective level as defined by the proposed storage classification system. In the study, ranges developed by DOE have been improved upon, and the study established new, effective storage coefficients that can be applied to the CSLF method. Specifically, the values for the effective storage coefficients at the formation level for the DOE E_E and the CSLF $C_c * (1 - S_{wirr})$ range from 1.4% to 6.0%, within an 80% confidence interval. It is worth noting that the effective storage coefficient reported in the Carbon Sequestration Atlas for the United States and Canada (DOE, 2007, 2008), developed through Monte Carlo simulation, for the P50 of E_E is approximately 1.8% to 2.2%, which is in close agreement with the P50 values of the effective storage coefficients E_E of 2.0% to 3.3% as calculated through numerical simulations in this study.

Key findings of this project include the following:

- A new and improved storage classification system was developed and related to the most relevant CCS terminology.
- Three different resource estimation methods were examined, two for open systems (DOE and CSLF) and one for closed systems. The DOE and CSLF methodologies were related to the proposed storage classification system.
- Since previous work had demonstrated that the DOE and CSLF methods are basically equivalent, the two methods were related to each other through a series of variables and equations so that storage estimates made with one system can be easily compared to estimates made with the other. This also means that any storage coefficients developed for one method can be translated to the other.
- A series of parameters that affect the storage coefficients were tested to determine the amount of influence they have on the effective storage resource estimates.
- A series of storage coefficients were developed for open systems for both the DOE and CSLF resource estimation methods. These coefficients were developed for both the site-specific level for different lithologies, depositional environments, and structures and for the formation level for different lithologies, since it is unlikely that any one structure or depositional environment could be extrapolated to the entire formation.

- It is suggested that future work should focus on the modeling and injection simulations on entire formations and even basins to determine the effect of an individual injection operation on other injection projects in the same formation or basin.

REFERENCES

- Bachu, S., Bonijoy, D., Bradshaw, J., Burruss, R., Holloway, S., Christensen, N.P., and Mathiassen, O.M., 2007, CO₂ storage capacity estimation—methodology and gaps: *International Journal of Greenhouse Gas Control I*, Elsevier, p. 430–443.
- Bennion, B., and Bachu, S., 2008, Drainage and imbibition relative permeability relationships for supercritical CO₂/brine systems in intergranular sandstone, carbonate, shale, and anhydrite rocks: *SPE Reservoir Evaluation & Engineering*, June, p. 487–496.
- Benson, S.M., 2009, Relative permeability explorer: A database of relative permeability curves: <http://pangea.stanford.edu/research/bensonlab/relperm/index.html> (accessed: July 27, 2009).
- Bradshaw, J.; Bachu, S.; Bonijoly, D.; Burruss, R.; Holloway, S.; Christensen, N.P.; and Mathiassen, O.M., 2007, CO₂ storage capacity estimation—issues and development of standards: *International Journal of Greenhouse Gas Control I*, Elsevier, p. 62–68.
- CO₂CRC, 2008, Storage capacity estimation, site selection and characterisation for CO₂ storage projects: Cooperative Research Centre for Greenhouse Gas Technologies, Canberra, CO₂CRC Report No. RPT08-1001, 52 pp.
- Carbon Sequestration Leadership Forum, 2005, A task force for review and development of standards with regards to storage capacity measurement—Phase I: CSLF-T-2005-9 15, August 2005, 16 p., www.cslforum.org/publications/documents/PhaseIReportStorageCapacityMeasurementTaskForce.pdf (accessed June 2009).
- Carbon Sequestration Leadership Forum, 2007, Estimation of CO₂ storage capacity in geological media—Phase II report: June 15, 2007, www.cslforum.org/publications/documents/PhaseIIReportStorageCapacityMeasurementTaskForce.pdf (accessed June 2009).
- Carbon Sequestration Leadership Forum, 2008, Comparison between methodologies recommended for estimation of CO₂ storage capacity in geologic media—Phase III report: April 21, 2008, www.cslforum.org/publications/documents/PhaseIIIReportStorageCapacityEstimationTaskForce0408.pdf (accessed June 2009).
- Deutsch, C.V., 2008, *Fundamentals of geostatistics—principles and hands-on practice* (2008 ed.).
- Deutsch, C.V., and Journel, A.G., 1998, *GSLIB—geostatistical software library and user's guide*: Oxford.

- Ennis-King, J., and Paterson, L., 2005, Role of convective mixing in the long-term storage of carbon dioxide in deep saline formations: SPE Paper 84344 presented at the SPE Annual Technical Conference and Exhibition, Denver, CO., Oct 5–8, 2003, Paper Peer Approved May 5, 2005.
- Gas Information System (GASIS release 2, NETL Version), 1999—a national database of geological, engineering, production and ultimate recovery data for U.S. oil and natural gas reservoirs: U.S. Department of Energy National Energy Technology Laboratory Strategic Center for Natural Gas.
- Hall, M., 2002, Integrating well observations with seismic interpretation, Canadian Society of Petroleum Engineers: www.cspg.org/conventions/abstracts/2002abstracts/extended/270S0125.pdf.
- Hyne, N.J., 2006, Dictionary of petroleum exploration, drilling and production: PennWell Corporation, p. 34–35.
- IEA Greenhouse Gas R&D Programme (IEA-GHG), November 2008, Aquifer storage—development issues: 2008/12.
- Metz, B., Davidson, O., de Coninck, H.C., Loos, M., and Mayer, L.A., eds., 2005, Intergovernmental Panel on Climate Change special report on carbon dioxide capture and storage: Cambridge University Press, Cambridge, United Kingdom, 442 p.
- Kopp, A.; Class, H.; and Helmig, R. 2009, Investigations on CO₂ storage capacity in saline aquifers—part 2—estimation of storage capacity coefficients: International Journal of Greenhouse Gas Control, Elsevier, in press.
- Merriam–Webster Online, 2009: [www.merriam-webster.com/dictionary/continent\[2\]](http://www.merriam-webster.com/dictionary/continent[2]) (accessed 2009).
- Span, R., and Wagner, W., 1996, A new equation of state for carbon dioxide covering the fluid region from the triple-point temperature to 1100°K at pressures up to 800 MPa: Journal of Physical Chemistry, v. 25, no. 6, Ref. Data.
- Society of Petroleum Engineers, World Petroleum Council, American Association of Petroleum Geologists, 2007, Petroleum resources management system.
- Total Oil Recovery Information System (TORIS), 1995—an integrated decision support system database for petroleum E&P policy evaluation: U.S. Department of Energy National Energy Technology Laboratory National Petroleum Technology Office.
- U.S. Department of Energy, [n.d.], Glossary of terms: draft. www.directives.doe.gov/pdfs/doegeninfo/draft/glossary.pdf, accessed 2009.

U.S. Department of Energy National Energy Technology Laboratory Office of Fossil Energy, 2007, Carbon sequestration atlas of the United States and Canada.

U.S. Department of Energy National Energy Technology Laboratory Office of Fossil Energy, 2008, Carbon sequestration atlas of the United States and Canada.

United States Geological Survey, [n.d.], Organic origins of petroleum: http://energy.er.usgs.gov/gg/research/petroleum_origins.html, accessed April 17, 2009.

Zhou, Q., Birkholzer, J. T., Tsang, C.-F., and Rutqvist, J., 2008, A method for quick assessment of CO₂ storage capacity in closed and semiclosed saline formations: *International Journal of Greenhouse Gas Control*, v. 2, no. 4, p. 626–639.

APPENDIX A

REFERENCES FOR THE AVERAGE GLOBAL DATABASE

Appendix A – References for the Average Global Database (AGD)

The AGD is made up of smaller databases whose sources are too numerous to list in the document and as a result have been listed here.

- Al-Hashami, A, Ren, S.R., and Tohidi, B., 2005, CO₂ injection for enhanced gas recovery and geo-storage—reservoir simulation and economics: SPE International Paper No. 94129.
- Allen, M., 2003, The application of Nadeland Gussman Permian L.L.C. for permanent field rules for the Moelson (Clear Fork) Field, Irion County, Texas: Oil and Gas Docket No. 7C-0233649.
- Alsharhan, A.S., and Nairn, A.E.M., 1997, Sedimentary basins and petroleum geology of the Middle East: Elsevier Science Ltd.
- Arkansas Geological Survey, 2007, Petroleum geology of South Arkansas and the Gulf Coastal Plain: www.geology.arkansas.gov/fossil_fuels/oil_geol_prodarea.htm, accessed March 18, 2009.
- Barnaby, R.J., and Ward, W.B., 2007, Outcrop analog for mixed siliciclastic—carbonate ramp reservoirs—stratigraphic hierarchy, facies architecture and geologic heterogeneity [abs.]: Grayburg Formation, Permian Basin, U.S.A., Abstract, Journal of Sedimentary Research, v. 77, no. 1.
- Bennion, B., and Bachu, S., 2005, Relative permeability characteristics for supercritical CO₂ displacing water in a variety of potential sequestration zones in the western Canada sedimentary basin: SPE International Paper No. 95547.
- Brenner, R., 1978, Sussex sandstone of Wyoming—example of Cretaceous offshore sedimentation: The American Association of Petroleum Geologists Bulletin, v.62, no. 2, p. 181–200.
- Brister, B., and Ulmer-Scholle, D., 2003, Interpretation of depositional environments of Upper Seven Rivers Formation from core and well logs, Grayburg Jackson Pool, Eddy County, New Mexico: Adapted from poster presentation at Southwest Section, AAPG Annual meeting, Texas, Search and Discovery Article #20023 (2004).
- Bruce, A., 1979, Atoka Formation (Pennsylvanian) deposition and contemporaneous structural movement, southwestern Arkoma Basin [abs.]: Oklahoma, American Association of Petroleum Geologists Bulletin v. 63, no. 11, p. 2114–2120.
- Chadwick, R.A., Zweigel, P., Gregersen, U., Kirby, G.A., Holloway, S., and Johannessen, P.N., 2004, Geological reservoir characterization of a CO₂ storage site—the Utsira Sand, Sleipner, northern North Sea: Energy, vol. 29, p. 1371–1381.

- Changsu, R., and Popp, R., 2004, Sequence stratigraphic controls of hydrocarbon reservoir architecture—case study of Late Permian (Guadalupian) Queen Formation, Means Field, Andrews County, Texas: Texas A&M.
- Chowdhury, A.H., and Turco, M., [n.d], Geology of the Gulf Coast Aquifer, Texas: [unknown publication].
- Cinar, Y., and others, 2007, Geo-engineering and economic assessment of a potential carbon capture and storage site in southeast Queensland, Australia: SPE International Paper No. 108924.
- Cook, P., 2006, House of Representatives Science and Innovation Committee inquiry into geosequestration: Cooperative Research Centre for Greenhouse Gas Technologies
- Davis, G.H., and Reynolds, S.J., 1996, Structural geology of rocks and regions (2d ed.): John Wiley & Sons, Inc.
- Davis, N., Riddiford, F., Bishop, C., Taylor, B., and Froukhi, R., 2001, The In Salah gas project, central Algeria—bringing an eight-field gas development to sanction: SPE International Paper No. 68180.
- Doughty, C., and others, 2006, Capacity investigation of brine-bearing sands of the Frio Formation for geologic sequestration of CO₂: U.S. Department of Energy National Energy Technology Laboratory.
- Dutton, S., Finley, R., and Herrington, K., 1987, Organic geochemistry of the Lower Cretaceous Travis Peak Formation, East Texas Basin: Bureau of Economic Geology, University of Texas at Austin.
- Emmons, W., 1921, Geology of petroleum: McGraw-Hill Book Company, Inc.
- Flett, M., and others, 2008, Gorgon Project—subsurface evaluation of carbon dioxide disposal under Barrow Island: SPE International Paper No. 116372.
- Fowler, G.M., 1933, Oil and oil structures in Oklahoma—Kansas zinc—lead mining field: Bulletin of the American Association of Petroleum Geologists, v. 17, no. 12, p. 1436–1445.
- Frykman, P., Zink-Jorgensen, K., Bech, N., Norden, B., Forster, A., and Larsen, M., 2006, Site characterization of fluvial, incised valley deposits, in CO₂SC Symposium [Proceedings].
- Gahring, R.R., 1958, History and development of north Madill Field, Marshall County, Oklahoma: Sinclair Oil and Gas Company.
- The GasGun, 2000, Field results, Kansas: http://thegasgun.com/?page_id=31, accessed March 18, 2009.

- The GasGun, 2000, Field results, Oklahoma: http://thegasgun.com/?page_id=38, accessed March 18, 2009.
- Gas Information System (GASIS release 2, NETL Version), 1999—a national database of geological, engineering, production and ultimate recovery data for U.S. oil and natural gas reservoirs: U.S. Department of Energy National Energy Technology Laboratory Strategic Center for Natural Gas.
- Geel, K., Arts, R., van Eijs, R., Kreft, E., Hargman, J., D’Hoore, D., 2006, Geological site characterization of the nearly depleted K12-B Gas Field, offshore The Netherlands: TNO. http://esd.lbl.gov/CO2SC/co2sc_presentations/Site_Characterization_Case_Studies/Geel.pdf, accessed April 2009.
- Gupta, N., Jaguki, P., Sminchak, J., Kelley, M., Spitznogle, G., and Sherrick, B., 2008, Integration and deployment of geologic storage and monitoring across two deep saline reservoirs with post-combustion capture at American Electric Power Mountaineer Plant: Presented at 9th International Conference on Greenhouse Gas Control Technologies (GHGT 9), Washington, D.C., November 16–20, 2008, Energy Procedia 00, Elsevier Science Ltd.
- Hartig, K., [n.d.], Origin of dolomite in loessitic paleosols of the Abo and Tubb Units, northeastern New Mexico: University of Oklahoma.
- Hortle, A., Xu, J., and Dance, T., 2008, Hydrodynamic interpretation of the Waarre Fm Aquifer in the Onshore Otway Basin—implications for the CO2CRC Otway Project: Energy Procedia 00, Elsevier Science Ltd.
- Hovorka, S.D., Doughty, C., Knox, P.R., Green, C.T., Pruess, K., and Benson, S.M., [n.d.], Evaluation of brine-bearing sands of the Frio Formation, Upper Texas Gulf Coast, for geological sequestration of CO₂: [unknown publication].
- IEA Greenhouse Gas R&D Programme, 2004, IEA GHG Weyburn CO₂ Monitoring & Storage Project: IEA GHG.
- Jarrell, P.M., Fox, C.E., Stein, M.H., and Webb, S.L., 2002, Practical aspects of CO₂ flooding: Society of Petroleum Engineers, Monograph Series v. 22.
- Jones, W., 1945, Bacon Limestone, East Texas: Geological Notes.
- Justen, J., 1957, Canada’s Pembina Field: Society of Petroleum Engineers Paper No. 856-G.
- Kansas Geological Survey, 1943, Forest City Basin stratigraphy: http://www.kgs.ku.edu/Publications/Bulletins/51/03_strat.html, accessed March 18, 2009.

- Land, L.S., and Fisher, R.S., 1987, Wilcox Sandstone diagenesis, Texas Gulf Coast—a regional isotropic comparison with the Frio Formation [abs.]: Geological Society, London, Special Publications, v. 36, p. 291–235.
- Love, J.D., and Christiansen, A.C., 1985, Explanation for geological map of Wyoming: The Geological Survey of Wyoming, U.S. Department of the Interior.
- Lyons, W.C., and Plisga, G.J., 2005, Standard handbook of petroleum and natural gas engineering (2d ed.): Elsevier Inc.
- Maldal, T. and I.M. Tappel, 2004, CO₂ Underground Storage for Snohvit Gas Field Development, Energy 29, 1403-1411, Elsevier Science Ltd
- Maslyn, M., 1996, Mineralized Late-Mississippian paleokarst features and paleogeography in the Leadville, Colorado Area: NSS Convention Guidebook.
- Mitchell-Tapping, H.J., 1981, Petrophysical properties of the Sligo Formation of northern Louisiana and Arkansas: Gulf Coast Association of Geological Societies, v. XXXI.
- Moore, C., 1947, Subsurface geological cross section McAlester Basin to Anadarko Basin, central Oklahoma: Academy of Science.
- Ohsumi, T., 2003, Regulatory issues in RITE's field test of CO₂ aquifer sequestration: Research Institute of Innovative Technology for the Earth.
- Petermen, J., 2001, Petrographic and petrophysical characteristics of the McCracken Sandstone member of Elbert Formation, Lisbon Field, Paradox Basin, Utah [abs.]: Rocky Mountain and South Central Sections, GSA, Joint Annual Meeting.
- Playnski, S., Lani, B., and Nemeth, K., 2008, Southeast regional carbon sequestration partnership —deployment phase: National Energy Technology Laboratory.
- Preston, R.D., [n.d.], The Yegua–Jackson Aquifer: [unknown publication].
- Roth, R., 1934, Type section of Hermosa Formation, Colorado: Geological Notes.
- Rouse, 1944, Correlation of the Pecan Gap, Wolfe City, and Annona Formations in East Texas: Bulletin of the American Association of Petroleum Geologists, v. 28, no. 4, p. 522–530.
- Smith, J., 2008, The handbook of Texas online: Texas State Historical Association, www.tshaonline.org/handbook/online/articles/SS/dosqw.html, accessed March 18, 2009.
- Spooner, W.C., 1928, Stephens Oil Field, Columbia and Ouachita Counties, Arkansas: Arkansas Geological Survey.

- Tokar, R.J., and Evans, J., 1993, Depositional environments of the Pictured Cliffs Sandstone, Late Cretaceous near Durango, Colorado: *Ohio Journal of Science*.
- Total Oil Recovery Information System (TORIS), 1995—an integrated decision support system database for petroleum E&P policy evaluation: U.S. Department of Energy National Energy Technology Laboratory National Petroleum Technology Office.
- Triyana, Y.Y., 2003, Characterization of Rodessa Formation reservoir (Lower Cretaceous) in Van Field, Van Zandt County, Texas: Texas A&M.
- United States Geological Survey, 2006, Stratigraphy of Canyonlands National Park: U.S. Department of the Interior, U.S. Geological Survey, http://3dparks.wr.usgs.gov/coloradoplateau/canyonlands_strat.htm, accessed March 18, 2009.
- Valasek, D., [n.d.], The Tocito Sandstone in a sequence stratigraphic framework—an example of landward-stepping small-scale genetic sequences, [unknown publication].
- Whitbread, T., 2002, The structural and stratigraphic history of the prolific gas-bearing Vicksburg Province of south Texas—an integrated study of 3D mapping and well correlation [abs.]: AAPG Annual Meeting.
- Wilhelm, C.J., Harris, H.M., and Harlin, M.N., 1950, Petroleum-engineering study of the Carthage Gas Field, Panola County, Texas: Bureau of Mines Report of Investigations 4698, U.S. Department of the Interior.
- Winham, H., 1942, An engineering study of the Magnolia Field in Arkansas [abs.]: Technical Publications and Contributions.
- Zerai, B., 2005, CO₂ sequestration in saline aquifer—geochemical modeling, reactive transport simulation and single-phase flow experiment: Case Western Reserve University.

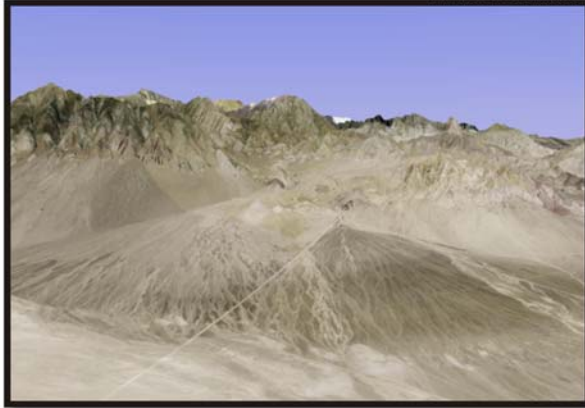
APPENDIX B

REVIEW OF DEPOSITIONAL ENVIRONMENTS

Appendix B – Review of Depositional Environments

Ten depositional environments representing the most common settings for sedimentary rock accumulation were chosen for heterogeneous simulation runs. Each situation possesses unique properties that impact the behavior and, inevitably, the storage capacity of the system. This section presents a summary of each system as well as satellite images of modern examples. Material for this section was taken from Boggs, S., Jr., 2001, Principles of sedimentology and stratigraphy (3rd ed.): Prentice Hall.

EERC ES34646.CDR



Alluvial Fan – Alluvial fans are continental deposits commonly found in mountainous terrain. The deposits form from sedimentary erosion and are transported by a combination of stream and debris flow from the highland to a depositional surface below. Sediments are typically poorly sorted and angular shaped. *Example: Death Valley margin, California, image from Google Earth.*



Delta – Deltas are marginal marine sedimentary deposits that form when a fluvial system such as a river enters a larger body of stagnant water, such as the ocean. Deposits consist of materials that have been transported from the river watershed and are generally well-rounded and well-sorted. *Example: Mississippi Delta, Louisiana, image from Google Earth.*



Eolian – Eolian deposits are continental deposits that form from windblown materials. These deposits are typically found in deserts but also include massive loess deposits. Eolian deposits are typically very well sorted and well rounded and tend to be very fine grained. Cross-bedding is a prevalent depositional feature in this environment. *Example: Namibian Coast, Africa, image from Google Earth.*



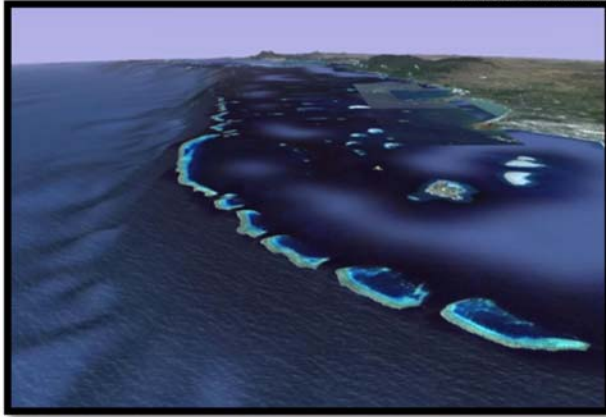
Fluvial – Fluvial systems are water-driven systems, including rivers and streams. Fluvial systems are dynamic and consist of numerous small-scale structures made of materials eroded from the watershed. Sediments are of variable size depending on the velocity of the water, ranging from silt and clay to large boulders. *Example: Southern Alaska, image from Google Earth.*



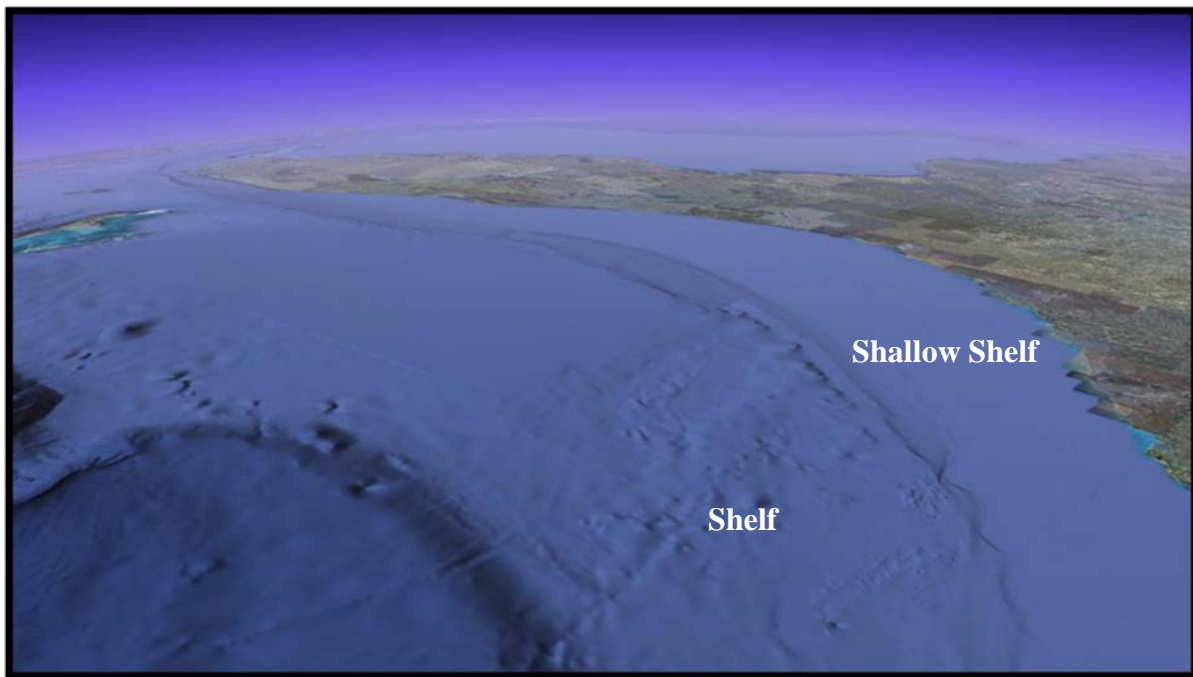
Peritidal – Peritidal systems cover nearshore marine environments, including subtidal, intertidal, and supratidal areas. This type of environment is also referred to as tidal flats and also incorporates the very shallow water as well as the land slightly above high-tide level, which is prone to flooding from storm surge. Sediments can be sands and clays washed from the shore, carbonates from organisms, or even salts left behind from saltwater pool evaporation. *Example: Northern Coast, Saudi Arabia, image from Google Earth.*



Slope/Basin – Beyond the shelf lies the continental slope, which is a steep decline (4 to 45 degrees) from the end of the shelf (average water depth 130 m) to the basin plane (approximately 1500–4000 m deep). Fine mud particles, ash, and organic skeletal material accumulate along the slope and in the associated turbidite and submarine fan deposits. *Example: Offshore, North Carolina, image from Google Earth.*



Reef – Reefs are complex organic communities that form in marine environments. They include barrier reefs, pinnacle reefs, bioherms, and atolls. Reefs possess vast diversity depending on the organisms that are present, ranging from algae-like microbes to skeletal corals, which secrete carbonate as a by-product or as an exoskeleton. *Example: Great Barrier Reef, Australia, image from Google Earth.*



Shallow Shelf and Shelf– Shallow Shelf environments are nearshore depositional settings on the continental slope, which is dominated by tidal, wind, and storm wave processes. The shallow shelf is a more chaotic setting, where sands and clays accumulate from the continent, limestones and dolomites are formed by biologic and chemical activity, and erosional forces mix, sort, and transport deposited materials. Water depth in the shallow shelf extends to about 30 m. Shelf environments are more densely populated by marine organisms and represent a calmer, more consistent landscape made of very fine grained material, such as clay, or biological limestone, such as shells or pellets. Ocean currents and tidal forces continue to move clastic materials along this zone, and much of the surface becomes bioturbated by organisms. *Example: Offshore Florida, image from Google Earth.*



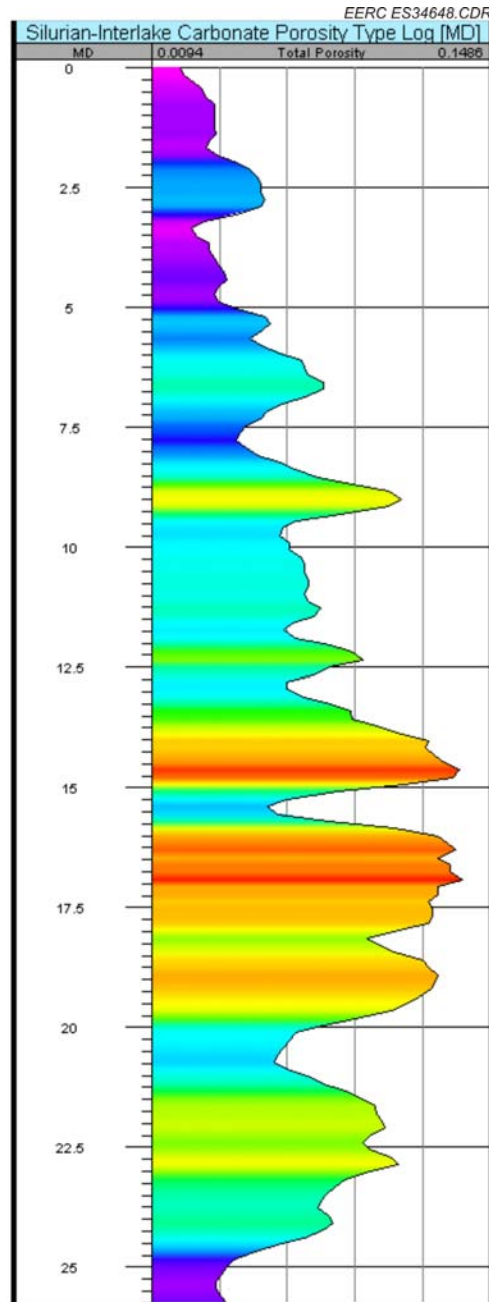
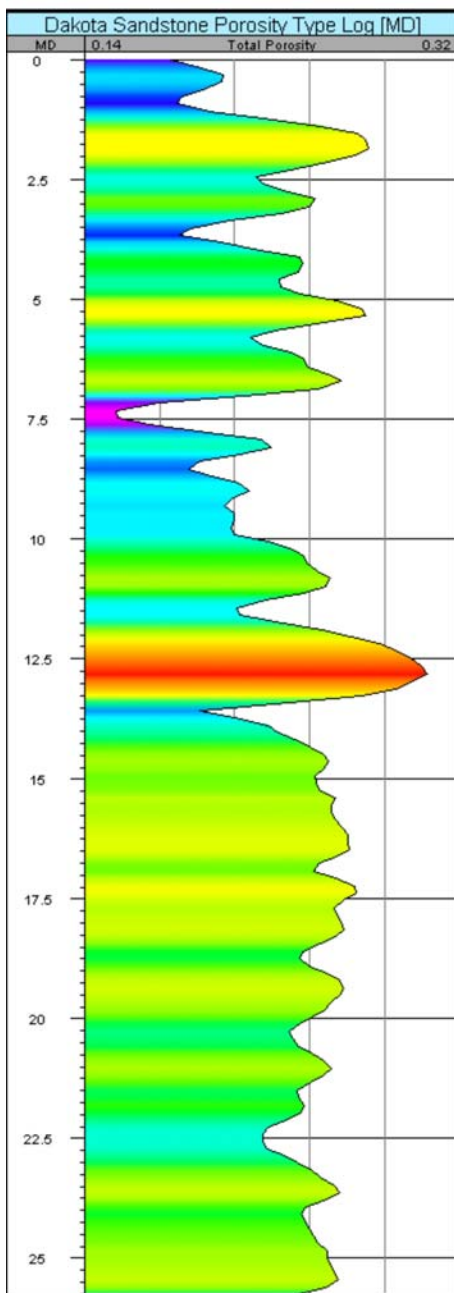
Strand Plain – Strand plains are nearshore marine deposits, including beaches and beach–ridge systems consisting of multiple ridges and parallel swales. Strand plains typically contain various sizes of sand deposited in long, thin lobes. The strand plain environment also includes barrier islands and the lagoons associated with them. *Example: Eastern Australia, image from Google Earth.*

APPENDIX C

CLASTIC AND CARBONATE TYPE LOGS

Appendix C – Clastic and Carbonate Type Logs

Two type logs, one for clastics and one for carbonates, were used that fit the P50 reservoir thickness for each lithology. The clastic sandstone type log was acquired from the Cretaceous Dakota Sandstone interval in the Foreman Butte oil field of North Dakota, USA. The limestone and dolomite type log was acquired from the Silurian Interlake Formation in the Beaver Lodge oil field of North Dakota, USA. The Interlake Formation is an alternating dolomite and limestone mixture, allowing for the use of this single type log for both limestone and dolomite lithologies.



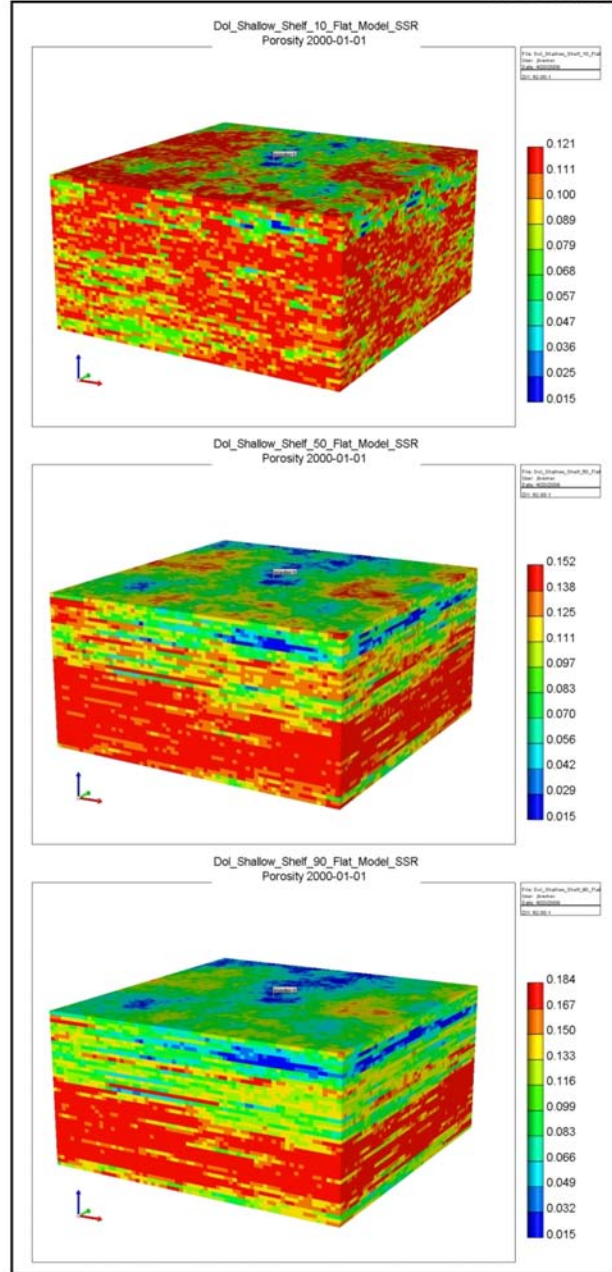
APPENDIX D

POROSITY DISTRIBUTION FOR EACH LITHOLOGY AND DEPOSITIONAL ENVIRONMENT

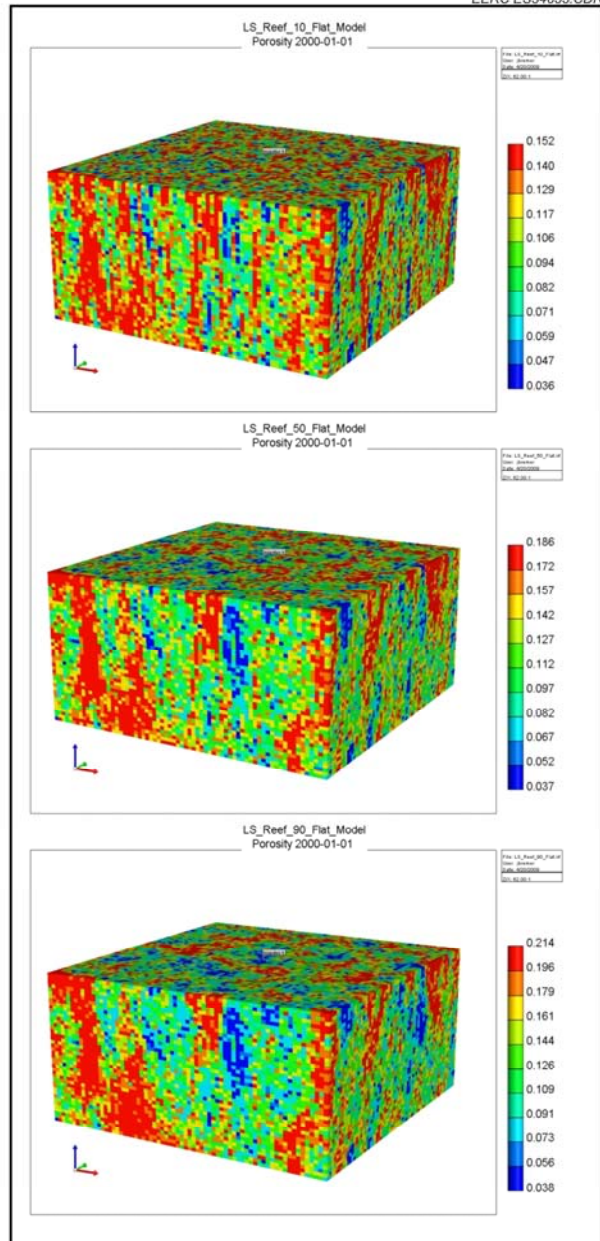
Appendix D – Porosity Distribution for Each Lithology and Depositional Environment

EERC ES34649.CDR

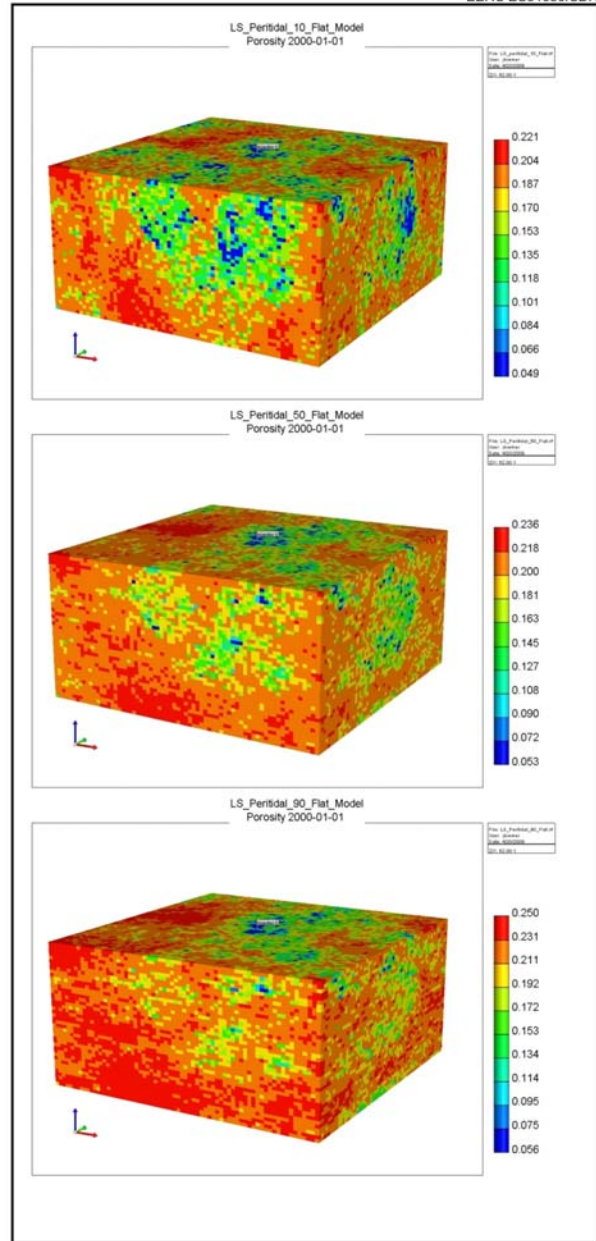
Dolomite Shallow Shelf			
Model Properties	P10	P50	P90
Horizontal Variogram Range Short (m)	397	1081	1764
Horizontal Variogram Range Long (m)	5111	13892	22674
Vertical Variogram Range Short (m)	1	1	1
Vertical Variogram Range Long (m)	14	14	14
Rock Compressibility (1/kPa)	5.26E-07	5.26E-07	5.26E-07
Effective Φ Min %	1	1	1
Effective Φ Mean %	10	12	14
Effective Φ Max %	12	15	18
Permeability Min (m ²)	2.87E-16	9.19E-16	2.94E-15
Permeability Mean (m ²)	5.82E-11	8.81E-11	1.50E-10
Permeability Max (m ²)	1.34E-13	2.18E-13	3.55E-13
k_v/k_h Ratio	0.209	0.487	0.835
Salinity (ppm) P50	53,080	53,080	53,080
Reservoir Depth (MD) (m) P50	2336	2336	2336
Temp (°C) P50	75	75	75
Reference Pressure at 2336 m (kPa)	23,900	23,900	23,900



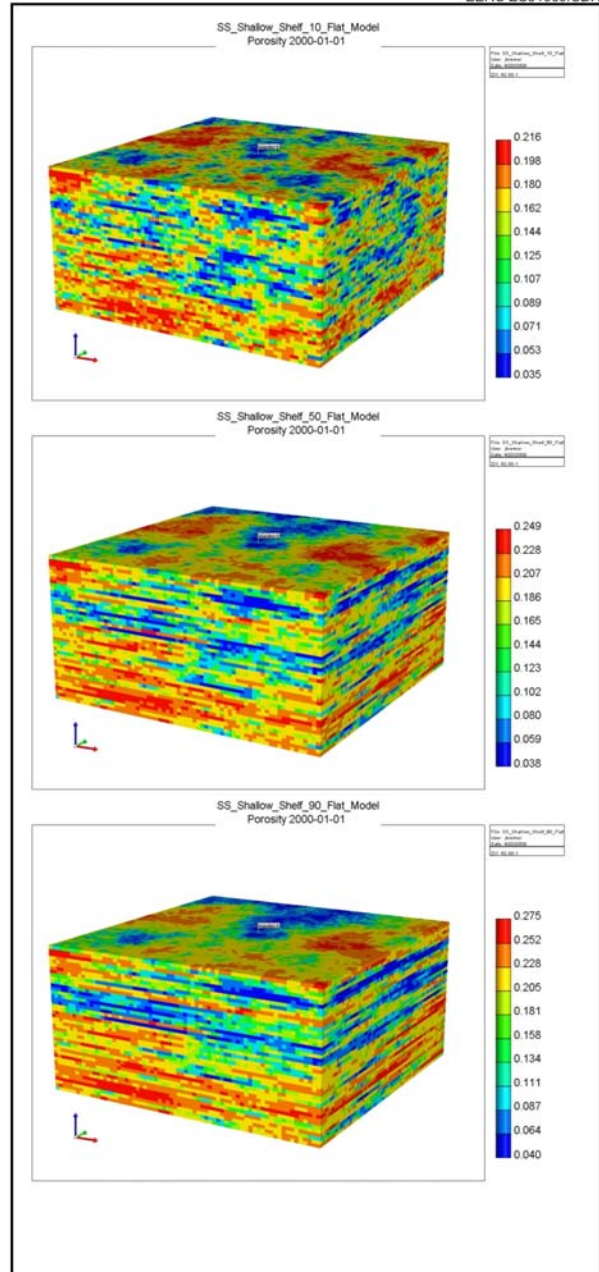
Limestone Reef			
Model Properties	P10	P50	P90
Horizontal Variogram Range Short (m)	9	16	23
Horizontal Variogram Range Long (m)	116	203	290
Vertical Variogram Range Short (m)	1	1	1
Vertical Variogram Range Long (m)	14	14	14
Rock Compressibility (1/kPa)	6.87E-07	6.87E-07	6.87E-07
Effective Φ Min %	4	4	4
Effective Φ Mean %	11	13	14
Effective Φ Max %	15	19	21
Permeability Min (m ²)	5.64E-16	1.31E-15	3.04E-15
Permeability Mean (m ²)	6.05E-11	1.01E-10	1.67E-10
Permeability Max (m ²)	2.04E-13	3.23E-13	5.12E-13
k_v/k_h Ratio	0.031	0.314	0.596
Salinity (ppm) P50	53,080	53,080	53,080
Reservoir Depth (MD) (m) P50	2336	2336	2336
Temp (°C) P50	75	75	75
Reference Pressure at 2336 m (kPa)	23,900	23,900	23,900



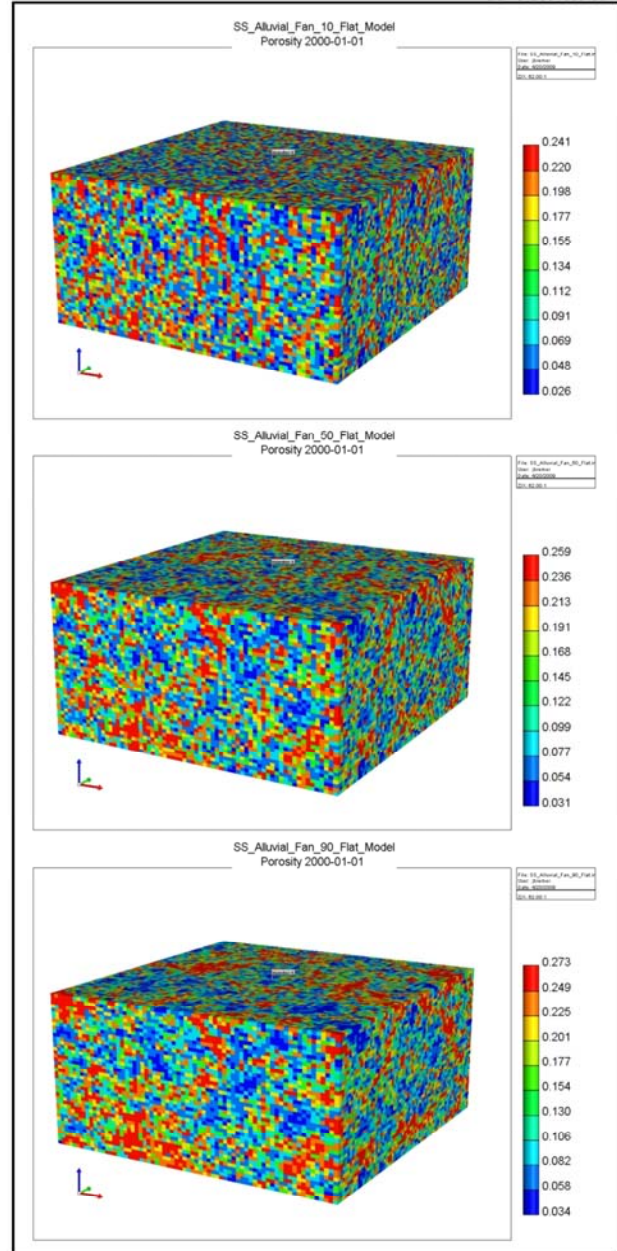
Limestone Peritidal			
Model Properties	P10	P50	P90
Horizontal Variogram Range Short (m)	44	120	196
Horizontal Variogram Range Long (m)	571	1543	2515
Vertical Variogram Range Short (m)	1	1	1
Vertical Variogram Range Long (m)	14	14	14
Rock Compressibility (1/kPa)	4.45E-07	4.45E-07	4.45E-07
Effective Φ Min %	5	5	6
Effective Φ Mean %	18	20	22
Effective Φ Max %	22	24	25
Permeability Min (m ²)	1.12E-15	2.92E-15	7.67E-15
Permeability Mean (m ²)	2.73E-10	4.33E-10	6.12E-10
Permeability Max (m ²)	6.37E-13	8.02E-13	1.01E-12
k_v/k_h Ratio	0.031	0.314	0.596
Salinity (ppm) P50	53,080	53,080	53,080
Reservoir Depth (MD) (m) P50	2336	2336	2336
Temp (°C) P50	75	75	75
Reference Pressure at 2336 m (kPa)	23,900	23,900	23,900



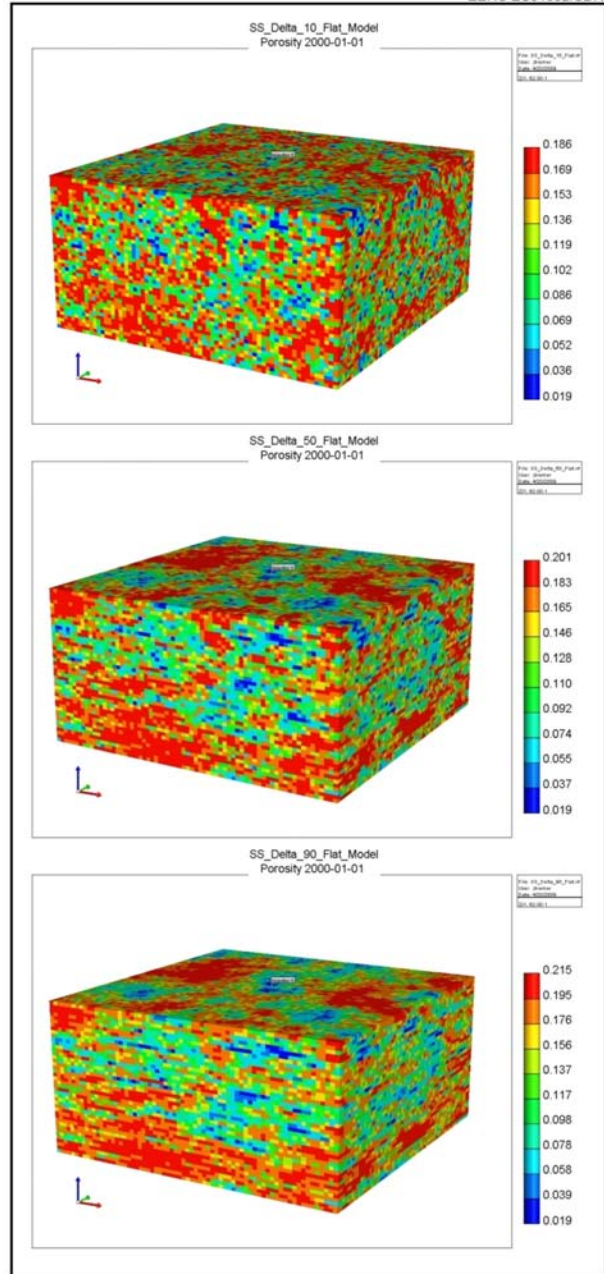
Sandstone Shallow Shelf			
Model Properties	P10	P50	P90
Horizontal Variogram Range Short (m)	681	1852	3023
Horizontal Variogram Range Long (m)	2499	6792	11085
Vertical Variogram Range Short (m)	2	2	2
Vertical Variogram Range Long (m)	7	7	7
Rock Compressibility (1/kPa)	3.18E -07	3.18E -07	3.18E -07
Effective Φ Min %	3	4	4
Effective Φ Mean %	15	17	19
Effective Φ Max %	22	25	28
Permeability Min (m ²)	2.04E -16	4.92E -16	1.19E -15
Permeability Mean (m ²)	1.77E -10	3.15E -10	5.30E -10
Permeability Max (m ²)	6.15E -13	1.00E -12	1.63E -12
k_v/k_h Ratio	0.013	0.108	0.876
Salinity (ppm) P50	53,080	53,080	53,080
Reservoir Depth (MD) (m) P50	2336	2336	2336
Temp (°C) P50	75	75	75
Reference Pressure at 2336 m (kPa)	23,900	23,900	23,900



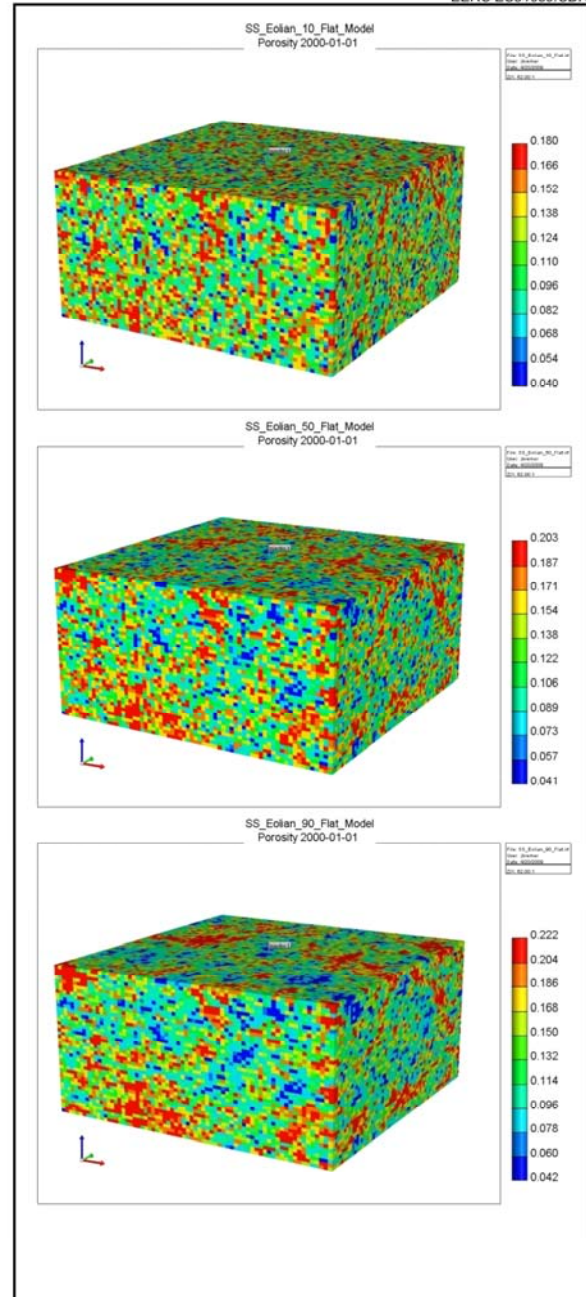
Sandstone Alluvial Fan			
Model Properties	P10	P50	P90
Horizontal Variogram Range Short (m)	40	108	177
Horizontal Variogram Range Long (m)	145	398	650
Vertical Variogram Range Short (m)	2	2	2
Vertical Variogram Range Long (m)	7	7	7
Rock Compressibility (1/kPa)	4.41E-07	4.41E-07	4.41E-07
Effective Φ Min %	3	3	3
Effective Φ Mean %	13	14	15
Effective Φ Max %	24	26	27
Permeability Min (m ²)	4.87E-17	1.17E-16	2.80E-16
Permeability Mean (m ²)	2.13E-10	3.18E-10	4.83E-10
Permeability Max (m ²)	8.71E-13	1.28E-12	1.89E-12
k_v/k_h Ratio	0.013	0.108	0.876
Salinity (ppm) P50	53,080	53,080	53,080
Reservoir Depth (MD) (m) P50	2336	2336	2336
Temp (°C) P50	75	75	75
Reference Pressure at 2336 m (kPa)	23,900	23,900	23,900



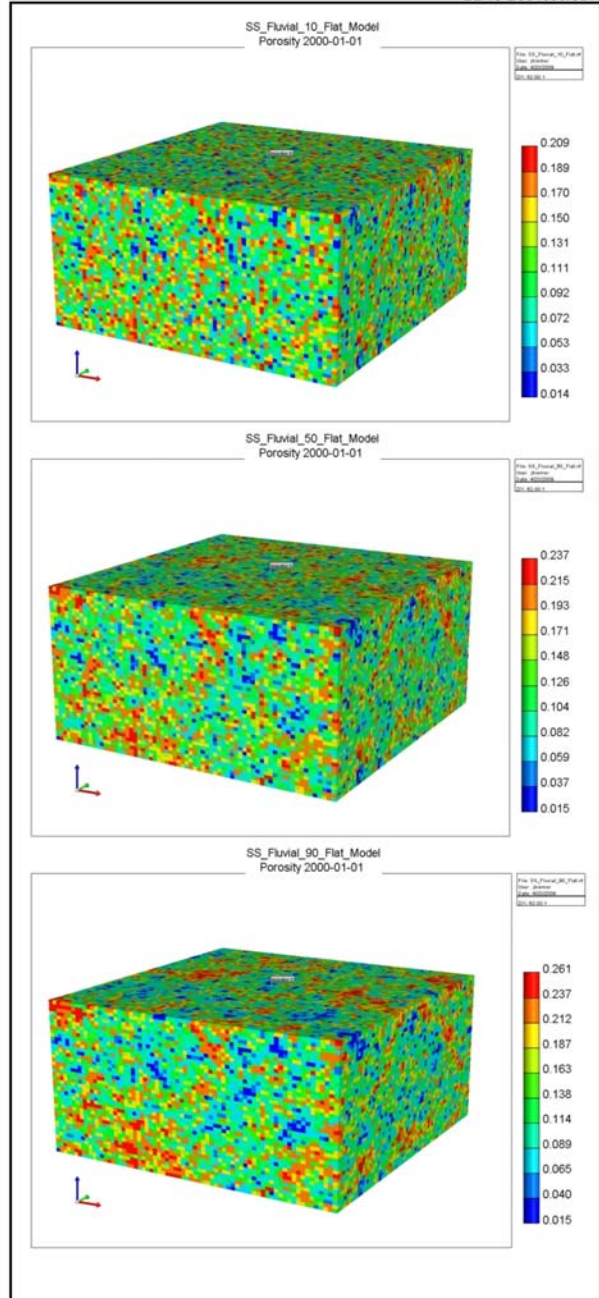
Sandstone Delta			
Model Properties	P10	P50	P90
Horizontal Variogram Range Short (m)	150	410	671
Horizontal Variogram Range Long (m)	550	1504	2459
Vertical Variogram Range Short (m)	2	2	2
Vertical Variogram Range Long (m)	7	7	7
Rock Compressibility (1/kPa)	3.60E-07	3.60E-07	3.60E-07
Effective Φ Min %	2	2	2
Effective Φ Mean %	13	14	15
Effective Φ Max %	19	20	21
Permeability Min (m ²)	8.20E-17	1.29E-16	2.02E-16
Permeability Mean (m ²)	1.27E-10	1.62E-10	2.07E-10
Permeability Max (m ²)	4.35E-13	5.15E-13	6.09E-13
k_v/k_h Ratio	0.013	0.108	0.876
Salinity (ppm) P50	53,080	53,080	53,080
Reservoir Depth (MD) (m) P50	2336	2336	2336
Temp (°C) P50	75	75	75
Reference Pressure at 2336 m (kPa)	23,900	23,900	23,900



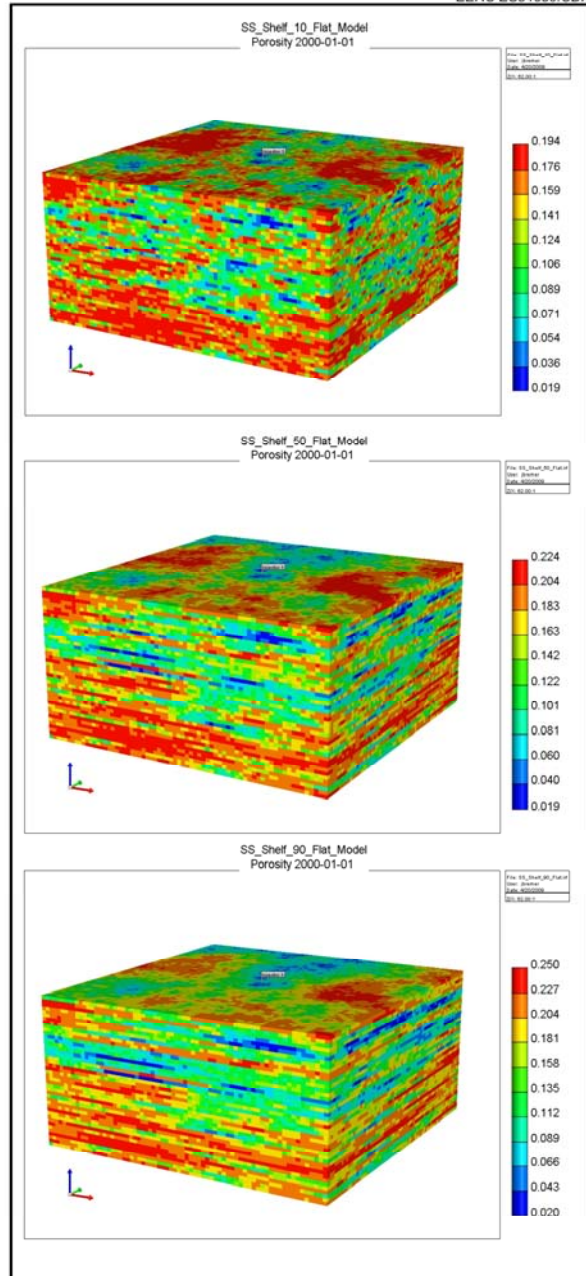
Sandstone Eolian			
Model Properties	P10	P50	P90
Horizontal Variogram Range Short (m)	54	144	234
Horizontal Variogram Range Long (m)	198	529	860
Vertical Variogram Range Short (m)	2	2	2
Vertical Variogram Range Long (m)	7	7	7
Rock Compressibility (1/kPa)	4.73E-07	4.73E-07	4.73E-07
Effective Φ Min %	4	4	4
Effective Φ Mean %	12	13	14
Effective Φ Max %	18	20	22
Permeability Min (m ²)	9.56E-16	1.75E-15	3.20E-15
Permeability Mean (m ²)	7.95E-11	1.17E-10	1.75E-10
Permeability Max (m ²)	2.93E-13	4.19E-13	5.98E-13
k_v/k_h Ratio	0.013	0.108	0.876
Salinity (ppm) P50	53,080	53,080	53,080
Reservoir Depth (MD) (m) P50	2336	2336	2336
Temp (°C) P50	75	75	75
Reference Pressure at 2336 m (kPa)	23,900	23,900	23,900



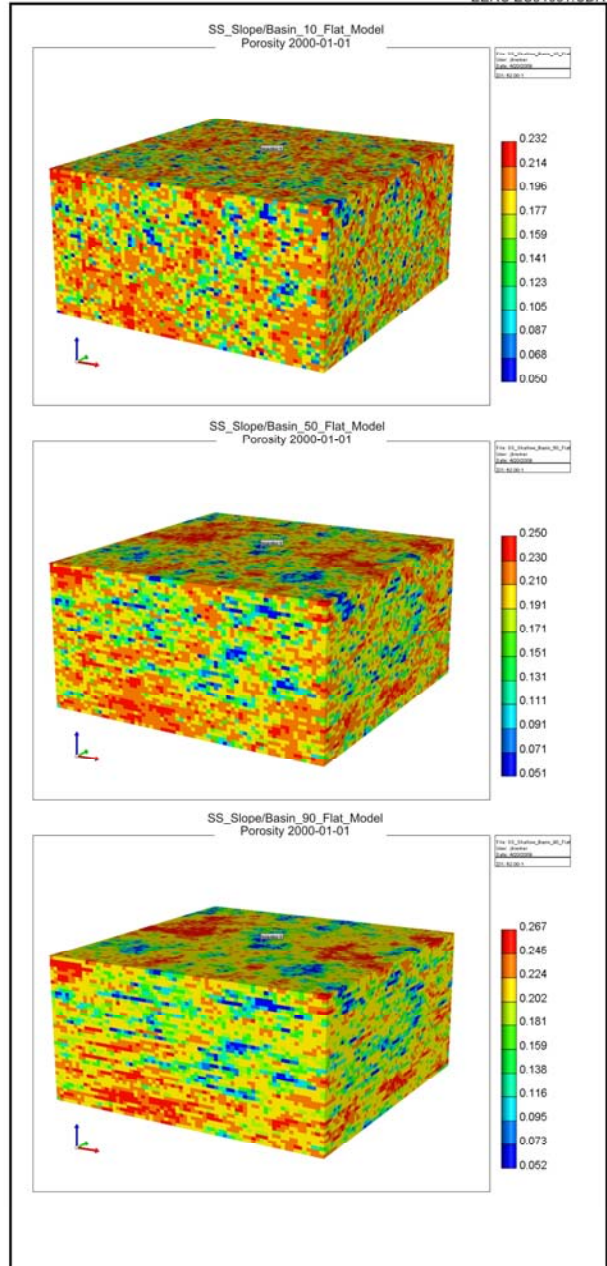
Sandstone Fluvial			
Model Properties	P10	P50	P90
Horizontal Variogram Range Short (m)	40	108	177
Horizontal Variogram Range Long (m)	145	398	650
Vertical Variogram Range Short (m)	2	2	2
Vertical Variogram Range Long (m)	7	7	7
Rock Compressibility (1/kPa)	4.44E -07	4.44E -07	4.44E -07
Effective Φ Min %	1	1	2
Effective Φ Mean %	12	13	14
Effective Φ Max %	21	24	26
Permeability Min (m ²)	4.34E -18	1.05E -17	2.52E -17
Permeability Mean (m ²)	9.44E -11	1.43E -10	2.19E -10
Permeability Max (m ²)	5.70E -13	8.37E -13	1.23E -12
k_v/k_h Ratio	0.013	0.108	0.876
Salinity (ppm) P50	53,080	53,080	53,080
Reservoir Depth (MD) (m) P50	2336	2336	2336
Temp (°C) P50	75	75	75
Reference Pressure at 2336 m (kPa)	23,900	23,900	23,900



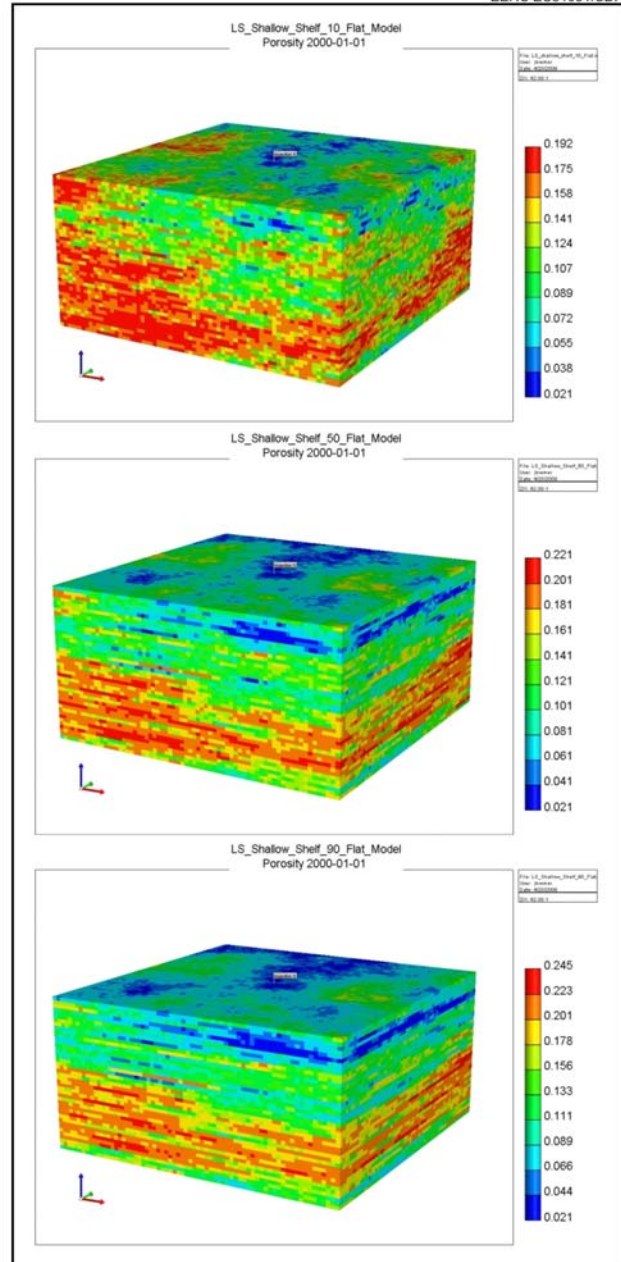
Sandstone Shelf			
Model Properties	P10	P50	P90
Horizontal Variogram Range Short (m)	681	1852	3023
Horizontal Variogram Range Long (m)	2499	6792	11085
Vertical Variogram Range Short (m)	2	2	2
Vertical Variogram Range Long (m)	7	7	7
Rock Compressibility (1/kPa)	3.34E-07	3.34E-07	3.34E-07
Effective Φ Min %	2	2	2
Effective Φ Mean %	14	16	17
Effective Φ Max %	19	22	25
Permeability Min (m ²)	9.36E-17	2.19E-16	5.12E-16
Permeability Mean (m ²)	1.46E-10	2.26E-10	3.29E-10
Permeability Max (m ²)	5.65E-13	7.78E-13	1.07E-12
k_v/k_h Ratio	0.013	0.108	0.876
Salinity (ppm) P50	53,080	53,080	53,080
Reservoir Depth (MD) (m) P50	2336	2336	2336
Temp (°C) P50	75	75	75
Reference Pressure at 2336 m (kPa)	23,900	23,900	23,900



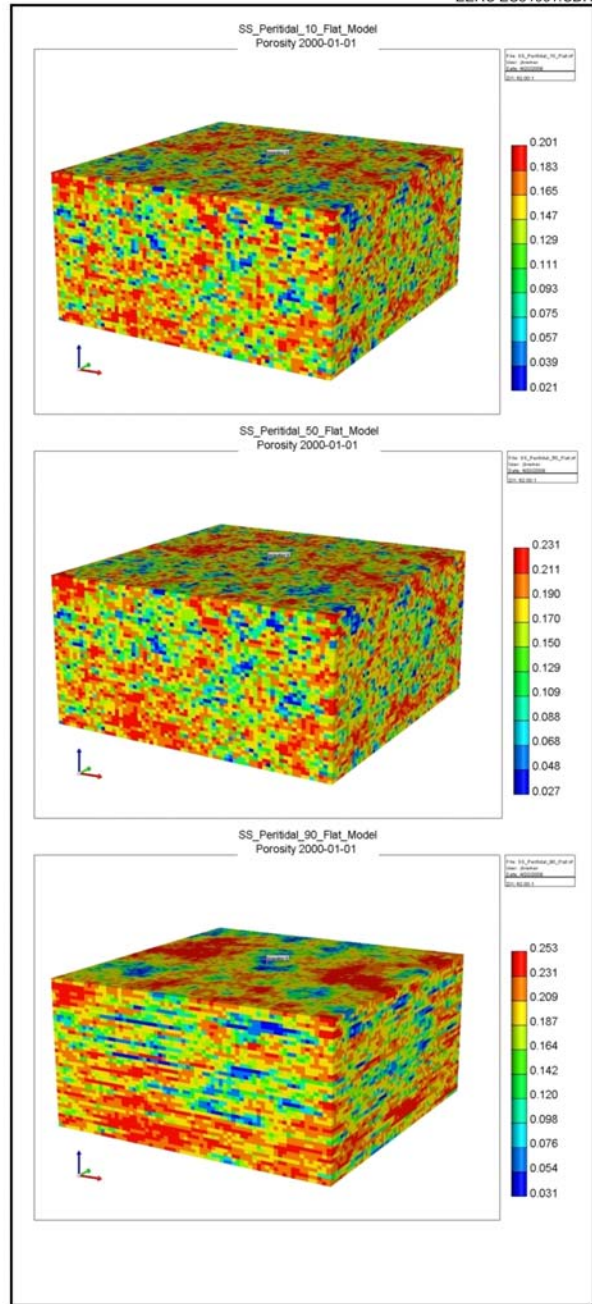
Sandstone Slope/Basin			
Model Properties	P10	P50	P90
Horizontal Variogram Range Short (m)	134	367	600
Horizontal Variogram Range Long (m)	492	1346	2200
Vertical Variogram Range Short (m)	2	2	2
Vertical Variogram Range Long (m)	7	7	7
Rock Compressibility (1/kPa)	2.80E-07	2.80E-07	2.80E-07
Effective Φ Min %	5	5	5
Effective Φ Mean %	18	19	20
Effective Φ Max %	23	25	27
Permeability Min (m ²)	4.04E-15	6.42E-15	1.02E-14
Permeability Mean (m ²)	3.00E-10	3.98E-10	5.31E-10
Permeability Max (m ²)	8.84E-13	1.10E-12	1.37E-12
k_v/k_h Ratio	0.013	0.108	0.876
Salinity (ppm) P50	53,080	53,080	53,080
Reservoir Depth (MD) (m) P50	2336	2336	2336
Temp (°C) P50	75	75	75
Reference Pressure at 2336 m (kPa)	23,900	23,900	23,900



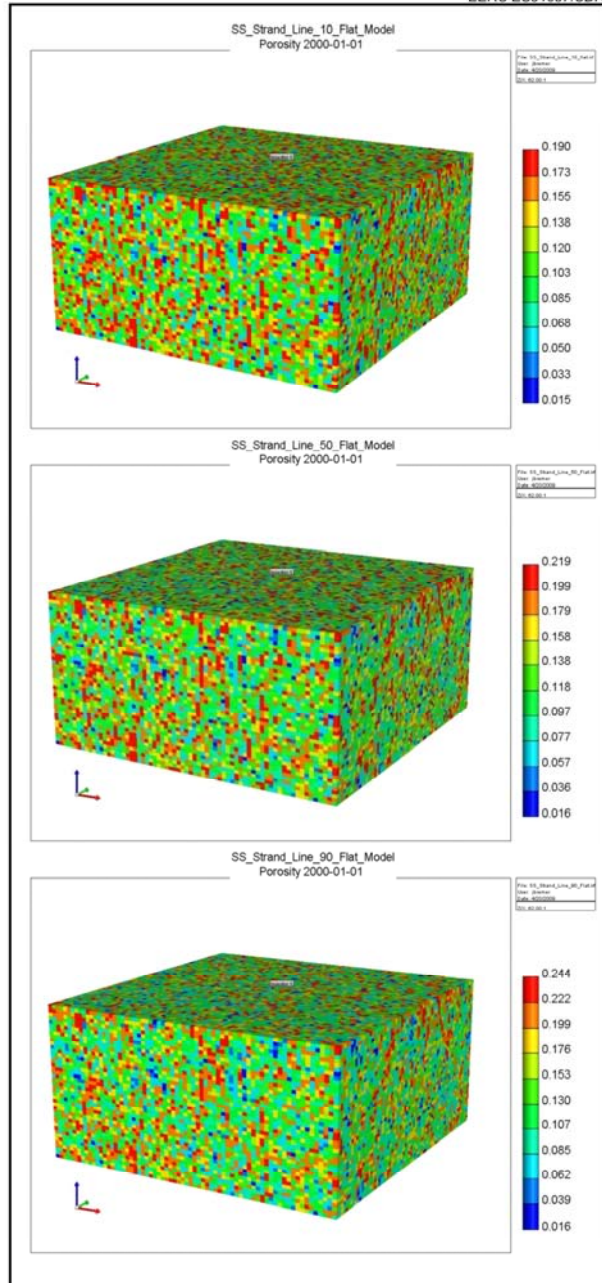
Limestone Shallow Shelf			
Model Properties	P10	P50	P90
Horizontal Variogram Range Short (m)	397	1081	1764
Horizontal Variogram Range Long (m)	5111	13892	22674
Vertical Variogram Range Short (m)	1	1	1
Vertical Variogram Range Long (m)	14	14	14
Rock Compressibility (1/kPa)	6.27E -07	6.27E -07	6.27E -07
Effective Φ Min %	2	2	2
Effective Φ Mean %	14	14	15
Effective Φ Max %	19	22	25
Permeability Min (m ²)	9.15E -17	1.59E -16	2.74E -16
Permeability Mean (m ²)	1.33E -10	1.54E -10	2.04E -10
Permeability Max (m ²)	5.17E -13	7.10E -13	9.74E -13
k _v /k _h Ratio	0.031	0.314	0.596
Salinity (ppm) P50	53,080	53,080	53,080
Reservoir Depth (MD) (m) P50	2336	2336	2336
Temp (°C) P50	75	75	75
Reference Pressure at 2336 m (kPa)	23,900	23,900	23,900



Sandstone Peritidal			
Model Properties	P10	P50	P90
Horizontal Variogram Range Short (m)	76	206	335
Horizontal Variogram Range Long (m)	279	754	1230
Vertical Variogram Range Short (m)	2	2	2
Vertical Variogram Range Long (m)	7	7	7
Rock Compressibility (1/kPa)	4.45E-07	4.45E-07	4.45E-07
Effective Φ Min %	2	3	3
Effective Φ Mean %	15	17	19
Effective Φ Max %	20	23	25
Permeability Min (m ²)	3.10E-17	6.03E-17	1.18E-16
Permeability Mean (m ²)	1.54E-10	2.63E-10	4.69E-10
Permeability Max (m ²)	4.24E-13	7.10E-13	1.19E-12
k _v /k _h Ratio	0.013	0.108	0.876
Salinity (ppm) P50	53,080	53,080	53,080
Reservoir Depth (MD) (m) P50	2336	2336	2336
Temp (°C) P50	75	75	75
Reference Pressure at 2336 m (kPa)	23,900	23,900	23,900



Sandstone Strand Plain			
Model Properties	P10	P50	P90
Horizontal Variogram Range Short (m)	15	27	39
Horizontal Variogram Range Long (m)	57	99	142
Vertical Variogram Range Short (m)	2	2	2
Vertical Variogram Range Long (m)	7	7	7
Rock Compressibility (1/kPa)	4.22E-07	4.22E-07	4.22E-07
Effective Φ Min %	2	2	2
Effective Φ Mean %	12	13	14
Effective Φ Max %	19	22	24
Permeability Min (m ²)	2.98E-17	5.47E-17	1.00E-16
Permeability Mean (m ²)	1.00E-10	1.45E-10	2.10E-10
Permeability Max (m ²)	4.69E-13	6.63E-13	9.37E-13
k _v /k _h Ratio	0.013	0.108	0.876
Salinity (ppm) P50	53,080	53,080	53,080
Reservoir Depth (MD) (m) P50	2336	2336	2336
Temp (°C) P50	75	75	75
Reference Pressure at 2336 m (kPa)	23,900	23,900	23,900



APPENDIX E

SITE-SPECIFIC STORAGE COEFFICIENTS FOR DIFFERENT LITHOLOGIES, DEPOSITIONAL ENVIRONMENTS, STRUCTURES, AND PROBABILITY LEVELS

Appendix E – Site-Specific Storage Coefficients for Different Lithologies, Depositional Environments, Structures, and Probability Levels

The following table contains all of the heterogeneous model runs that were used to calculate storage coefficients for the site-specific lithologies and depositional environments and the formation-level storage coefficients for lithologies.

Num	Lithology	Depositional Environment	Structure	P value	A_n/A_t P90	h_n/h_g P90	Φ_{eff}/Φ_{tot}	E_v	E_d	$(1 - S_{wave})$	E_E and $C_c * (1 - S_{wirr})$
										$(1 - S_{wirr})$	
1	Sandstone	Alluvial Fan	Anticline	10	0.8	0.76	0.70	0.41	0.37	0.46	6.42%
2	Sandstone	Alluvial Fan	Dome	10	0.8	0.76	0.70	0.46	0.42	0.52	8.12%
3	Sandstone	Alluvial Fan	10° Incline	10	0.8	0.76	0.70	0.34	0.32	0.40	4.60%
4	Sandstone	Alluvial Fan	5° Incline	10	0.8	0.76	0.70	0.33	0.32	0.40	4.57%
5	Sandstone	Alluvial Fan	Flat	10	0.8	0.76	0.70	0.31	0.32	0.40	4.22%
6	Sandstone	Alluvial Fan	Anticline	50	0.8	0.76	0.76	0.46	0.51	0.64	10.85%
7	Sandstone	Alluvial Fan	Dome	50	0.8	0.76	0.76	0.56	0.57	0.70	14.76%
8	Sandstone	Alluvial Fan	10° Incline	50	0.8	0.76	0.76	0.23	0.45	0.55	4.85%
9	Sandstone	Alluvial Fan	5° Incline	50	0.8	0.76	0.76	0.26	0.46	0.57	5.59%
10	Sandstone	Alluvial Fan	Flat	50	0.8	0.76	0.76	0.22	0.46	0.57	4.60%
11	Sandstone	Alluvial Fan	Anticline	90	0.8	0.76	0.82	0.35	0.72	0.89	12.42%
12	Sandstone	Alluvial Fan	Dome	90	0.8	0.76	0.82	0.61	0.74	0.93	22.48%
13	Sandstone	Alluvial Fan	10° Incline	90	0.8	0.76	0.82	0.18	0.67	0.83	6.07%
14	Sandstone	Alluvial Fan	5° Incline	90	0.8	0.76	0.82	0.15	0.70	0.87	5.29%
15	Sandstone	Alluvial Fan	Flat	90	0.8	0.76	0.82	0.18	0.69	0.86	6.08%
16	Sandstone	Delta	Anticline	10	0.8	0.76	0.61	0.46	0.44	0.55	7.56%
17	Sandstone	Delta	Dome	10	0.8	0.76	0.61	0.57	0.50	0.63	10.62%
18	Sandstone	Delta	10° Incline	10	0.8	0.76	0.61	0.39	0.36	0.44	5.22%
19	Sandstone	Delta	5° Incline	10	0.8	0.76	0.61	0.37	0.37	0.46	5.14%
20	Sandstone	Delta	Flat	10	0.8	0.76	0.61	0.38	0.37	0.46	5.21%
21	Sandstone	Delta	Anticline	50	0.8	0.76	0.66	0.46	0.60	0.74	10.96%
22	Sandstone	Delta	Dome	50	0.8	0.76	0.66	0.59	0.66	0.82	15.51%
23	Sandstone	Delta	10° Incline	50	0.8	0.76	0.66	0.22	0.54	0.67	4.85%
24	Sandstone	Delta	5° Incline	50	0.8	0.76	0.66	0.25	0.54	0.67	5.48%
25	Sandstone	Delta	Flat	50	0.8	0.76	0.66	0.30	0.53	0.66	6.29%
26	Sandstone	Delta	Anticline	90	0.8	0.76	0.71	0.37	0.79	0.98	12.40%
27	Sandstone	Delta	Dome	90	0.8	0.76	0.71	0.59	0.79	0.99	19.98%
28	Sandstone	Delta	10° Incline	90	0.8	0.76	0.71	0.17	0.75	0.94	5.53%
29	Sandstone	Delta	5° Incline	90	0.8	0.76	0.71	0.18	0.75	0.94	5.84%
30	Sandstone	Delta	Flat	90	0.8	0.76	0.71	0.19	0.75	0.93	6.00%
31	Sandstone	Eolian	Anticline	10	0.8	0.76	0.69	0.49	0.41	0.52	8.46%
32	Sandstone	Eolian	Dome	10	0.8	0.76	0.69	0.56	0.46	0.57	10.78%
33	Sandstone	Eolian	10° Incline	10	0.8	0.76	0.69	0.43	0.37	0.46	6.70%
34	Sandstone	Eolian	5° Incline	10	0.8	0.76	0.69	0.39	0.37	0.46	6.03%
35	Sandstone	Eolian	Flat	10	0.8	0.76	0.69	0.44	0.37	0.46	6.79%
36	Sandstone	Eolian	Anticline	50	0.8	0.76	0.74	0.38	0.63	0.78	10.78%
37	Sandstone	Eolian	Dome	50	0.8	0.76	0.74	0.57	0.67	0.83	17.19%
38	Sandstone	Eolian	10° Incline	50	0.8	0.76	0.74	0.21	0.59	0.74	5.56%
39	Sandstone	Eolian	5° Incline	50	0.8	0.76	0.74	0.24	0.59	0.73	6.52%
40	Sandstone	Eolian	Flat	50	0.8	0.76	0.74	0.23	0.58	0.73	5.97%
41	Sandstone	Eolian	Anticline	90	0.8	0.76	0.79	0.38	0.76	0.95	13.93%
42	Sandstone	Eolian	Dome	90	0.8	0.76	0.79	0.68	0.78	0.97	25.73%
43	Sandstone	Eolian	10° Incline	90	0.8	0.76	0.79	0.16	0.73	0.91	5.62%
44	Sandstone	Eolian	5° Incline	90	0.8	0.76	0.79	0.17	0.74	0.92	6.17%

Continued . . .

Num	Lithology	Depositional Environment	Structure	Pvalue	A_n/A_t , P90	h_n/h_g , P9)	Φ_{eff}/Φ_{tot}	E_v	E_d	$(1 - S_{wave})$	E_E and $C_c * (1 - S_{wirr})$
										$(1 - S_{wirr})$	
45	Sandstone	Eolian	Flat	90	0.8	0.76	0.79	0.20	0.73	0.90	6.96%
46	Sandstone	Fluvial	Anticline	10	0.8	0.76	0.63	0.44	0.37	0.47	6.36%
47	Sandstone	Fluvial	Dome	10	0.8	0.76	0.63	0.51	0.41	0.51	8.02%
48	Sandstone	Fluvial	10° Incline	10	0.8	0.76	0.63	0.42	0.34	0.43	5.48%
49	Sandstone	Fluvial	5° Incline	10	0.8	0.76	0.63	0.43	0.34	0.42	5.53%
50	Sandstone	Fluvial	Flat	10	0.8	0.76	0.63	0.41	0.33	0.42	5.23%
51	Sandstone	Fluvial	Anticline	50	0.8	0.76	0.71	0.38	0.54	0.67	8.92%
52	Sandstone	Fluvial	Dome	50	0.8	0.76	0.71	0.55	0.58	0.73	13.73%
53	Sandstone	Fluvial	10° Incline	50	0.8	0.76	0.71	0.26	0.50	0.62	5.62%
54	Sandstone	Fluvial	5° Incline	50	0.8	0.76	0.71	0.25	0.50	0.62	5.44%
55	Sandstone	Fluvial	Flat	50	0.8	0.76	0.71	0.24	0.50	0.62	5.07%
56	Sandstone	Fluvial	Anticline	90	0.8	0.76	0.77	0.39	0.72	0.90	12.97%
57	Sandstone	Fluvial	Dome	90	0.8	0.76	0.77	0.56	0.75	0.93	19.61%
58	Sandstone	Fluvial	10° Incline	90	0.8	0.76	0.77	0.17	0.70	0.87	5.54%
59	Sandstone	Fluvial	5° Incline	90	0.8	0.76	0.77	0.19	0.70	0.87	6.12%
60	Sandstone	Fluvial	Flat	90	0.8	0.76	0.77	0.19	0.69	0.86	6.11%
61	Sandstone	Peritidal	Anticline	10	0.8	0.76	0.60	0.44	0.47	0.59	7.60%
62	Sandstone	Peritidal	Dome	10	0.8	0.76	0.60	0.64	0.55	0.69	12.78%
63	Sandstone	Peritidal	10° Incline	10	0.8	0.76	0.60	0.30	0.37	0.46	4.01%
64	Sandstone	Peritidal	5° Incline	10	0.8	0.76	0.60	0.34	0.39	0.48	4.74%
65	Sandstone	Peritidal	Flat	10	0.8	0.76	0.60	0.34	0.39	0.49	4.84%
66	Sandstone	Peritidal	Anticline	50	0.8	0.76	0.69	0.34	0.65	0.81	9.29%
67	Sandstone	Peritidal	Dome	50	0.8	0.76	0.69	0.57	0.71	0.88	16.97%
68	Sandstone	Peritidal	10° Incline	50	0.8	0.76	0.69	0.19	0.58	0.72	4.71%
69	Sandstone	Peritidal	5° Incline	50	0.8	0.76	0.69	0.17	0.60	0.74	4.21%
70	Sandstone	Peritidal	Flat	50	0.8	0.76	0.69	0.20	0.59	0.73	4.82%
71	Sandstone	Peritidal	Anticline	90	0.8	0.76	0.78	0.31	0.80	0.99	11.76%
72	Sandstone	Peritidal	Dome	90	0.8	0.76	0.78	0.69	0.79	0.98	25.74%
73	Sandstone	Peritidal	10° Incline	90	0.8	0.76	0.78	0.13	0.73	0.91	4.56%
74	Sandstone	Peritidal	5° Incline	90	0.8	0.76	0.78	0.14	0.75	0.94	4.98%
75	Sandstone	Peritidal	Flat	90	0.8	0.76	0.78	0.15	0.75	0.94	5.38%
76	Sandstone	Slope Basin	Anticline	10	0.8	0.76	0.68	0.37	0.57	0.71	8.82%
77	Sandstone	Slope Basin	Dome	10	0.8	0.76	0.68	0.59	0.66	0.82	16.11%
78	Sandstone	Slope Basin	10° Incline	10	0.8	0.76	0.68	0.24	0.43	0.54	4.37%
79	Sandstone	Slope Basin	5° Incline	10	0.8	0.76	0.68	0.23	0.47	0.58	4.56%
80	Sandstone	Slope Basin	Flat	10	0.8	0.76	0.68	0.25	0.48	0.60	4.94%
81	Sandstone	Slope Basin	Anticline	50	0.8	0.76	0.73	0.30	0.74	0.92	9.91%
82	Sandstone	Slope Basin	Dome	50	0.8	0.76	0.73	0.68	0.78	0.97	23.42%
83	Sandstone	Slope Basin	10° Incline	50	0.8	0.76	0.73	0.16	0.67	0.83	4.59%
84	Sandstone	Slope Basin	5° Incline	50	0.8	0.76	0.73	0.14	0.70	0.87	4.37%
85	Sandstone	Slope Basin	Flat	50	0.8	0.76	0.73	0.16	0.68	0.85	4.92%
86	Sandstone	Slope Basin	Anticline	90	0.8	0.76	0.77	0.30	0.80	1.00	11.12%
87	Sandstone	Slope Basin	Dome	90	0.8	0.76	0.77	0.66	0.80	0.99	24.43%
88	Sandstone	Slope Basin	10° Incline	90	0.8	0.76	0.77	0.11	0.74	0.92	3.96%
89	Sandstone	Slope Basin	5° Incline	90	0.8	0.76	0.77	0.13	0.77	0.96	4.74%
90	Sandstone	Slope Basin	Flat	90	0.8	0.76	0.77	0.15	0.77	0.96	5.50%

Continued . . .

Num	Lithology	Depositional Environment	Structure	Pvalue	A_n/A_t , P90	h_n/h_g , P90	Φ_{eff}/Φ_{tot}	E_v	E_d	$(1 - S_{wave})$	E_E and $C_c * (1 - S_{wirr})$
										$(1 - S_{wirr})$	
91	Sandstone	Shallow Shelf	Anticline	10	0.8	0.76	0.62	0.48	0.47	0.59	8.58%
92	Sandstone	Shallow Shelf	Dome	10	0.8	0.76	0.62	0.64	0.54	0.67	12.97%
93	Sandstone	Shallow Shelf	10° Incline	10	0.8	0.76	0.62	0.34	0.36	0.45	4.67%
94	Sandstone	Shallow Shelf	5° Incline	10	0.8	0.76	0.62	0.36	0.39	0.49	5.26%
95	Sandstone	Shallow Shelf	Flat	10	0.8	0.76	0.62	0.35	0.40	0.50	5.26%
96	Sandstone	Shallow Shelf	Anticline	50	0.8	0.76	0.72	0.38	0.62	0.77	10.21%
97	Sandstone	Shallow Shelf	Dome	50	0.8	0.76	0.72	0.62	0.69	0.86	18.53%
98	Sandstone	Shallow Shelf	10° Incline	50	0.8	0.76	0.72	0.31	0.51	0.63	6.90%
99	Sandstone	Shallow Shelf	5° Incline	50	0.8	0.76	0.72	0.28	0.54	0.67	6.63%
100	Sandstone	Shallow Shelf	Flat	50	0.8	0.76	0.72	0.29	0.52	0.65	6.67%
101	Sandstone	Shallow Shelf	Anticline	90	0.8	0.76	0.78	0.32	0.80	1.00	12.33%
102	Sandstone	Shallow Shelf	Dome	90	0.8	0.76	0.78	0.73	0.80	1.00	27.77%
103	Sandstone	Shallow Shelf	10° Incline	90	0.8	0.76	0.78	0.13	0.80	1.00	5.00%
104	Sandstone	Shallow Shelf	5° Incline	90	0.8	0.76	0.78	0.16	0.80	1.00	6.12%
105	Sandstone	Shallow Shelf	Flat	90	0.8	0.76	0.78	0.18	0.80	1.00	6.78%
106	Sandstone	Shelf	Anticline	10	0.8	0.76	0.62	0.46	0.46	0.58	8.02%
107	Sandstone	Shelf	Dome	10	0.8	0.76	0.62	0.66	0.54	0.67	13.39%
108	Sandstone	Shelf	10° Incline	10	0.8	0.76	0.62	0.38	0.36	0.45	5.19%
109	Sandstone	Shelf	5° Incline	10	0.8	0.76	0.62	0.40	0.38	0.47	5.65%
110	Sandstone	Shelf	Flat	10	0.8	0.76	0.62	0.39	0.38	0.48	5.65%
111	Sandstone	Shelf	Anticline	50	0.8	0.76	0.69	0.39	0.68	0.85	11.24%
112	Sandstone	Shelf	Dome	50	0.8	0.76	0.69	0.56	0.73	0.91	17.22%
113	Sandstone	Shelf	10° Incline	50	0.8	0.76	0.69	0.25	0.63	0.78	6.47%
114	Sandstone	Shelf	5° Incline	50	0.8	0.76	0.69	0.24	0.63	0.78	6.34%
115	Sandstone	Shelf	Flat	50	0.8	0.76	0.69	0.27	0.61	0.76	6.79%
116	Sandstone	Shelf	Anticline	90	0.8	0.76	0.74	0.32	0.80	1.00	11.59%
117	Sandstone	Shelf	Dome	90	0.8	0.76	0.74	0.64	0.80	1.00	23.17%
118	Sandstone	Shelf	10° Incline	90	0.8	0.76	0.74	0.20	0.80	1.00	7.11%
119	Sandstone	Shelf	5° Incline	90	0.8	0.76	0.74	0.18	0.80	1.00	6.46%
120	Sandstone	Shelf	Flat	90	0.8	0.76	0.74	0.19	0.80	1.00	6.94%
121	Sandstone	Strand Plain	Anticline	10	0.8	0.76	0.64	0.47	0.40	0.50	7.48%
122	Sandstone	Strand Plain	Dome	10	0.8	0.76	0.64	0.56	0.45	0.56	9.75%
123	Sandstone	Strand Plain	10° Incline	10	0.8	0.76	0.64	0.44	0.36	0.45	6.20%
124	Sandstone	Strand Plain	5° Incline	10	0.8	0.76	0.64	0.44	0.36	0.45	6.15%
125	Sandstone	Strand Plain	Flat	10	0.8	0.76	0.64	0.47	0.36	0.45	6.56%
126	Sandstone	Strand Plain	Anticline	50	0.8	0.76	0.71	0.37	0.60	0.75	9.48%
127	Sandstone	Strand Plain	Dome	50	0.8	0.76	0.71	0.55	0.64	0.80	15.28%
128	Sandstone	Strand Plain	10° Incline	50	0.8	0.76	0.71	0.22	0.56	0.70	5.35%
129	Sandstone	Strand Plain	5° Incline	50	0.8	0.76	0.71	0.23	0.57	0.70	5.58%
130	Sandstone	Strand Plain	Flat	50	0.8	0.76	0.71	0.25	0.56	0.70	5.91%
131	Sandstone	Strand Plain	Anticline	90	0.8	0.76	0.76	0.34	0.73	0.90	11.41%
132	Sandstone	Strand Plain	Dome	90	0.8	0.76	0.76	0.51	0.77	0.95	17.91%
133	Sandstone	Strand Plain	10° Incline	90	0.8	0.76	0.76	0.17	0.68	0.85	5.39%
134	Sandstone	Strand Plain	5° Incline	90	0.8	0.76	0.76	0.18	0.69	0.86	5.58%
135	Sandstone	Strand Plain	Flat	90	0.8	0.76	0.76	0.18	0.69	0.86	5.80%

Continued . . .

Num	Lithology	Depositional Environment	Structure	Pvalue	A_n/A_t (P90)	h_n/h_g (P90)	Φ_{eff}/Φ_{tot}	E_v	E_d	$(1 - S_{wave})$	E_E and $C_c * (1 - S_{wirr})$
										$(1 - S_{wirr})$	
136	Dolomite	Shallow Shelf	Anticline	10	0.8	0.68	0.53	0.52	0.64	0.79	9.57%
137	Dolomite	Shallow Shelf	Dome	10	0.8	0.68	0.53	0.61	0.66	0.82	11.57%
138	Dolomite	Shallow Shelf	10° Incline	10	0.8	0.68	0.53	0.42	0.61	0.75	7.40%
139	Dolomite	Shallow Shelf	5° Incline	10	0.8	0.68	0.53	0.42	0.61	0.75	7.40%
140	Dolomite	Shallow Shelf	Flat	10	0.8	0.68	0.53	0.41	0.61	0.76	7.21%
141	Dolomite	Shallow Shelf	Anticline	50	0.8	0.68	0.64	0.49	0.68	0.85	11.53%
142	Dolomite	Shallow Shelf	Dome	50	0.8	0.68	0.64	0.59	0.73	0.91	15.01%
143	Dolomite	Shallow Shelf	10° Incline	50	0.8	0.68	0.64	0.36	0.63	0.79	7.76%
144	Dolomite	Shallow Shelf	5° Incline	50	0.8	0.68	0.64	0.35	0.63	0.78	7.72%
145	Dolomite	Shallow Shelf	Flat	50	0.8	0.68	0.64	0.35	0.63	0.78	7.50%
146	Dolomite	Shallow Shelf	Anticline	90	0.8	0.68	0.71	0.47	0.65	0.81	11.77%
147	Dolomite	Shallow Shelf	Dome	90	0.8	0.68	0.71	0.60	0.78	0.97	18.20%
148	Dolomite	Shallow Shelf	10° Incline	90	0.8	0.68	0.71	0.30	0.57	0.71	6.57%
149	Dolomite	Shallow Shelf	5° Incline	90	0.8	0.68	0.71	0.29	0.58	0.72	6.55%
150	Dolomite	Shallow Shelf	Flat	90	0.8	0.68	0.71	0.28	0.58	0.72	6.37%
151	Limestone	Peritidal	Anticline	10	0.8	0.62	0.61	0.57	0.38	0.88	6.62%
152	Limestone	Peritidal	Dome	10	0.8	0.62	0.61	0.70	0.41	0.95	8.78%
153	Limestone	Peritidal	10° Incline	10	0.8	0.62	0.61	0.44	0.37	0.86	4.95%
154	Limestone	Peritidal	5° Incline	10	0.8	0.62	0.61	0.43	0.38	0.88	4.99%
155	Limestone	Peritidal	Flat	10	0.8	0.62	0.61	0.42	0.38	0.88	4.91%
156	Limestone	Peritidal	Anticline	50	0.8	0.62	0.70	0.53	0.39	0.90	7.12%
157	Limestone	Peritidal	Dome	50	0.8	0.62	0.70	0.74	0.42	0.97	10.82%
158	Limestone	Peritidal	10° Incline	50	0.8	0.62	0.70	0.32	0.39	0.90	4.33%
159	Limestone	Peritidal	5° Incline	50	0.8	0.62	0.70	0.37	0.39	0.90	4.97%
160	Limestone	Peritidal	Flat	50	0.8	0.62	0.70	0.37	0.38	0.88	4.81%
161	Limestone	Peritidal	Anticline	90	0.8	0.62	0.75	0.51	0.40	0.93	7.65%
162	Limestone	Peritidal	Dome	90	0.8	0.62	0.75	0.73	0.43	1.00	11.74%
163	Limestone	Peritidal	10° Incline	90	0.8	0.62	0.75	0.30	0.41	0.95	4.53%
164	Limestone	Peritidal	5° Incline	90	0.8	0.62	0.75	0.31	0.41	0.95	4.81%
165	Limestone	Peritidal	Flat	90	0.8	0.62	0.75	0.34	0.40	0.93	5.14%
166	Limestone	Reef	Anticline	10	0.8	0.62	0.62	0.58	0.29	0.67	5.11%
167	Limestone	Reef	Dome	10	0.8	0.62	0.62	0.57	0.30	0.69	5.19%
168	Limestone	Reef	10° Incline	10	0.8	0.62	0.62	0.47	0.28	0.65	4.03%
169	Limestone	Reef	5° Incline	10	0.8	0.62	0.62	0.47	0.28	0.65	4.03%
170	Limestone	Reef	Flat	10	0.8	0.62	0.62	0.46	0.28	0.65	3.94%
171	Limestone	Reef	Anticline	50	0.8	0.62	0.71	0.55	0.36	0.85	6.98%
172	Limestone	Reef	Dome	50	0.8	0.62	0.71	0.66	0.38	0.89	8.89%
173	Limestone	Reef	10° Incline	50	0.8	0.62	0.71	0.39	0.37	0.87	5.05%
174	Limestone	Reef	5° Incline	50	0.8	0.62	0.71	0.39	0.35	0.81	4.81%
175	Limestone	Reef	Flat	50	0.8	0.62	0.71	0.42	0.35	0.81	5.14%
176	Limestone	Reef	Anticline	90	0.8	0.62	0.77	0.51	0.40	0.92	7.86%
177	Limestone	Reef	Dome	90	0.8	0.62	0.77	0.74	0.43	1.00	12.27%
178	Limestone	Reef	10° Incline	90	0.8	0.62	0.77	0.34	0.40	0.93	5.25%
179	Limestone	Reef	5° Incline	90	0.8	0.62	0.77	0.38	0.41	0.95	5.92%
180	Limestone	Reef	Flat	90	0.8	0.62	0.77	0.40	0.41	0.96	6.31%

Continued . . .

Num	Lithology	Depositional Environment	Structure	Pvalue	A_n/A_t P90	h_n/h_g P90	Φ_{eff}/Φ_{tot}	E_v	E_d	$(1 - S_{wave})$	E_E and $C_c * (1 - S_{wirr})$
										$(1 - S_{wirr})$	
181	Limestone	Shallow Shelf	Anticline	10	0.8	0.62	0.69	0.53	0.39	0.90	7.09%
182	Limestone	Shallow Shelf	Dome	10	0.8	0.62	0.69	0.64	0.40	0.93	8.75%
183	Limestone	Shallow Shelf	10° Incline	10	0.8	0.62	0.69	0.43	0.22	0.51	3.28%
184	Limestone	Shallow Shelf	5° Incline	10	0.8	0.62	0.69	0.44	0.36	0.84	5.52%
185	Limestone	Shallow Shelf	Flat	10	0.8	0.62	0.69	0.44	0.36	0.84	5.55%
186	Limestone	Shallow Shelf	Anticline	50	0.8	0.62	0.70	0.65	0.38	0.89	8.64%
187	Limestone	Shallow Shelf	Dome	50	0.8	0.62	0.70	0.74	0.40	0.93	10.38%
188	Limestone	Shallow Shelf	10° Incline	50	0.8	0.62	0.70	0.53	0.35	0.81	6.46%
189	Limestone	Shallow Shelf	5° Incline	50	0.8	0.62	0.70	0.57	0.36	0.83	7.10%
190	Limestone	Shallow Shelf	Flat	50	0.8	0.62	0.70	0.61	0.36	0.84	7.68%
191	Limestone	Shallow Shelf	Anticline	90	0.8	0.62	0.73	0.68	0.41	0.95	10.11%
192	Limestone	Shallow Shelf	Dome	90	0.8	0.62	0.73	0.80	0.43	1.00	12.62%
193	Limestone	Shallow Shelf	10° Incline	90	0.8	0.62	0.73	0.53	0.38	0.87	7.31%
194	Limestone	Shallow Shelf	5° Incline	90	0.8	0.62	0.73	0.56	0.38	0.88	7.82%
195	Limestone	Shallow Shelf	Flat	90	0.8	0.62	0.73	0.59	0.26	0.60	5.52%